Aus dem Department für Veterinärwissenschaften

der Tierärztlichen Fakultät

der Ludwig-Maximilians-Universität München

Arbeit angefertigt unter der Leitung von

Univ.-Prof. Dr. Bernhard Aigner

Molecular genetic and phenotypic analysis of ENU-induced mutant mouse models for biomedical research

Inaugural-Dissertation

zur Erlangung der tiermedizinischen Doktorwürde

der Tierärztlichen Fakultät der Ludwig-Maximilians-Universität

München

von

Sudhir Kumar

aus

Majra, India

München 2011

From the Department of Veterinary Sciences

Faculty of Veterinary Medicine

Ludwig-Maximilians-University Munich

Under the supervision of Prof. Dr. Bernhard Aigner

Molecular genetic and phenotypic analysis of ENU-induced mutant mouse models for biomedical research

Inaugural-Dissertation

to achieve the title Doctor of Veterinary Medicine

at the Faculty of Veterinary Medicine of the

Ludwig-Maximilians-University Munich

By

Sudhir Kumar

from

Majra, India

Munich 2011

Gedruckt mit Genehmigung der Tierärztlichen Fakultät

der Ludwig-Maximilians-Universität München

Dekan:	Univ.-Prof. Dr. J. Braun
Berichterstatter:	Univ.-Prof. Dr. B. Aigner
Korreferent:	Priv.-Doz. Dr. M. Schneider

Tag der Promotion: 30.07.2011

To my beloved parents

TABLE OF CONTENTS

1 Introduction 1

2 Review of the literature 2

2.1 Mice in biomedical research 2

2.2 Single gene vs. multifactorial genetic disorders 2

2.2.1 Genetic mapping of monogenic diseases 3

2.2.2 Genome-wide association studies (GWAS) 4

2.2.3 Exome sequencing 6

2.3 Mouse models for functional genome analysis 7

2.4 ENU mutagenesis 7

2.4.1 History and mechanism of action 7

2.4.2 ENU mouse mutagenesis 9

2.4.3 Spectrum of ENU-induced mutations 11

2.4.4 Outcome of the ENU mouse mutagenesis projects 12

2.5 The phenotype-driven Munich ENU mouse mutagenesis project 13

2.5.1 The clinical chemical screen for dominant and recessive mutations 13

2.5.2 Establishment of mutant lines in the clinical chemical screen 14

2.5.3 Analysis of the causative mutation 15

3 Research methodology 18

3.1 ENU-induced mutant lines analyzed in this study 18

3.1.1 Line HST014 18

3.1.2 Line HST011 18

3.1.3 Line HST015 19

3.1.4 Line CLP001 19

3.2 Animal husbandry and maintenance of the mutant lines 20

3.3 Analysis of the causative mutation 20

3.3.1 Line HST014 20

3.3.1.1 Linkage analysis 20

3.3.1.2 Fine mapping and selection of candidate genes 21

3.3.1.3 Analysis of the candidate genes 22

3.3.1.4 Genotyping of the animals of line HST014 23

3.3.2 Line HST011 24

3.3.2.1 Fine mapping of chromosome 1 24

3.3.2.2 Selection and analysis of the candidate gene 25

3.3.2.3 Genotyping of the animals of line HST011 26

3.3.3 Line HST015 26

3.3.3.1 Linkage analysis 26

3.3.3.2 Fine mapping of chromosome 7 27

3.3.3.3 Selection and analysis of the candidate genes 27

3.3.4 Line CLP001 28

3.3.4.1 Selection and analysis of the candidate gene 28

3.3.4.2 Genotyping of the animals of line CLP001 29

3.4 Molecular genetic methodologies 30

3.4.1 Genomic DNA isolation and analysis 30

3.4.2 RNA isolation and analysis 31

3.4.3 First strand cDNA synthesis 32

3.4.4 PCR 32

3.4.5 Elution of PCR products from the agarose gel 33

3.4.6 Sequencing of purified PCR products 33

3.5 Phenotype analysis 34

3.5.1 Blood plasma analysis 34

3.5.2 Metabolic cage analysis 34

3.5.3 Morphological studies 35

3.5.4 SDS-PAGE analysis for the detection of albuminuria 35

3.5.5 Generation of a congenic line 36

3.6 Data presentation and statistical analysis of the data 36

4 Results 37

4.1 Line HST014 37

4.1.1 Linkage analysis of the causative mutation 37

4.1.2 Identification of the causative mutation 40

4.1.3 Allelic differentiation of the *Kctd1*^{I27N} mutation by PCR-RFLP 42

4.1.4 Analysis of *Kctd1*^{I27N} homozygous mutant mice 42

4.1.5 Clinical chemical analysis of *Kctd1*^{I27N} heterozygous mutant mice 43

4.1.6 Urine analysis of *Kctd1*^{I27N} heterozygous mutant mice 45

4.1.7 Morphological analysis of *Kctd1*^{I27N} heterozygous mutant mice 47

4.2 Line HST011 48

4.2.1 Re-analysis of line HST011 showed erroneous linkage analysis 48

4.2.2 Re-mapping of the causative mutation to chromosome 1 50

4.2.3 Sequence analysis of the gene *Pou3f3* 51

4.2.4 Allelic differentiation of the *Pou3f3*^{L423P} mutation by PCR-RFLP 52

4.2.5 Clinical chemical analysis of *Pou3f3*^{L423P} homozygous mutant mice 53

4.2.6 Urine analysis of *Pou3f3*^{L423P} homozygous mutant mice 55

4.2.7 Morphological analysis of *Pou3f3*^{L423P} homozygous mutant mice 56

4.3 Line HST015 59

4.3.1 Linkage analysis of the causative mutation 59

4.3.2 Fine mapping of chromosome 7 60

4.3.3 Candidate genes analysis 60

4.3.4 Clinical chemical analysis of phenotypically heterozygous mutant mice 62

4.3.5 Phenotypical analysis of backcross mice 62

4.4 Line CLP001 63

4.4.1 Sequence analysis of the gene *Gsdma3* 63

4.4.2 Allelic differentiation of the *Gsdma3*^{I359N} mutation by ARMS-PCR 64

4.4.3 Analysis of alopecia in *Gsdma3*^{I359N} mutant mice 65

4.4.4 Clinical chemical analysis of *Gsdma3*^{I359N} mutant mice 66

4.4.5 Morphological analysis of *Gsdma3*^{I359N} mutant mice 66

4.5 Generation of congenic lines 69

5 Discussion 70

5.1 Line HST014 exhibiting the mutation *Kctd1*^{I27N} 70

5.2 Line HST011 exhibiting the mutation *Pou3f3*^{L423P} 72

5.3 Line HST015 established by increased plasma urea levels 74

5.4 Line CLP001 exhibiting the mutation *Gsdma3*^{I359N} 74

6 Summary 77

7 Zusammenfassung 79

8 References 81

9 Acknowledgement 91

LIST OF ABBREVIATIONS

Aqp4	Aquaporin 4
Aqp11	Aquaporin 11
bp	Base pair
cDNA	Complementary deoxyribonucleic acid
Chd2	Chromodomain helicase DNA binding protein 2
DNA	Deoxyribonucleic acid
dNTP	Deoxyribonucleotide Triphosphate
DTT	Dithiothreitol
EDTA	Ethylene diamine tetraacetic acid
ENU	N-ethyl-N-nitrosourea
ES	Embryonic stem
Gsdma3	Gasdermin 3
h	Hour
Het	Heterozygous mutant
Hom	Homozygous mutant
Kctd1	Potassium channel tetramerization domain-containing 1
Mb	Megabase
Mep1b	Meprin 1 beta
nt	Nucleotide
PAGE	Polyacrylamide gel electrophoresis
PCR	Polymerase chain reaction
Pou3f3	POU domain, class 3, transcription factor 3
RE	Restriction endonuclease
RFLP	Restriction fragment length polymorphism

RNA	Ribonucleic acid
SDS	Sodium dodecyl sulphate
Sec	Second
SNP	Single nucleotide polymorphism
TE buffer	Tris EDTA buffer
Tomt	Transmembrane O-methyltransferase
Tris	Tris(hydroxymethyl)aminomethane
Umod	Uromodulin
Wnt11	Wingless-related MMTV integration site 11
Wt	Wild-type

I. INTRODUCTION

Functional genome research is conducted using model organisms such as mice. Mice are easy to handle, have a short generation period and a large litter size, and can be maintained in standardized conditions. A high number of genotypically and phenotypically characterized mouse inbred strains are available to study biochemical and physiological aspects of mammalian biology in a defined genetic background. In addition, mice can be easily genetically manipulated. Functional studies on mouse models are carried out by reverse genetics approaches or by forward genetics approaches. Reverse genetics represents transgenic techniques, whereas in forward genetics mice exhibiting aberrant phenotypes are analyzed to identify the causative mutations. For the generation of a large number of randomly mutant mice, the chemical N-ethyl-N-nitrosourea (ENU) is used. ENU is a potent mutagen and induces primarily point mutations in the spermatogonial stem cells at a frequency of ~150 × 10^{-5} per locus (Russell et al. 1979). In the phenotype-driven ENU mouse mutagenesis projects, screening of the offspring of ENU-mutagenized males is performed in the search of altered phenotypes for the establishment of novel mouse models for biomedical research (Hrabé de Angelis et al. 2000, Nolan et al. 2000). In the phenotype-driven Munich ENU mouse mutagenesis project, a high number of dominant and recessive mutant lines with aberrant phenotypes were established. In the present study, the mutant lines HST014, HST011 (= UREHR2), and HST015 showing nephropathies as well as CLP001 exhibiting alopecia, established previously in the Munich ENU project were analyzed with the following aims:

- Molecular genetic examination of the causative mutation.

- Examination of the basal pathophysiology of the altered phenotype associated with the mutation.

II. REVIEW OF THE LITERATURE

2.1 Mice in biomedical research

After completion of the human genome project, biomedical research focuses to unravel the functions of genes. Understanding the gene functions and their roles in different organ systems is the task of functional genomics. Mice are the most commonly used lab animals to generate animal models for the understanding of many aspects of mammalian biology and diseases (Acevedo-Arozena et al. 2008). Mice are easy to handle and require less space compared with other lab animals. Phylogenetic analysis of the mammalian genomes revealed a high percentage of similarity. In addition, a high number of inbred mouse strains having an identical genotype in all individuals of the strain are available which provides the opportunity for carrying out experiments under standardized and controlled conditions leading to valid and reproducible data. The Mouse Genome Informatics (MGI) database (http://www.informatics.jax.org) represents a comprehensive public resource providing integrated access to curated genetic and phenotypic information for thousands of gene mutations in mice (Bult et al. 2008).

2.2 Single gene vs. multifactorial genetic disorders

Human and mouse sequence projects predicted 20,000 to 25,000 genes in both species. Alteration in genes may lead to abnormalities in the translated protein or in the regulatory system which may cause genetic diseases. Genetic diseases can be divided in two categories: 1) monogenic single gene diseases, and 2) multifactorial complex diseases. Monogenic disorders are caused due to a mutation in a single gene; they are inherited in a dominant or recessive manner and can be autosomal or sex-linked. The inheritance pattern of monogenic disorders is mostly revealed by pedigree analysis of affected families. In contrast, multifactorial complex diseases involve the combined action of many genes, show non-mendelian inheritance, and are ultimately determined by a number of genetic and environmental factors (Fig. 2.1).

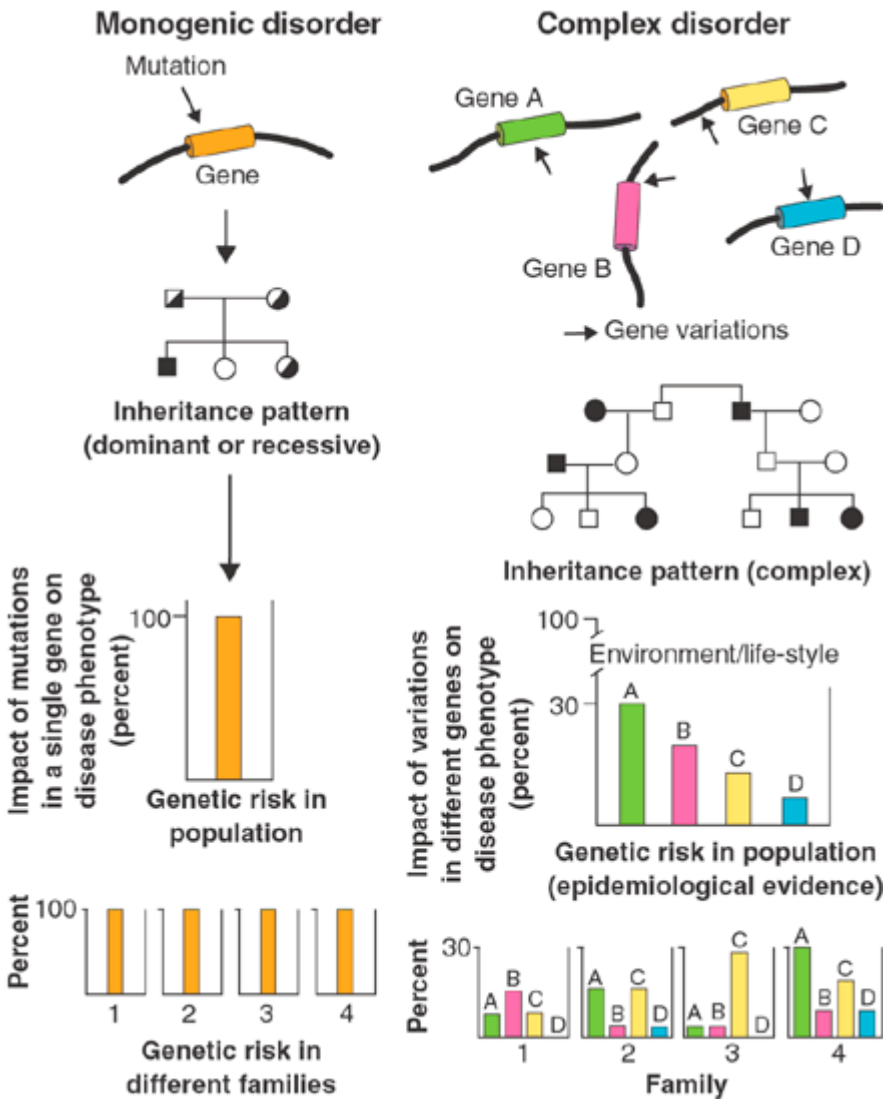

Fig. 2.1: Inheritance and outcome of monogenic and complex disorders (taken from: Peltonen and McKusick 2001).

2.2.1 Genetic mapping of monogenic diseases

The causative mutation of monogenic disorders can be identified by different approaches. Sequence analysis of candidate genes can be carried out which are chosen based on the phenotypic characterization of the disease without prior knowledge of the chromosomal position of the genes. For example, globin gene mutations responsible for certain forms of anemia were identified using this approach. This strategy relies on detailed informations of the disease and the affected gene. A combined strategy can be carried out by using informations about the chromosomal site of a disease locus as well as of a candidate gene locus which is chosen based on the known or predicted biological function (Xu and Li 2000). Once the disease locus and the candidate gene locus are mapped on the identical chromosomal region, sequence analysis and/or expression analysis is

carried out for the identification of the causative mutation (Moore and Nagle 2000).

If suitable candidate genes as well as the chromosomal site of the disease locus are not known, identification of the causative mutation starts with the mapping of the chromosomal region of the mutant gene (linkage analysis, positional cloning). High-density chromosome maps of polymorphic genetic markers have been developed for several mammals including the mouse. Linkage analysis aims to identify genetic markers that are linked to the causative mutation. Therefore, phenotypically mutant mice with the genetic background of an inbred strain are crossed for two generations with another inbred strain exhibiting a normal phenotype of the trait in question. For the mapping of a dominant mutation, heterozygous mutant animals are mated to the second inbred strain. The G1 offspring are phenotypically classified into two categories, the phenotypic mutant and the phenotypic wild-type animals. Phenotypic mutant G1 mice are backcrossed to wild-type mice of the second inbred strain. Mapping of recessive mutations is carried out by mating of homozygous mutant animals with wild-type animals of the second inbred strain and the G2 generation is produced by intercrossing of G1 offspring. For both dominant and recessive mutations, the G2 offspring are again phenotypically characterized. Usually, phenotypically mutant G2 animals are used for the genotype analysis with genome-wide polymorphic markers to find the chromosomal position of the causative mutation. Single-nucleotide polymorphisms (SNPs) of a large number of inbred strains are available as polymorphic genetic marker for the genetic mapping of mutations (http://www.ensembl.org/Mus_musculus/, http://mousesnp.roche.com/cgi-bin/msnp_public.pl, http://www.broad.mit.edu/snp/mouse/, http://www.nervenet.org/MMfiles/MMlist.html, http://snp.gnf.org, http://www.ncbi.nlm.nih.gov/SNP/MouseSNP.cgi.). Further fine mapping of the identified defined chromosomal region with additional genetic markers is carried out. When linkage of the mutant phenotype and the chromosomal region is successfully done, suitable candidate genes are selected for sequence analysis (Silver 1995).

2.2.2 Genome-wide association studies (GWAS)

Genome-wide association studies (GWAS) involve the analysis of the genome of a high number of patients exhibiting a disease of interest with a dense array of

polymorphic genetic markers compared to an unaffected control population for identifying the genetic variations associated with the particular disease (Lander 2011, and refs. therein). High density, strain-specific single nucleotide polymorphism (SNP) data sets like the mouse HapMap resource (http://www.mousehapmap.org), the Broad Institute 149 K SNP Hapmap (Frazer et al. 2007; http://www.broadinstitute.org/) as well as the Wellcome-CTC Mouse Strain SNP Genotype Set (http://mus.well.ox.ac.uk/mouse/INBREDS) are freely accessible to design SNP arrays to carry out GWAS in mice. There are also some commercially arrays available like the JAX® Mouse Diversity Genotyping Array and the Affymetrix® Mouse Diversity Genotyping Array. GWAS can be performed on outbred stocks (Yalcin et al. 2010), on inbred and recombinant inbred strains (Bennett et al. 2010) as well as on heterozygous stock mice (Valder et al. 2006). Outbred stocks are defined as closed populations of genetically variable animals that are bred using defined strategies to maintain maximum heterozygosity (Festing 1993). Recombinant inbred strains are derived from the systematic inbreeding of randomly selected pairs of G2 hybrid mice produced from a cross between two inbred strains (Justice et al. 1992). Su et al. (2010) performed GWAS in 370 mice from 19 mouse strains for more than 1,000 expression traits. The results showed that the statistical power of GWAS was low and false-positive associations were frequent. In another mouse GWAS study, 18 genes with significant association to defined SNPs were identified for the phenotype of ventilator-induced lung injury (VILI). Of these, the four genes *Asap1*, *Adcy8*, *Wisp1*, and *Ndrg1* are located in a single region (64.1-66.7 Mb) on chromosome 15 (Li et al. 2010). Another GWAS performed in inbred mouse strains for the analysis of lung tumor susceptibility, showed the association of SNP rs3681853 on Chromosome 5 for spontaneous tumor incidence, of two SNPs in the pulmonary adenoma susceptibility 1 (*Pas1*) locus for urethane-induced tumor incidence and of SNP rs4174648 on Chromosome 16 for urethane-induced tumor multiplicity. However, linkage analysis showed that only the *Pas1* locus had a significant effect. In summary, GWAS in mouse inbred strains often show false-positive results. Therefore, GWAS combined with linkage analysis may produce more significant results (Manenti et al. 2009). In humans, genome-wide association studies have identified more than 350 common variants associated with risk alleles that contribute to a wide range of complex diseases (Lander 2011, Table 2.1).

Table 2.1: Number of loci identified for different phenotypes in GWAS in humans (taken from: Lander 2011)

Phenotype	Number of GWAS loci	Proportion of heritability explained (%)
Type 1 diabetes	41	~60
Fetal haemoglobin level	3	~50
Macular degeneration	3	~50
Type 2 diabetes	39	20-25
Crohn's disease	71	20-25
LDL and HDL levels	95	20-25
Height	180	~12

LDL: low density lipoprotein; HDL: high density lipoprotein

2.2.3 Exome sequencing

With the advent of next-generation sequencing technologies, cost of DNA sequencing decreased. Sequencing of the protein coding regions of the genome is by far cheaper than whole genome sequencing as the coding regions only represent ~ 1% or ~ 30 Mb of the whole genome known as exome. In total, about 180,000 exons are found in the human genome (Ng et al. 2009). Furthermore, about 85% of the disease-causing mutations are found in the coding regions (Choi et al. 2009). Therefore, exome sequencing is performed to identify genes underlying rare monogenic diseases and to discover the coding variants associated with common diseases (Coffey et al. 2011). It is a powerful method to identify new disease-causing variants in small kindreds for phenotypically and genetically heterogeneous disorders where traditional linkage studies are not feasible (Bilgüvar et al. 2010, Ng et al. 2010). The consensus coding sequence (CCDS) database is mostly targeted by commercial exome capture reagents. The two most widely used commercial kits are the NimbleGen Sequence Capture 2.1M Human Exome Array (http://www.nimblegen.com/products/seqcap) and the Agilent SureSelect Human All Exon Kit (http://www.genomics.agilent.com). Recently, Agilent Technologies introduced the Agilent SureSelect^{XT} Mouse all Exon Kit which is the first commercial system for the targeted enrichment of a model organism exome (http://www.genomics.agilent.com).

2.3 Mouse models for functional genome analysis

Functional studies on mouse models are carried out by reverse genetics approaches or by forward genetics approaches (Fig. 2.2). In the reverse genetics approaches (gene to phenotype), a DNA sequence of interest is used by transgenic techniques which results in the generation of genetically modified mice. Additive gene transfer including RNA interference and random insertional mutagenesis as well as gene knockout and knockin strategies can be carried out to achieve genetic modifications. However, the resulting phenotype due to the genetic modification in mouse models does not always reflect the pathophysiology of human diseases. Therefore, the complementary forward genetics approach (phenotype to gene) is also used to establish additional mouse models for human diseases. The forward genetics approach includes the examination of a large number of animals for altered phenotypes caused by spontaneous or induced mutations. Mice exhibiting altered phenotypes are further bred to establish a mutant line, and subsequently the mutant lines are analyzed for the mutations causing the altered phenotypes (Hrabé de Angelis et al. 2000, Nolan et al. 2000).

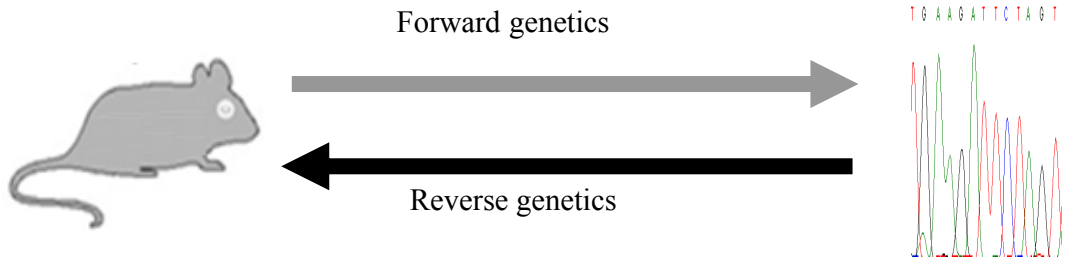

Fig. 2.2: Strategy of the forward genetics and reverse genetics approaches. In forward genetics, mice are analyzed from phenotype to gene, whereas in reverse genetics from gene to phenotype.

2.4 ENU mutagenesis

2.4.1 History and mechanism of action

N-ethyl-N-nitrosourea (ENU) is a synthetic alkylating compound which is toxic and carcinogenic to the cells (Fig. 2.3). It is a potent mutagen, and primarily affects spermatogonial stem cells. It induces random point mutations in the spermatogonial stem cells at a frequency of ~150×10^{-5} per locus in mice (Russell et al. 1979). It does not require any metabolic processing for its activation (Singer and Dosahjh 1990).

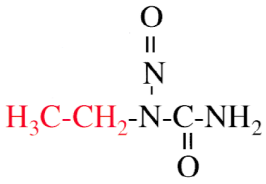

Fig. 2.3: Chemical formula of ENU

ENU transfers its ethyl group to oxygen and nitrogen reactive sites of the nucleotides (Table 2.2, Noveroske et al. 2000).

Table 2.2: Reactive sites of ENU alkylation (taken from: Noveroske et al. 2000)

Nucleotide	Reactive sites
Adenine	N1, N3, and N7
Thymine	O2, O4, and N3
Guanine	O6, N3, and N7
Cytosine	O2 and N3

The ethylated nucleotide is not recognised correctly during DNA replication which results in mispairing to a non-complementary nucleotide (Fig. 2.4).

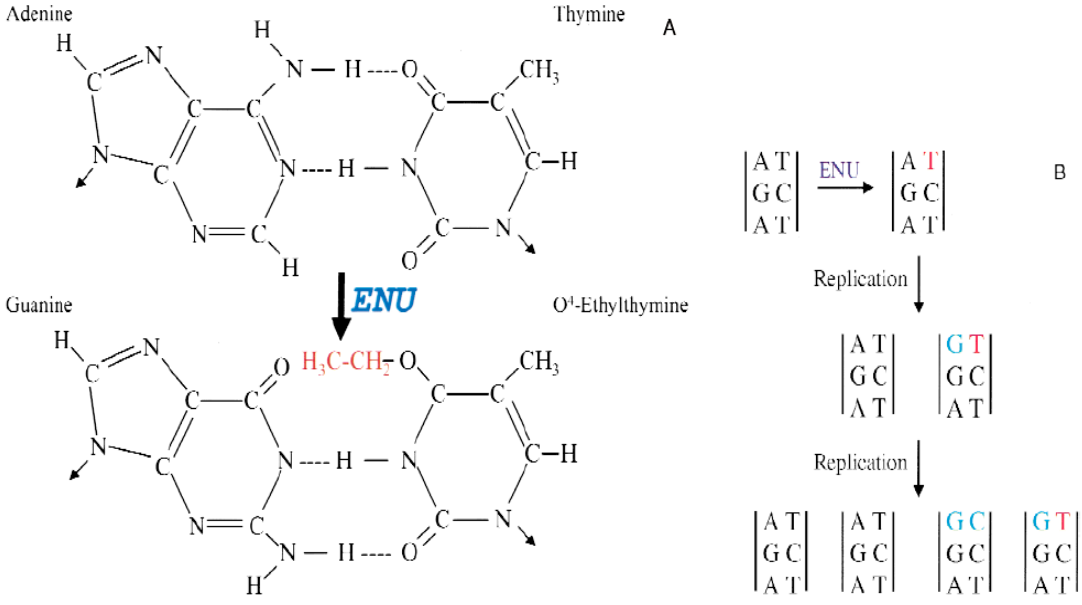

Fig. 2.4: Mechanism of action of ENU. A) Alkylation of thymine results in the formation of O^4-Ethylthymine which is recognised as cytosine and mispairs with guanine. B) Mispairing leads to the corresponding base exchange during DNA replication (taken from: Noveroske et al. 2000).

After two rounds of DNA replication, a single base pair substitution occurs which is not identified by the cellular DNA repair systems and therefore results in a

single base change mutation in the DNA (Bielas and Heddle 2000, Noveroske et al. 2000).

2.4.2 ENU mouse mutagenesis

The alkylating agent ENU is a powerful mutagen for the production of randomly mutant mouse models. Screening for ENU-induced mutations can be carried out by two strategies, the phenotype-driven screen and the gene-driven screen. In a phenotype-driven screen, a large number of offspring of ENU-mutagenized males are screened for the phenotypes of interest. Mice showing aberrant phenotypes are further bred to wild-type animals, and offspring are screened for the desired phenotype. Transmission of the altered phenotype to the subsequent generation shows a genetic mutation as the cause for the altered phenotypes (Balling 2001, Nolan et al. 2000). No assumptions are made about the genetic basis of a particular phenotype. The causative mutation of the altered phenotype is identified by linkage analysis (see 2.2.1).

The ENU gene-driven approach is performed on DNA by establishing both a sperm and a DNA archive from G1 offspring of ENU-mutagenized males (Coghill et al. 2002). Screening the DNA archive for mutations in a gene of interest followed by the recovery of mutant mice from the corresponding frozen sperm sample by *in vitro* fertilization (IVF) allows the subsequent phenotypic characterization of the mutation (Fig. 2.5).

DNA archive centres include the MRC Harwell UK (FESA), the German ENU mouse mutagenesis screening project, the RIKEN Bioresource Center and the Australian Phenomics facility (Acevado-Arozina et al. 2008). Alternatively, ENU gene-driven approaches can be performed on ENU treated mouse ES cells. Mutagenized ES cells are screened for mutations in a gene of interest and a parallel frozen cell archive can be used to generate mutant mice (Chen et al. 2000, Munroe et al. 2000).

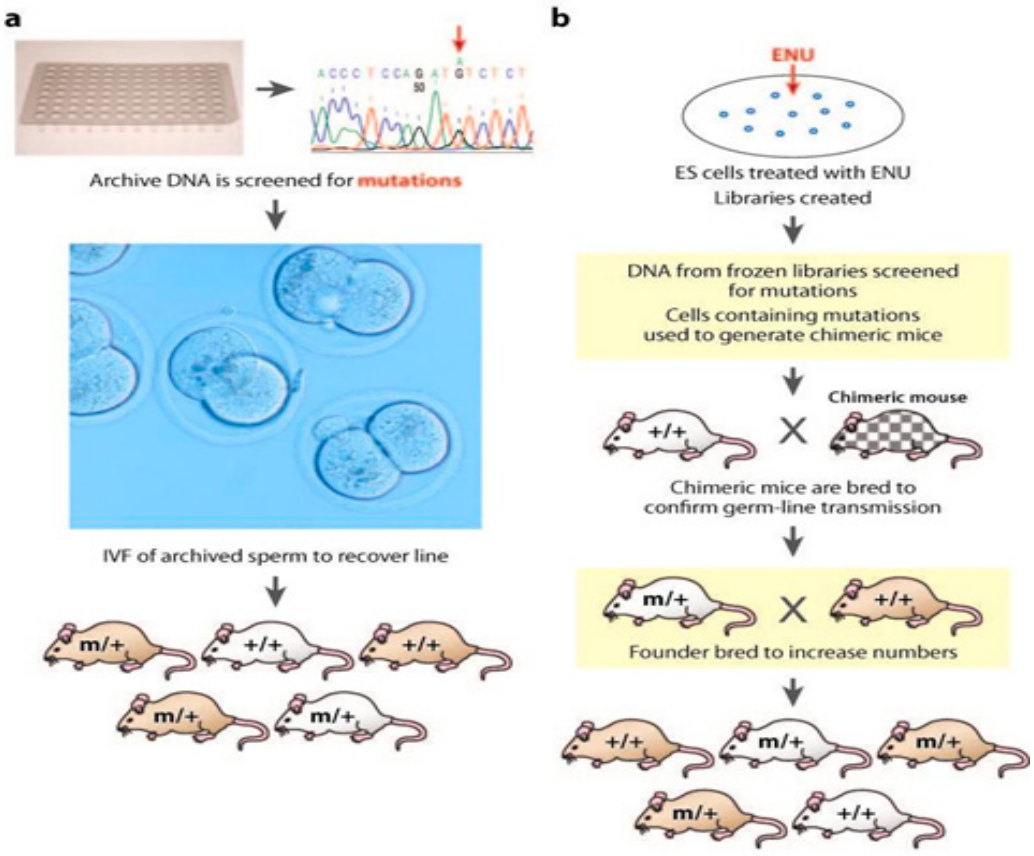

Fig. 2.5: Scheme for an ENU gene-driven screen. a) A DNA archive of G1 mice derived from ENU-mutagenized males is screened for mutations and mutant mice are recovered by *in vitro* fertilization (IVF) from the frozen sperm. b) A library of ENU-treated ES cells is screened for ENU mutations. Once a mutated clone is identified, ES cells are microinjected into mouse blastocysts to generate mutant mice for further examinations (taken from: Acevado-Arozina et al. 2008).

For ENU mutagenesis, one mutation has been estimated to occur in 1.0-2.5 Mb (Aigner et al. 2008, and refs. therein). Thus, G1 offspring of ENU-mutagenized males harbour less than 100 potentially functional mutations. A founder G1 mouse with an interesting phenotype is backcrossed using wild-type mice of the same inbred strain to eliminate additional mutations. The number of mutations will decline on average by 50% with each backcross generation; as the resulting genome will harbour about 97% of non-mutagenized genome of the recipient animals after five backcrosses (Keays et al. 2006).

After identifying the putative causative mutation, the proof that the sequenced mutation is the causative mutation has to be produced by functional analysis, e.g. by expression analysis of the affected gene, by performing complementation tests with another mutant allele or by rescue of the wild-type function of the gene in

transgenic mice. The mutants may carry loss-of-function, dominant-negative, hypomorphic, or gain-of-function alleles of the affected genes (Caspary and Anderson 2006).

2.4.3 Spectrum of ENU-induced mutations

ENU mostly generates random genome-wide point mutations by base substitutions. Around 70-85% of the base substitutions are A-T to T-A transversions or A-T to G-C transitions (Table 2.3, Noveroske et al. 2000, Takahasi et al. 2007). Conversely, the G-C to C-G transversion appears less often (Augustin et al. 2005). To a lower extent, few small deletions have been also reported as a consequence of ENU mutagenesis (Shibuya and Morimoto 1993).

Table 2.3: Genetic nature and frequencies of mutations found in ENU projects (taken from: Barbaric et al. 2007)

	AT to TA	AT to GC	AT to CG	GC to AT	GC to TA	GC to CG	Insertion	Deletion
Phenotype-driven (%)	29.5	30.2	7.4	18.1	10.7	1.3	0.7	2.0
Gene-driven (%)	27.3	37.0	3.9	18.7	12.1	0.8	0	0.4

About 70% non-synonymous amino acid exchanges occurred due to ENU-induced point mutations. 65% of these are missense amino acid exchanges and the rest are nonsense or splice mutations at the protein level (Table 2.4, Barbaric et al. 2007, Justice et al. 1999, Takahasi et al. 2007).

Table 2.4: Consequences of ENU-induced mutations at the protein level (taken from: Barbaric et al. 2007)

	Missense	Nonsense	Splicing	5', 3' UTR	Destroy start site	Make sense	Frameshift
Phenotype-driven (%)	58.9	16.6	21.9	0	1.3	0	1.3
Gene-driven (%)	83.3	6.5	5.7	3.7	0	0.8	0

2.4.4 Outcome of the ENU mouse mutagenesis projects

Major ENU mouse mutagenesis projects have been performed as phenotype-driven as well as gene-driven screens for the generation of novel mutant models (Table 2.5).

Table 2.5: Centres running ENU mouse mutagenesis projects (taken from: Cordes 2005)

ENU centre	Website	Genetic approach	Genetic region
ENU mutagenesis programme MRC Harvell UK	http://www.har.mrc.ac.uk/research/mutagenesis/	Dominant Recessive	Genome-wide Chr 13 36H
Munich ENU mouse mutagenesis project Germany	http://www.helmholtz-muenchen.de/en/ieg/group-functional-genetics/enu-screen/index.html	Dominant Recessive	Genome-wide Genome-wide
Australian phenomics facility	http://www.apf.edu.au/	Recessive	Genome-wide
Baylor College of Medicine Mouse Genome project	http://www.mouse-genome.bcm.tmc.edu/ENU/ENUHome.asp	Recessive	Chr 11 Chr 4
Centre for Modeling Human disease	http://www.cmhd.ca/	Dominant	Genome-wide
Genomics institute of the Novartis Research foundation	http://www.gnf.org/	Recessive	Genome-wide
Jackson Laboratory Neuroscience Mutagenesis Facility	http://nmf.jax.org/	Dominant Recessive Recessive	Genome-wide Genome-wide Chr 5
Jackson Laboratory Mouse Heart, Lung, Blood and Sleep Disorders Center	http://pga.jax.org/	Dominant Recessive	Genome-wide Genome-wide
Molecular Neurobiology at Northwestern University	http://www.neurobiology.northwestern.edu/	Dominant Recessive	Genome-wide Genome-wide
Mutagenesis Project at MRI	http://www.montana.edu/wwwmri/index.html	Recessive	Genome-wide
Oak Ridge National Laboratory	http://www.ornl.gov/	Recessive	Chr 7, chr 10, chr 15 & chr X
RIKEN Mutagenesis Center	http://www.brc.riken.jp/lab/gsc/mouse/	Dominant Recessive	Genome-wide Genome-wide
Tennessee Mouse Genome Consortium	http://www.tnmouse.org/	Recessive	Chr 7, chr 10, chr 15 & chr X
University of Pennsylvania, Philadephia	http://www.med.upenn.edu/ins/faculty/bucan.htm	Recessive	Chr 5

Search for published ENU-induced mutants (as of 31.03.11) in the “phenotypes and alleles” MGI database

(http://www.informatics.jax.org/searches/allele_form.shtml) revealed 2,282 alleles and 1,823 genes/markers. Among them, 73 alleles and 61 genes/markers are described for influencing the renal or urinary system as primary or secondary phenotype derived from phenotypic-driven or gene-driven approaches.

2.5 The phenotype-driven Munich ENU mouse mutagenesis project

The Munich ENU mouse mutagenesis project has been established for the genome-wide screen for dominant and recessive mutations in C3HeB/FeJ (C3H) inbred mice. Male C3H mice (10 weeks old, G0) are treated with three intraperitoneal injections of 90 mg/kg ENU at weekly intervals (Hrabé de Angelis et al. 2000). The treated male mice are mated with wild-type C3H females and the G1 offspring are screened for dominant mutations. After carrying out a defined breeding scheme (see Fig. 2.6), G3 mice are screened for recessive mutations. A large number of mutant mouse lines have been established in different phenotypic screens. The phenotypic screens are done in the German Mouse Clinic (GMC), which is an open-access technology platform established for the comprehensive phenotyping of mutant lines (Fuchs et al. 2009, Gailus-Durner et al. 2005).

2.5.1 The clinical chemical screen for dominant and recessive mutations

The Chair for Molecular Animal Breeding and Biotechnology (Prof. Dr. E. Wolf), LMU München conducts the clinical chemical screen in the Munich ENU mouse mutagenesis project. The focus of the clinical chemical screen is to detect alterations in blood parameters (substrates, enzyme activities, electrolytes) as well as haematological changes by common high-throughput laboratory diagnostic procedures. The list of parameters used in the clinical chemical screen is given in Table 2.6 (Rathkolb et al. 2000). More than 15,000 G1 offspring and 500 G3 pedigrees have been screened for alterations in clinical chemical parameters.

Table 2.6: Clinical chemical plasma parameters used (taken from: Rathkolb et al. 2000)

Enzyme Activities	Alkaline phosphatase (AP), α-amylase, creatine kinase (CK), aspartate-aminotransferase (AST), alanine-aminotransferase (ALT), lipase, c-reactive protein
Substrates	Glucose, cholesterol, triglycerides, total protein, uric acid, urea, creatinine, ferritin, transferritin, lactose, low density lipoprotein
Electrolytes	Potassium, sodium, chloride, calcium, inorganic phosphate (Pi)

2.5.2 Establishment of mutant lines in the clinical chemical screen

The screen for dominant mutations is performed on G1 animals that are derived from the mating of ENU-mutagenized G0 males to wild-type C3H females (Fig. 2.6).

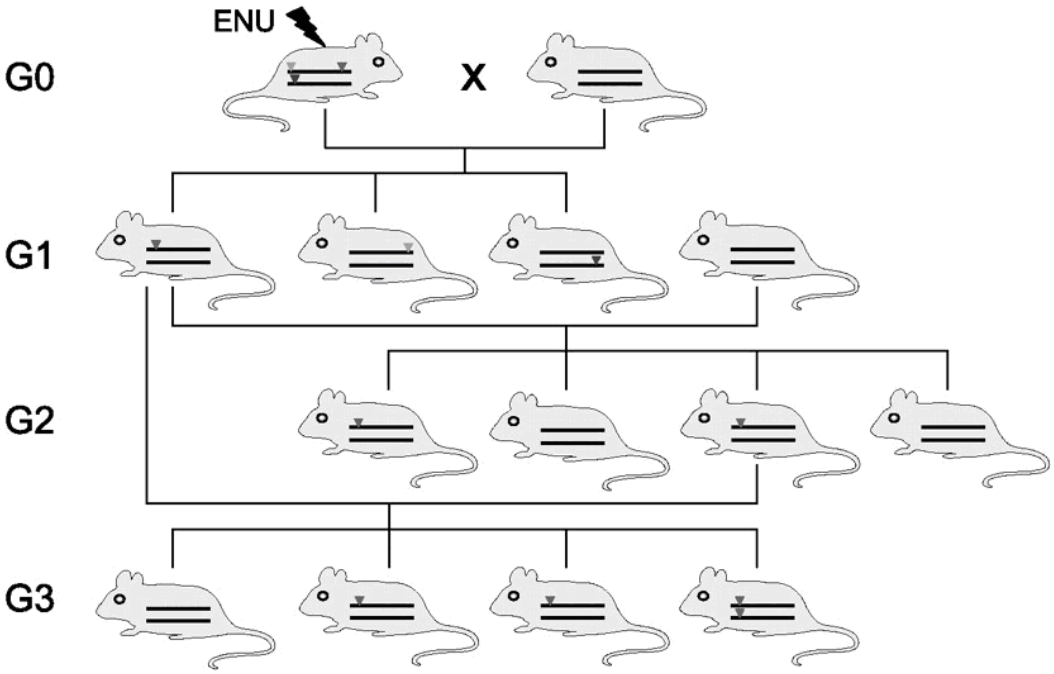

Fig. 2.6: ENU mutagenesis and breeding strategies for the screening for dominant and recessive mutation. ENU treated male (G0) mice are mated to female wild-type C3H mice to produce G1 mice. The dominant mutations are screened in the G1 offspring and the recessive mutations are screened in the G3 offspring produced from the backcross of G2 animals with G1 mice. Black triangles: causative mutation; light triangles: non-causative mutations (taken from: Aigner et al. 2008).

Animals with an aberrant phenotype associated with blood parameters are re-examined for the mutant phenotype. Animals showing the aberrant phenotype also in the second measurement are considered to be mutant for the screened parameter. Inheritance of the observed mutant phenotype is tested on G2 mice, which are derived from the mating of the G1 mice exhibiting the altered phenotype and wild-type mice. The appearance of the aberrant phenotype in G2 mice confirms that the mutant phenotype is caused by a dominant mutation and allows the generation of a mutant line.

The screen for recessive mutations is performed on G3 mice, which are produced in a two-step breeding scheme from G1 mice. Phenotypically normal G1 males are mated to wild-type females for the production of G2 animals. Subsequently

G2 females are backcrossed to the G1 male to produce the G3 mice (Fig. 2.6). G3 mice with an aberrant phenotype associated with blood parameters are re-examined for the mutant phenotype. Animals showing the aberrant phenotype also in the second measurement are considered to be mutant for the screened parameter. Inheritance of the aberrant phenotype is confirmed in G5 mice. Therefore, the phenotypically mutant G3 mice supposed to harbour a homozygous recessive mutation are mated to wild-type mice for the production of the presumably heterozygous mutant G4 mice with an inconspicuous phenotype. Intercrossing of the G4 heterozygous mutant mice is performed to produce G5 animals. The appearance of the aberrant phenotype in G5 mice confirms that the mutant phenotype is caused by a recessive mutation and allows the establishment of a mutant line. Provisional names are given to the established mutant lines, which are replaced according to the official nomenclature after identification of the mutation (http://www.informatics.jax.org/mgihome/nomen/index.shtml).

2.5.3 Analysis of the causative mutation

Linkage analysis is carried out to find the chromosomal position of the causative mutation after the establishment of a mutant line. C57BL/6 or BALB/c is used as second inbred strain for the linkage analysis in the Munich ENU mouse mutagenesis project. The breeding strategy to map the dominant mutation is given in Fig. 2.7. Phenotypically heterozygous mutant animals are mated to the second inbred strain. Phenotypically mutant G1 hybrid mice are backcrossed to wild-type mice of the second inbred strain (Aigner et al. 2008). The G2 offspring are phenotypically classified as mutant mice and wild-type mice. Usually, DNA samples from phenotypically mutant G2 mice are used in the genetic analysis using a panel of genome-wide polymorphic markers.

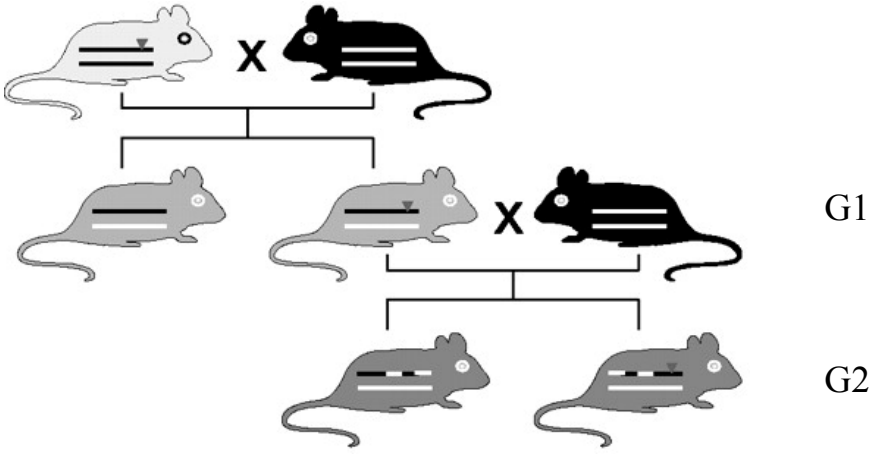

Fig. 2.7: Breeding strategy for mapping dominant mutations. Phenotypically heterozygous mutant animals are mated to a second inbred strain. G1 hybrid offspring showing the mutant phenotype are backcrossed to wild-type mice of the second inbred strain. Triangles: causative dominant mutation (taken from: Aigner et al. 2008).

For mapping a recessive mutation, phenotypically homozygous mutant animals are mated with a second inbred strain and the resulting G1 hybrid mice with inconspicuous phenotype are intercrossed for the production of the G2 offspring (Fig. 2.8).

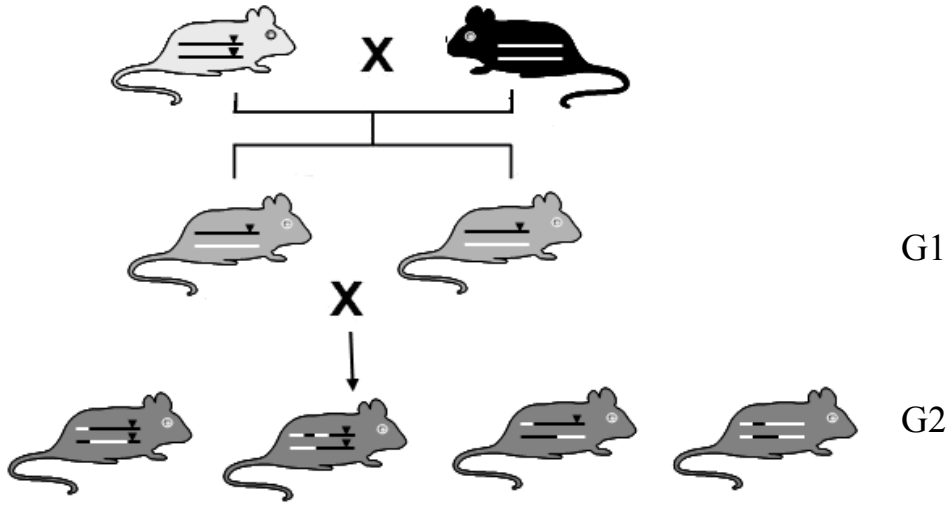

Fig. 2.8: Breeding strategy for mapping recessive mutations. Phenotypically homozygous mutant animals are mated with a second inbred strain and the resulting G1 hybrid mice are intercrossed for the production of the G2 offspring. Triangles: causative recessive mutation (taken from: Aigner et al. 2008).

G2 animals are phenotypically classified as mutant and wild-type mice. About 150 genome-wide polymorphic markers are used for the chromosomal mapping of the mutation. Further fine mapping with additional polymorphic markers is carried out. Subsequently, candidate genes within the identified defined genetic interval are analyzed to find the causative mutation for the mutant phenotype. In ENU-induced mutant lines, usually a single mutation has been proven to be the cause for the mutant phenotype (Barbaric et al. 2007). Causative mutations have already been successfully mapped and subsequently identified in many mutant lines established in the Munich ENU mouse mutagenesis project (Kemter et al. 2010, and refs. therein).

III. RESEARCH METHODOLOGY

3.1 ENU-induced mutant lines analyzed in this study

The mutant lines HST014, HST011, and HST015 showing increased plasma urea values established in the clinical chemical screen, as well as line CLP001 exhibiting alopecia as primary phenotypic alterations were analyzed in this study (Table 3.1).

Table 3.1: ENU-induced mutant lines analyzed in this study

Line	Aberrant phenotype	Founder animal	Year	Inheritance
HST014	Increased plasma urea	G1 male ID 10295828	2006	Dominant
HST011	Increased plasma urea	G3 male ID 20033899	2000	Recessive
HST015	Increased plasma urea	G1 male ID 10174676	2006	Dominant
CLP001	Alopecia	G1 female ID 20020972	2000	Dominant

Increased plasma urea values (>70 mg/dl for males and >65 mg/dl for females as cut-off values)

3.1.1 Line HST014

Line HST014 harbours a dominant mutation. Four-month-old phenotypically heterozygous mutant mice showed increased plasma urea values (>70 mg/dl for males and >65 mg/dl for females as cut-off values) as compared with littermate controls.

3.1.2 Line HST011

Line HST011 (= UREHR2) harbours a recessive mutation. Phenotypically homozygous mutant animals exhibited increased plasma urea and creatinine levels as compared to control littermates. In addition, four-month-old phenotypically homozygous mutants showed a decreased absolute and relative kidney weight (Fig. 3.1). Light microscopy showed no alterations in the kidneys of the phenotypically mutant animals (Aigner et al. 2007).

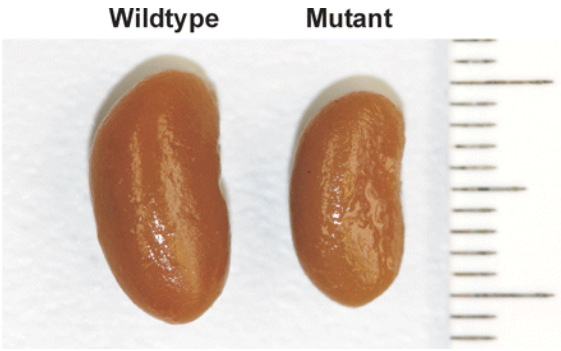

Fig. 3.1: Macroscopic appearance of the kidneys of HST011 mice. Kidneys of phenotypically homozygous mutant animals were smaller compared to phenotypically wild-type littermates (taken from: Aigner et al. 2007).

For the chromosomal mapping of the causative mutation, phenotypically homozygous mutant animals on the inbred C3H genetic background were bred with BALB/c inbred mice. The phenotypically inconspicuous heterozygous mutant G1 mice were intercrossed for the production of the G2 generation. G2 offspring were screened for increased plasma urea levels (>70 mg/dl for males and >65 mg/dl for females as cut-off values) at the age of 12 and 15 weeks, and subsequently 48 phenotypically mutant animals were selected for the linkage analysis. Linkage analysis was carried out using a panel of 116 genome-wide polymorphic markers in collaboration with the Institute of Experimental Genetics (Prof. Dr. M. Hrabé de Angelis), Helmholtz Zentrum München. Linkage analysis mapped the causative mutation to chromosome 7.

3.1.3 Line HST015

Line HST015 has a dominant mutation. Twelve-week-old phenotypically heterozygous mutant mice showed increased plasma urea values (>70 mg/dl for males and >65 mg/dl for females as cut-off values) as compared with littermate controls.

3.1.4 Line CLP001

Line CLP001 harbours a dominant mutation. Phenotypically heterozygous mutant mice showed alopecia. Onset of hair loss started from 3 weeks of age from the back. For linkage analysis, phenotypically heterozygous mutant mice on the inbred C3H genetic background were bred for two generations with C57BL/6 inbred mice. Phenotypically heterozygous mutant G2 mice exhibiting alopecia were selected for linkage analysis. Linkage analysis on 46 phenotypically mutant

G2 animals with 94 genome-wide polymorphic markers was carried out. The causative mutation was mapped on chromosome 11. Fine mapping was carried out with additional polymorphic markers in the defined chromosomal region and confirmed the mapping results.

3.2 Animal husbandry and maintenance of the mutant lines

The mutant lines were maintained in the mouse facility at the Chair for Molecular Animal Breeding and Biotechnology, Moorversuchsgut, Oberschleißheim under a controlled specific-pathogen-free (SPF) hygiene standard according to the Federation of European Laboratory Animals Science Associations (FELASA) protocols (Nicklas et al. 2002; http://www.felasa.eu/). Mouse husbandry was done under standard environmental conditions (22°C, 55% relative humidity, 12 h light : 12 h dark cycle) and mice were provided a standard rodent diet (V1124; Ssniff, Soest, Germany) and water ad libitum. All animal experiments were conducted under the approval of the responsible animal welfare authority (Regierung von Oberbayern). The dominant mutant lines HST014, HST015, and CLP001 were maintained by mating phenotypically heterozygous mutant animals to wild-type C3H mice. The recessive mutant line HST011 was maintained by mating phenotypically homozygous mutant animals to wild-type C3H mice and subsequently intercrossing of the heterozygous mutant offspring without aberrant phenotype. Offspring were weaned three weeks post partum and marked by ear punching.

3.3 Analysis of the causative mutation

3.3.1 Line HST014

3.3.1.1 Linkage analysis

Phenotypically heterozygous mutant mice on the inbred C3H genetic background with increased plasma urea levels were bred to BALB/c inbred mice. The G1 hybrid offspring were examined for increased plasma urea levels at the age of 9, 12, and 15 weeks. G1 animals showing increased plasma urea values (>70 mg/dl for males and >65 mg/dl for females as cut-off values) were bred with BALB/c mice. The G2 animals were analyzed for increased plasma urea levels at the age of 9, 12, and 15 weeks and classified as phenotypically heterozygous mutants exhibiting increased plasma urea values and wild-type mice. Tail samples of G2

mice were collected and stored at -80˚C. Linkage analysis was performed using a panel of 113 genome-wide polymorphic markers on the DNA samples of 45 phenotypically mutant G2 animals in cooperation with the Institute of Experimental Genetics (Prof. Dr. M. Hrabé de Angelis), Helmholtz Zentrum München.

3.3.1.2 Fine mapping and selection of candidate genes

Fine mapping was performed by using additional polymorphic microsatellites and SNP markers which are described to exhibit different alleles for C3H and BALB/c mice (http://www.informatics.jax.org/; http://www.ncbi.nlm.nih.gov) and which cover the previously defined chromosomal region. The PCR primers (Table 3.2) were designed according to the available sequence data (http://www.informatics.jax.org/; http://www.ensembl.org/) and were ordered for synthesis (Thermo Fisher Scientific, Ulm, Germany).

Table 3.2: Polymorphic markers of chromosome 18 used for fine mapping in the line HST014

Marker name	Chr. Position (Mb)	Forward primer (5'-3')	Reverse primer (5'-3')
rs52303422	9.5	caggacagttgtcacaggac	tcccatcatgtactgtaagcac
rs52534573	11.2	ccctccgttcccactttctc	tcaggatccatgtcaacaaag
rs46961948	11.4	cagcctttgtacatggtgac	tacagtggctgtcgtagtttac
rs52391350	12.9	actgtgtgctttagaacacaac	gctctctggtgctctctgg
rs52376653	13.6	tgggatgtatgtagcactc	gttttattgagtgtgggag
rs31073798	14.3	atgaggggaagcgctgaagg	cttctgttaagctgtaaaatgc
rs31158307	14.6	ctgggaaatgccttctcttgc	gatgaacttgtgagcccattag
rs31155567	14.6	gagtggttttggtatcagtg	tctcccaacccccctc
rs31158391	14.6	tctatcctaactgatctagtc	ggcttccatgatcagcagg
rs31243033	17.0	tgaaatgatgaaagaccatataatg	caaaggaagatgtttactataaag
rs31247952	17.0	atatttatttatgtaattaaataac	gatttgaaatactattgacag
rs31220775	17.5	ggcaaagaaccttttcctctc	tgtttgtctctctattctg gttg
D18Mit68	21.5	gcgtgagggttttgtttgtt	aatacttccagaaccttagacc
rs51268966	23.4	agaatttaaggatgaacttt actg	ccctgtgatccatccaatagc
rs52585890	26.1	gtgagtgtatgtatgtatctcag	aagttcatgggccagctagc
D18Mit70	35.0	ctgctagcgtttaccatatagc	ctgtggtctcccagccac

The marker position is given according to http://www.informatics.jax.org/.

The microsatellite markers D18Mit68 and D18Mit70 were analyzed by PCR whereas the SNP markers were analyzed by using a PCR-RFLP strategy. The genes which are located in the identified defined chromosomal region (http://www.ensembl.org/) were analyzed for published data about their wild-type and mutant function (http://www.informatics.jax.org/). Three genes were selected as the candidate genes for the mutant phenotype (Fig. 3.2).

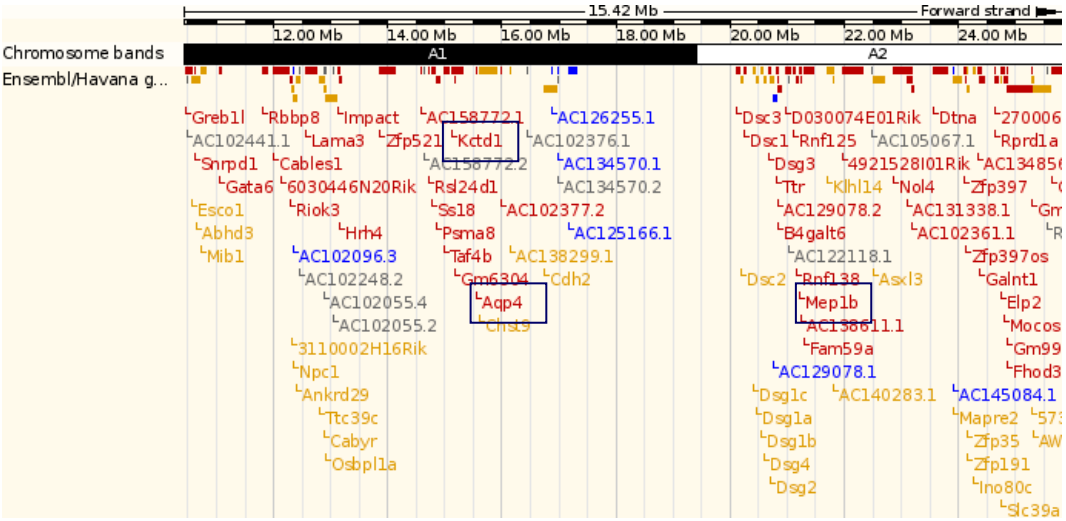

Fig. 3.2: Chromosomal position of the candidate genes for line HST014. The selected genes are shown in boxes. The figure is adopted from http://www.ensembl.org/.

3.3.1.3 Analysis of the candidate genes

PCR amplifications of the exonic or cDNA sequences of the candidate genes were carried out using specific primers (Table 3.3). Subsequently, sequencing of the PCR products was carried out. The obtained sequences were compared with published database sequences and C3H wild-type sequences.

Table 3.3: Candidate genes on chromosome 18 and their primer sequences

Gene	Primer and transcript ID	Forward primer (5'-3')	Reverse primer (5'-3')	Expected PCR product size (bp)
Aqp4	E_1(ENSMUST00000079081)	ctgtgtctataatgatcaggtacag	gctgttgctaccttctagattctg	305
	E_2(ENSMUST00000079081)	aaactgcaagactgcagcctgac	tgcaagcacatgaagttctagtac	550
	E_3(ENSMUST00000079081)	tggtagaagactcaagttaaccatg	agcttcagggtgaggataaatgag	337
	E_4(ENSMUST00000079081)	tgttcctctgaggagactacagc	agaaaccagtgagctaaattacgc	257
	E_5(ENSMUST00000079081)	tatatgcataggttgtccactgag	tgtaacaaggtgtgaagcaagaaac	402
	E_1(ENSMUST00000115856)	tcctatgagtgtgaacacatcagg	cacctgctcattcacacacctg	232
	E_2(ENSMUST00000115856)	acaggtgtgtgaatgagcaggtg	tctctgagagagactgtgagaac	287
Mep1b	P_1(ENSMUST00000082235)	agcttgcagctttcatctggaag	gaatcagacacactgtcattgtag	612
	P_2(ENSMUST00000082235)	agtcacgtgctgaccgggatg	aacagtctgctctccatcg	540
	P_3(ENSMUST00000082235)	agtgcaaagactctggcttcttc	ctccgctggttgaacatacgc	660
	P_4(ENSMUST00000082235)	tggccatgtccttggcaacaag	tggaaggtctcttttcatttcacc	660
	E_1(ENSMUST00000115840)	tgccttgtcaaccacatgactg	gatgacgtctgtatcctcttctg	284
Kctd1	P_1(ENSMUST00000025992)	tgtgcttcaatgtttcaggacag	cacaaatgtccctttctcatattg	861

3.3.1.4 Genotyping of the animals of line HST014

After identifying the causative mutation, the DNA sequence containing the point mutation was analyzed with the NEBcutter V2.0 tool (New England Biolabs, UK; http://tools.neb.com/NEBcutter2/). The point mutation resulted in the abolishment of the restriction site of the enzyme *Bsm*I in the mutant allele. For the genotypic analysis of homozygous mutant, heterozygous mutant and wild-type animals, a PCR-RFLP strategy was established. The PCR primers were designed encompassing the DNA sequence around the point mutation (Kctd1_F: 5' acggcaaaagtgagagaacctg 3' and Kctd1_R: 5' tggaattgcaggcagataatgcc 3'). PCR conditions were used as given.

Components of the PCR master mixture (1×)	Volume (µl)
Distilled H_2O	15.4
10× PCR buffer	2.5
dNTPs (2 mM)	2.5
$MgCl_2$ (25 mM)	2.5
Primer Kctd1_F (10 mM)	0.4
Primer Kctd1_R (10 mM)	0.4
Taq DNA Polymerase (10 U/µl)	0.3
Genomic DNA (100 ng/µl)	1.0

- 94˚C 5 min
- 94˚C 30 sec
- 66˚C 45 sec
- 72˚C 45 sec

35×

- 72˚C 5 min

For restriction enzyme digestion, 5 µl of the PCR products were incubated with 5 µl master mixture (3.5 µl distilled H_2O, 1 µl 10× restriction enzyme buffer, 5 U *Bsm*I (Fermentas, St. Leon-Rot, Germany)) at 37˚C for 2 h. Digested PCR products were analyzed on a 2% agarose gel stained with ethidium bromide. Homozygous mutant mice were produced by mating heterozygous mutant mice on the C3H genetic background.

3.3.2 Line HST011

3.3.2.1 Fine mapping of chromosome 1

Fine mapping was carried out on phenotypically mutant animals which exhibited the homozygous wild-type genotype for the *Umod* gene (see 4.2.1). Polymorphic markers which are described to have different alleles for C3H and BALB/c were selected for chromosome 1 (Table 3.4).

Table 3.4: Polymorphic markers used for fine mapping of chromosome 1 in line HST011

Marker name	Chr. Position (Mb)	Forward primer (5'-3')	Reverse primer (5'-3')
D1Mit64	12.8	agtgcattatgaagccccac	tcaaattttaaaacaacccatttg
D1Mit432	24.3	tctgctcttgttctcttctgagg	gcagattcatttctctctctataatc
D1Mit411	33.2	ggaaactggaaaaggggtga	tagcattgctctttggtttctg
D1Mit212	40.0	tctcatgaggtgtgtgagtttg	ggatccccttgcttcactaa
D1Mit156	65.8	tctgctgccacttctgag	gtgtgtctatggacatggatg
D1Mit415	88.3	ttggcacatgcctacaactc	agaacaccatatattgtgccc

The marker position is given according to http://www.informatics.jax.org/.

3.3.2.2 Selection and analysis of the candidate gene

According to the MGI data (http://www.informatics.jax.org/), the gene *Pou3f3* (Fig. 3.3) was selected as candidate gene for sequence analysis (Table 3.5).

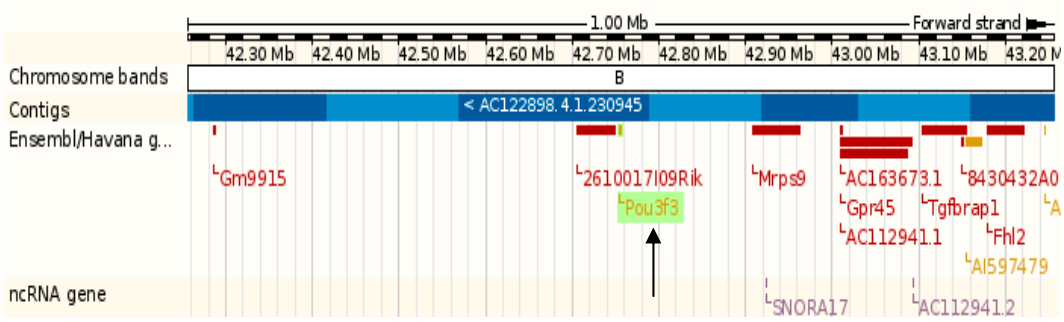

Fig. 3.3: Chromosomal position of the gene *Pou3f3* (shown by arrow). The figure is adopted from http://www.ensembl.org/.

Table 3.5: Primer sequences of the candidate gene *Pou3f3* (chr. 1, 42.7 Mb) of line HST011

Primer	Forward primer (5'-3')	Reverse primer (5'-3')	Expected PCR product size (bp)
P_1	gcggctgctgctgcggcg	tccgcggtgatgcagcgcgg	560
P_2	cagcagccgccacagccgc	tgaactgcttagcgaactgctc	682
P_3	gctcaacagccacgaccctc	tgctgacagcggctgcggag	658

The position is given according to http://www.ensembl.org/.

3.3.2.3 Genotyping of the animals of line HST011

Genotyping of the animals of line HST011 was also carried out with PCR-RFLP because a restriction site of the enzyme *Sml*I was abolished due to the causative mutation (NEBcutter V2.0 tool; New England Biolabs, UK; http://tools.neb.com/NEBcutter2/). Primers were synthesised 5' and 3' of the causative mutation (Pou3f3_F: 5' cactggcagtcccaccagc 3' and Pou3f3_R: 5' agcagcagcggtggttctcg 3'). PCR conditions are shown below.

Components of the PCR master mixture (1×)	Volume (µl)
Distilled H_2O	15.4
10× PCR buffer	2.5
dNTPs (2 mM)	2.5
$MgCl_2$ (25 mM)	2.5
Primer Pou3f3_F (10 mM)	0.4
Primer Pou3f3_R (10 mM)	0.4
Taq DNA Polymerase (10 U/µl)	0.3
Genomic DNA (100 ng/µl)	1.0

- 94˚C 5 min
- 94˚C 30 sec
- 64˚C 45 sec
- 72˚C 45 sec

35×

- 72˚C 5 min

For restriction enzyme digestion, 5 µl PCR products were incubated with 5 µl master mixture (analogous to 3.3.1.4) using *Sml*I at 55˚C for 2 h. The digested PCR products were analyzed on a 2% agarose gel and stained with ethidium bromide.

3.3.3 Line HST015

3.3.3.1 Linkage analysis

Phenotypically heterozygous mutant mice on the inbred C3H genetic background

with increased plasma urea levels were bred to BALB/c inbred mice. The G1 hybrid offspring were examined for increased plasma urea values (>70 mg/dl for males and >65 mg/dl for females as cut-off values) at the age of 12 and 15 weeks. G1 animals showing increased plasma urea values were bred with BALB/c inbred mice. The G2 animals were analyzed for increased plasma urea values (>70 mg/dl for males and >65 mg/dl for females as cut-off values) at the age of 12, 15 and 18 weeks and classified as phenotypically heterozygous mutants exhibiting increased plasma urea values and wild-type mice.

3.3.3.2 Fine mapping of chromosome 7

Fine mapping was carried out on phenotypically mutant G2 mice using polymorphic markers of chromosome 7 (Table 3.6).

Table 3.6: Polymorphic markers used for fine mapping of chromosome 7 in line HST015

Marker name	Locus (Mb)	Forward primer (5'-3')	Reverse primer (5'-3')
D7Mit230	56.7	ggttaactgctttt taaaagtgc	acttctgcatgttgccctct
D7Mit276	69.4	ctgggaggaatgttctccaa	atgcccagtgtagaagaaacc
D7Mit90	87.5	cacaccaagtctccccaact	caaaactgacccagagaggc
D7Mit323	108.0	caccttctaatcctacttcctg	ccagaacaggaaatagagtacc
D7Mit40	123.9	gtcaacagtcaggaaagctgg	cagatgcttgtatttgcaaagc
D7Mit68	132.4	ctcccacacagggtctttgt	gatacccaaagtacacctctgtca

The marker position is given according to http://www.informatics.jax.org/.

3.3.3.3 Selection and analysis of the candidate genes

The genes which are located in the identified defined chromosomal region (http://www.ensembl.org/) were analyzed for published data for wild-type and mutant function (http://www.informatics.jax.org/). The genes *Tomt* and *Chd2* were selected as candidate genes and used for sequence analysis (Table 3.7).

Table 3.7: Candidate genes on chromosome 7 and their primer sequences

Gene	Primer	Forward primer (5'-3')	Reverse primer (5'-3')	Expected PCR product size (bp)
Tomt	E2	cagacatgtttgtataagcgtgg	aggtaagcagtgggccatgc	472
	E3	agcacagcaggtttgattctg	gaaagaggcctggtctgagc	335
	E4	taaatcagccagatcccggtg	attctgaggtctgcttgaatgg	458
Chd2	P1	atgcgtggtggccagcagtag	catcatcctaggaagcagaaaac	711
	P2	gcgggtctgagagtgggag	gttgctgtaaggagtcttcac	600
	P3	aatggagatcctagcgatgac	tcaaagccacaaatctcggcc	547
	P4	ggaagatgaagccttgattgg	aagagtcatcattcttcaaccg	602
	P5	aatgcacttataacaacatatgag	tgctcctaattagagactgaag	601
	P6	cttccttaatatcgtgatggag	tcctgccagtggtatccatg	596
	P7	tgaatatttaccgcctggttac	atcagagtcgtccgtctcac	599
	P8	gcctcggattcgcagttccac	cagacgagaatcgtcctccac	598
	P9	tgagatgctgcataaatctatcc	atcaccacctttgaccttctc	607
	P10	aaccagtgagctctcggaagg	aatcccggcttgagcccgag	561
	P11	aagttatataagatggctcataag	gtctcggtcgctgttgtactg	474
	P12	aggaccaccactatggtgacc	caacagcagcagcatatccag	599

3.3.4 Line CLP001

3.3.4.1 Selection and analysis of the candidate gene

Linkage analysis and fine mapping was done earlier and independent of this study. The causative mutation was mapped to a defined region around 100 Mb on chromosome 11. In the present study, the gene *Gsdma3* (Table 3.8) was chosen for the sequence analysis as alopecia is described for *Gsdma3* mutant phenotype (http://www.informatics.jax.org).

Table 3.8: Primer sequences of the candidate gene *Gsdma3* (chr. 11, 98.4 Mb) of the line CLP001

Primer	Forward primer (5'-3')	Reverse primer (5'-3')	Expected PCR product size (bp)
E_1	tgatggatgcataaagcagc	tgaggcctactataagtcc	278
E_2	tctactctaggagtgaagcc	agccccacagcatccttcagag	368
E_3	agagctgggctctgaagg	agatacttccaatctctacactgc	477
E_4	cttggtgaagaaatgttgagg	tgtctctctccatccctgtc	226
E_5-6	ggttctcagagaattcacag	gtaagttataggagctgctgc	735
E_7	gaggctgtcttagcctatgg	accatcttcccggtcagtcc	178
E_8-9	tgaagcctacagaacctatg	acagaaagaaactcgtctgac	848
E_10-11	tgatcagagtgtgctaacac	tatcctcagactggaggctc	725

The position is given according to http://www.ensembl.org.

3.3.4.2 Genotyping of the animals of line CLP001

A novel missense point mutation in the gene *Gsdma3* was identified as causative mutation in the line CLP001. No restriction enzyme site was affected due to the mutation. Therefore, genotyping of the animals of line CLP001 was done using the amplification refractory mutation system PCR (ARMS-PCR; Newton et al. 1989). The concept of the ARMS-PCR is the selective amplification of the wild-type allele and the mutant allele by allele-specific internal primers in which the first nucleotide at the 3' end binds either the wild-type nucleotide or the mutant nucleotide. The insertion of an additional mismatch at the third nucleotide of the 3' end increases the primer specificity for the respective alleles. ARMS-PCR is preferentially performed in a single reaction (single tube allele-specific PCR). The allele-specific internal primers with their respective external primers amplify the specific PCR products. An additional common PCR product is also amplified because of the external primers (Zinovieva et al. 1996, and refs. therein). The allele-specific reverse primer INT1 (5' tttctccaaggattttactaaaa 3') and the forward primer EXT1 (5' caaatgagcatatgaatgaatag 3') for amplifying the wild-type allele, and the allele-specific forward primer INT2 (5' ctaactgaagaacaactgaataa 3') and the reverse primer EXT2 (5' atgttcccacaagttctagcg 3') for the amplification of the mutant allele, were designed (Fig. 3.4). The PCR conditions are given below.

Components of the PCR master mixture (1×)	Volume (µl)
Distilled H_2O	14.5
10× PCR buffer	2.5
dNTPs (2 mM)	2.5
$MgCl_2$ (25 mM)	2.5
Primer EXT1 (10 mM)	0.1
Primer EXT2 (10 mM)	0.1
Primer INT1 (10 mM)	0.2
Primer INT2 (10 mM)	0.2
Taq DNA Polymerase (10 U/µl)	0.3
Genomic DNA (100 ng/µl)	2.0

- 94˚C 5 min
- 94˚C 30 sec
- 49˚C 55 sec
- 72˚C 55 sec

35×

- 72˚C 20 min

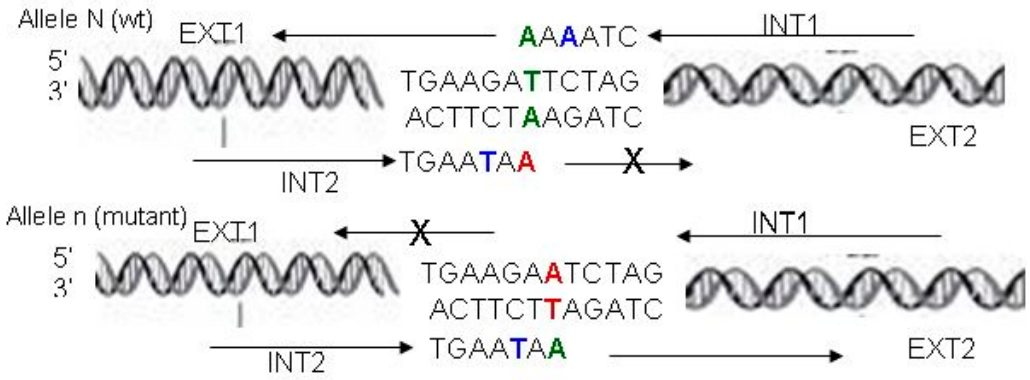

Fig. 3.4: Principle of the ARMS-PCR. Primer INT1 is specific for the wild-type allele, as the complementary base binds at the 3' end and allows the amplification of the wild-type allele. Primer INT2 is specific for the mutant allele and leads to the amplification of the mutant allele.

3.4 Molecular genetic methodologies

3.4.1 Genomic DNA isolation and analysis

Genomic DNA was isolated from mouse tail tips. Tail tips were incubated in 400

µl master mixture (375 µl cutting buffer (2.5 ml 1 M Tris/HCl pH 7.5, 5 ml 0.5 M EDTA pH 8.0, 1 ml 5 M NaCl, 250 µl 1 M DTT, 127 µl Spermidine and add distilled H_2O to make 50 ml), 20 µl 20% SDS, and 5 µl proteinase K) at 60˚C overnight. Digested samples were centrifuged at 13,000 rpm for 2 min and supernatant was transferred to a 1.5 ml tube (Eppendorf, Hamburg, Germany). DNA was precipitated by adding 400 µl 100% isopropanol. The DNA pellet was washed twice with 70% ethanol and air dried. Further on, the pellet was resolved in 10 mM Tris buffer pH 8.0 by incubating at 50˚C for 90 min. The genomic DNA concentration was determined using a Gene Quant Pro spectrophotometer (Amersham Biosciences, Freiburg, Germany) and the final concentration was adjusted to 100 ng/µl.

3.4.2 RNA isolation and analysis

RNA was isolated from kidney tissues using the TRIzol® reagent (Invitrogen, Darmstadt, Germany). Both kidneys of phenotypically mutant mice and wild-type mice from the lines HST014, HST011, and HST015 were dissected from 3-to 4-month-old mice and stored at -80˚C. One third of the kidney tissue was transferred into a 2 ml RNase-free reaction tube containing 1 ml TRIzol® Reagent. Subsequently, the tissue was homogenized using the Polytron PT 1200 E tissue homogenizer (Kinematica, Lucerne, Switzerland). The rotor was washed serially with distilled H_2O, 0.2 N NaOH, and again with distilled H_2O after each sample to avoid cross contamination. Homogenized tissues were incubated at room temperature for 10 min. 200 µl chloroform was added; the suspension was mixed and again incubated at room temperature for 10 min. The samples were centrifuged at 10,500 rpm at 4˚C for 15 min and the supernatant was transferred to a new tube. 500 µl isopropanol was added; the samples were mixed and again centrifuged at 10,500 rpm at 4˚C for 15 min. The RNA pellet was washed twice with 75% ethanol and air dried. The RNA pellet was resolved in RNase-free H_2O and incubated at 55˚C for 10 min. RNA concentration was determined using the Gene Quant Pro spectrophotometer (Amersham Biosciences, Freiburg, Germany), and the final concentration was adjusted to 500 ng/µl. RNA quality was checked by formaldehyde gel electrophoresis. A 1.5% agarose gel (Bio & Sell, Nürnberg, Germany) of volume 150 ml was prepared containing 6 ml 25× MOPS and 7.5 ml formaldehyde. RNA samples for loading were prepared by mixing 2 µl RNA (500 ng/µl), 5 µl denaturing buffer (750 µl formamide, 250 µl formaldehyde, 150 µl

25× MOPS, 116 µl 86% glycerol, 122 µl 0.25% bromphenol blue, 122 µl 0.25% xylene cyanol, 6 µl ethidium bromide), and 10 µl distilled H_2O. The samples were incubated at 55˚C for 10 min and subsequently put on ice for 2 min. RNA samples were loaded on the agarose gel and run at 120 volts for 50 min using 1× MOPS as running buffer. The signal quality of the 28S and 18S ribosomal RNA was visualised under UV light (Gel documentation system, Bio-Rad, California, USA).

3.4.3 First strand cDNA synthesis

Five µl RNA (500 ng/µl) samples were mixed with 15 µl DNA digest mixture (5 µl DNaseI (1 U/µl), 2 µl RNasin (100 U/µl), 2 µl 10× buffer, and 6 µl H_2O) and incubated at 37˚C for 60 min for removing contaminant DNA. Enzymes were inactivated at 75˚C for 10 min. Purification of the RNA samples was carried out by washing with 150 µl PCIA (25 ml Tris saturated phenol, 24 ml chloroform, and 1 ml isoamyl alcohol). The samples were mixed with 15 µl 3 M NaOAc and 400 µl ethanol and frozen at -80˚C for 30 min. The samples were centrifuged at 13,000 rpm at 4˚C for 30 min and the resulting pellet was washed with 75% ethanol. The pellet was air dried and dissolved in 20 µl RNase-free H_2O. First strand cDNA synthesis was carried out by incubating 11 µl DNaseI digested RNA mixed with 1 µl 50 µM cDNAvor (Fermentas, St. Leon-Rot, Germany) at 70˚C for 10 min, and subsequently on ice for 2 min. Further on, 7 µl reaction buffer (4 µl 5× buffer, 1 µl 10 mM dNTP and 2 µl 100 mM DTT) was added to the samples and incubated at 42˚C for 5 min. After that, 1 µl superscript reverse transcriptase (SuperScript® II RT; Invitrogen, Darmstadt, Germany) was added and further incubation was carried out for 60 min. Enzymes were inactivated at 75˚C for 15 min and samples were stored at -20˚C.

3.4.4 PCR

PCR was carried out with standard conditions (10× PCR buffer, 2 mM dNTPs, 25 mM $MgCl_2$, 10 mM primers and 5 U Taq DNA polymerase) using the GeneAmp® PCR System 9700 Thermocycler (Applied Biosystem, California, USA). PCR conditions were optimized for the product lengths and the annealing temperature of the primers. After carrying out the amplification of the templates, PCR products were mixed with 2.5 µl 6× loading dye (Fermentas, St. Leon-Rot, Germany) and loaded on a 0.7% agarose gel stained with ethidium bromide

(Merck, Darmstadt, Germany). The gel electrophoresis (Biorad PowerPac 300, Bio-Rad, California, USA) was carried out at 80 volts for 45 min. The pUC mix marker 8 (Fermentas, St. Leon-Rot, Germany) was used as molecular weight marker. PCR products were visualised under UV light.

3.4.5 Elution of the PCR products from the agarose gel

Gel elution of the PCR products was carried out using the QIAEX II gel extraction kit (QIAGEN, Hilden, Germany). PCR product bands were excised from the gel with the scalpel under the UV light. Three volumes QX 1 buffer and 10 µl QIAEX II buffer were added to the gel slice and incubated at 50˚C for 10 min for solubilizing the gel. Solubilized samples were centrifuged at 13,000 rpm for 30 sec. Further washing of the pellet was carried out with 500 µl QX 1 and subsequently with 500 µl PE buffer. The pellet was air dried and dissolved in 20 µl 10 mM Tris buffer pH 8.0 for eluting the PCR product. The samples were centrifuged at 13,000 rpm for 30 sec and the supernatant containing the PCR products was transferred in a new tube. The concentration of the gel eluted PCR products was determined using a 0.7% agarose gel with a1 kb molecular marker.

3.4.6 Sequencing of purified PCR products

Sequencing of purified PCR products was performed in collaboration with the sequencing service of the Helmholtz Zentrum München. The purified PCR products were diluted as per formula (DNA amount in ng = length in bp/100 × 1.5). Two µl of the purified PCR products was mixed with the sequencing master mixture (4 µl 5× sequencing buffer, 1 µl terminator big dye (Applied Biosystem, California, USA), 1 µl primer, and 2 µl H_2O). The sequencing PCR conditions are described below.

•	95˚C	1 min	
•	95˚C	5 sec	40×
•	50˚C	10 sec	
•	60˚C	4 min	

The sequencing samples were purified by ethanol precipitation. Samples were mixed with 2.5 µl 125 mM EDTA and 30 µl 100% ethanol and put on ice for 15 min. After that, samples were centrifuged at 13,000 rpm at 4˚C for 30 min. The pellet was washed with 70% ethanol and air dried. The pellet was dissolved in 30 µl distilled H_2O and transferred to the sequencing plate. Sequencing of the samples was carried in collaboration with the Helmholtz Zentrum München.

3.5 Phenotype analysis

3.5.1 Blood plasma analysis

Blood samples were collected by puncturing the retro orbital sinus under ether anaesthesia using Na-heparin treated glass capillaries (Hirschmann Laborgeraete, Eberstadt, Germany) in 1 ml lithium-heparin treated tubes (Kabe Labortechnik, Nümbrecht-Elsenroth, Germany) for the clinical chemical analysis of the blood plasma. Plasma samples were prepared by centrifuging the blood at 7,000 rpm for 10 min. Approximately 150 µl plasma was collected. The plasma parameters were measured in collaboration with the clinical chemical screen (Dr. B. Rathkolb, Chair for Molecular Animal Breeding and Biotechnology, LMU München) within the German Mouse Clinic (Prof. Dr. M. Hrabé de Angelis) of the Helmholtz Zentrum München (see Table 2.6). An Olympus AU400 autoanalyzer (Olympus, Hamburg, Germany) was used with the respective kits. Plasma creatinine was determined using two different methods, Jaffe's kinetic method (OSR6178, Beckman Coulter, California, USA; creatinine-J) and the enzymatic method (OSR61204, Beckman Coulter, California, USA; creatinine-E).

3.5.2 Metabolic cage analysis

Phenotypically mutant mice of the lines HST014 and HST011 exhibited increased plasma urea values as compared to wild-type littermate controls. Therefore, analysis of the renal function of phenotypically mutant mice of both lines was carried out using metabolic cages (Tecniplast, Hohenpeissenberg, Germany). At the age of 14 weeks, phenotypically mutant animals and wild-type littermate controls were separated in single metabolic cages for 1-2 h for 3 consecutive days for habituation providing crushed food and water ad libitum. On day 4 (0 h), the metabolic cages were cleaned. Body weight, food weight, and water weight were measured before the mice were put in the cages. Urine was collected for 24 h and stored at -20˚C, and parameters (body weight, 24 h water intake, 24 food intake,

24 h urine volume, and 24 h faeces excretion) were measured, and the mice were again provided with fresh water and food. After 24 h (48 h from 0 h), all parameters stated above were measured again, and the metabolic cages were cleaned. For the next 24 h, the mice were kept under water deprivation, and all parameters were measured. To avoid urine evaporation, 1 ml paraffin was added in the urine collecting tubes. Urine samples were stored at -80˚C for further analysis. The clinical chemical analysis of blood and urine was performed in collaboration with the clinical chemical screen (Dr. B. Rathkolb, Chair for Molecular Animal Breeding and Biotechnology, LMU München) within the German Mouse Clinic (Prof. Dr. M. Hrabé de Angelis) of the Helmholtz Zentrum München.

3.5.3 Morphological studies

Three-to four-month-old phenotypically mutant animals and sex-matched control animals of the lines HST014, HST011, and CLP001 were analyzed for growth parameters. Body weight was measured before euthanasia. Mice were euthanized by bleeding from the retro-orbital sinus under ether anaesthesia followed by cervical dislocation for the determination of the organ weights. Nose-to-rump length was measured in dorsal position. The organs were dissected, blotted on tissue paper to dry, and weighed to the nearest 0.1 mg. The organs kidney, liver, spleen, urinary bladder, testis/uterus, lung, heart and brain were weighed. Carcass weight was measured with skin and body fat. Tail samples were collected for genotype analysis and stored at -20˚C. For the lines HST014 and HST011, both kidneys were stored in 4% paraformaldehyde. Histopathological studies were carried out at the Institute of Veterinary Pathology (Prof. Dr. R. Wanke), LMU München. In line CLP001, the course of hair loss was also assessed.

3.5.4 SDS-PAGE analysis for the detection of albuminuria

Examination of albuminuria in mutant lines with renal disorder was carried out by the qualitative analysis of urinary proteins using SDS-polyacrylamide gel electrophoresis (SDS-PAGE). 20 µl spot urine samples or collected in the metabolic cage were taken from 3-to 4-month-old mice and stored at -20˚C. For SDS-PAGE analysis, urine samples were boiled for 10 min after 1:2 dilutions with sample buffer (62.5 mM Tris-HCl pH 6.8, 2% SDS, 25% glycerol, 0.01% bromophenol blue, 5% 2-mercaptoethanol). 10 µl of the samples were

electrophoresed (25 mM Tris, 200 mM glycine, 0.1% SDS) in a 10% Tris-HCl-polyacrylamide gel using the Bio-Rad Mini Protean II system (Bio-Rad Laboratories, California, USA). Protein bands were visualized by staining with Coomassie Brilliant Blue dye. The prestained SDS-PAGE Standard Broad (catalog: 161-0318; Bio-Rad Laboratories, California, USA) was used as molecular weight standard for the detected bands. Wild-type littermates were used as controls.

3.5.5 Generation of a congenic line

Congenic lines harbour the mutant allele on different genetic backgrounds and therefore, they are used to study the mutant phenotype of a given allele on different genetic backgrounds (Silver 1995). After carrying out 10 backcrosses, a congenic line harbouring more than 99% genome of the recipient strain is established. After identification of the causative mutations in the lines HST014 and HST011, establishment of congenic lines on the C57BL/6 and BALB/c inbred genetic backgrounds was started. Therefore heterozygous mutant mice on the C3H genetic background were bred to the recipient strain. The offspring were genotyped by PCR-RFLP, and heterozygous mutant mice were again bred with the recipient strain. In line HST015, phenotypically heterozygous mutant backcross mice were used for breeding.

3.6 Data presentation and statistical analysis of the data

Data are presented as means ± standard deviation (SD). Data charts were plotted with GraphPad Prism 5.0 (GraphPad Software, California USA). Data were analyzed using the Student's t-test and p values <0.05, <0.01 and <0.001 were considered to be significant.

IV. RESULTS

4.1 Line HST014

4.1.1 Linkage analysis of the causative mutation

After having carried out matings of phenotypically heterozygous mutant mice of line HST014 with the genetic background of the C3H inbred strain to inbred BALB/c mice for two generations, the complete penetrance of the mutant phenotype (increased plasma urea levels) was observed in the backcross animals in both sexes (Table 4.1) as expected by the rules of Mendelian inheritance. Linkage analysis was carried out with 113 SNPs using 45 phenotypically mutant G2 animals in collaboration with the Institute of Experimental Genetics (Prof. Dr. M. Hrabé de Angelis), Helmholtz Zentrum München (Table 4.2). The analysis showed that the mutant phenotype is linked to chromosome 18.

Table 4.1: Total number of backcross animals of line HST014

Generation	Total (m/f)	Phenotypically mutant (m/f)	Phenotypically wild-type (m/f)
G1	49 (28/21)	24 (14/10)	25 (14/11)
G1 (%)		49%	51%
G2	296 (152/144)	145 (73/72)	151 (79/72)
G2 (%)		49%	51%

m: males; f: females.

Table 4.2: Genetic mapping of phenotypically mutant G2 backcross animals of line HST014

Chromosome	rSNP	Locus (Mb)	Num_het	Num_wt	Failed	Total	χ^2 value	P value
1	rs13475764	23.5	28	16	1	45	N.S.	>0.01
1	rs13475818	38.1	27	14	4	45	N.S	>0.01
1	rs32716288	65.6	31	14	0	45	N.S.	>0.01
1	rs3678148	76.2	30	15	0	45	N.S	>0.01
1	rs13476065	116.7	26	19	0	45	N.S.	>0.01
1	rs30551255	126.9	21	18	6	45	N.S	>0.01
1	rs30942489	144.1	26	19	0	45	N.S.	>0.01
1	rs31593281	159.9	25	20	0	45	N.S	>0.01
1	rs33777727	172.7	25	20	0	45	N.S.	>0.01
1	rs13499691	195.1	29	16	0	45	N.S	>0.01
2	rs13476355	14.3	28	17	0	45	N.S.	>0.01
2	rs27120459	20.2	25	18	2	45	N.S	>0.01
2	rs13476434	37.0	27	16	2	45	N.S.	>0.01
2	rs13476490	50.7	23	19	3	45	N.S	>0.01

2	rs13476567	70.8	22	23	0	45	N.S.	>0.01
2	rs3679193	95.6	18	21	6	45	N.S	>0.01
2	rs27441842	114.2	21	24	0	45	N.S.	>0.01
2	rs27257388	129.5	21	24	0	45	N.S	>0.01
2	rs3696248	164.2	20	25	0	45	N.S.	>0.01
2	r13476909	169.3	19	26	0	45	N.S	>0.01
2	rs3691120	181.6	17	27	1	45	N.S.	>0.01
3	rs13477026	26.3	25	20	0	45	N.S	>0.01
3	rs3151604	36.9	22	22	1	45	N.S.	>0.01
3	rs3685081	52.2	25	20	0	45	N.S	>0.01
3	rs13477178	69.6	25	20	0	45	N.S.	>0.01
3	rs8259135	89.0	21	24	0	45	N.S	>0.01
3	rs13477302	103.3	21	24	0	45	N.S.	>0.01
3	rs13477321	109.0	25	20	0	45	N.S	>0.01
3	rs16799508	129.6	25	19	1	45	N.S.	>0.01
4	rs27731305	10.9	27	17	1	45	N.S	>0.01
4	rs27781503	35.2	27	18	0	45	N.S	>0.01
4	rs28056583	86.8	24	21	0	45	N.S.	>0.01
4	rs28307021	101.2	21	24	0	45	N.S	>0.01
4	rs13477989	133.1	20	25	0	45	N.S.	>0.01
4	rs3711383	141.9	18	26	1	45	N.S	>0.01
5	rs13481347	14.0	21	24	0	45	N.S.	>0.01
5	rs13478148	24.9	21	24	0	45	N.S	>0.01
5	rs13478204	41.0	20	24	1	45	N.S.	>0.01
5	rs13478263	55.6	21	24	0	45	N.S	>0.01
5	rs29635956	67.9	22	23	0	45	N.S.	>0.01
5	rs31585424	79.4	23	22	0	45	N.S	>0.01
5	rs31610566	81.9	19	20	6	45	N.S.	>0.01
5	rs13478429	103.3	25	20	0	45	N.S	>0.01
5	rs32067291	111.7	24	21	0	45	N.S.	>0.01
5	rs13478514	127.2	23	22	0	45	N.S	>0.01
6	rs13478670	26.1	24	20	1	45	N.S.	>0.01
6	rs13478756	52.7	23	20	0	45	N.S	>0.01
6	rs13478816	72.3	22	23	0	45	N.S.	>0.01
6	rs13478872	85.9	21	20	4	45	N.S	>0.01
6	rs13478987	115.2	25	20	0	45	N.S.	>0.01
6	rs16815348	137.6	27	18	0	45	N.S	>0.01
6	rs13479084	144.5	25	19	1	45	N.S.	>0.01
7	rs13479164	28.1	19	26	0	45	N.S	>0.01
7	rs13479256	60.7	14	31	0	45	N.S.	>0.01
7	rs16805799	73.2	13	31	1	45	N.S	>0.01
7	rs4226783	100.1	15	30	0	45	N.S.	>0.01
7	rs13479476	124.0	19	26	0	45	N.S	>0.01
8	rs13479604	9.8	21	24	0	45	N.S.	>0.01
8	rs13479662	28.1	20	22	3	45	N.S	>0.01
8	rs13479741	48.2	26	19	0	45	N.S.	>0.01
8	rs13479814	70.9	24	21	0	45	N.S	>0.01
8	rs13479998	116.7	20	25	0	45	N.S.	>0.01
9	rs13480217	57.7	26	16	3	45	N.S	>0.01
9	rs13480245	65.0	26	19	0	45	N.S.	>0.01
9	rs3673055	96.2	44	1	0	45	N.S	>0.01
10	rs13480484	8.2	19	26	0	45	N.S.	>0.01
10	rs13480541	22.6	18	27	0	45	N.S	>0.01
10	rs13480638	68.9	26	19	0	45	N.S.	>0.01
10	rs8258500	99.5	26	19	0	45	N.S	>0.01
10	rs13480784	117.8	26	17	2	45	N.S.	>0.01
11	rs13480851	7.1	20	22	3	45	N.S	>0.01
11	rs13480905	21.6	24	21	0	45	N.S.	>0.01
11	rs26822879	32.3	24	21	0	45	N.S	>0.01
11	rs26982471	53.9	22	23	0	45	N.S.	>0.01
11	rs13481061	62.8	22	22	1	45	N.S	>0.01
11	rs13481127	83.2	19	26	0	45	N.S.	>0.01
11	rs27041242	98.6	21	24	0	45	N.S	>0.01
11	rs27000576	114.3	20	23	2	45	N.S.	>0.01
12	rs13481307	13.2	16	29	0	45	N.S	>0.01
12	rs13481351	25.7	0	44	1	45	N.S.	>0.01
12	rs8259450	75.0	17	23	5	45	N.S	>0.01
12	rs6194112	83.4	22	22	1	45	N.S.	>0.01
12	rs13481604	99.3	22	22	1	45	N.S	>0.01
12	rs13459138	114.1	24	21	0	45	N.S.	>0.01
13	rs6345767	19.5	20	25	0	45	N.S	>0.01
13	rs13481783	42.9	25	20	0	45	N.S.	>0.01
13	rs13481863	69.3	27	18	0	45	N.S	>0.01
13	rs13481910	83.1	26	19	0	45	N.S.	>0.01
13	rs29566800	97.2	26	18	1	45	N.S	>0.01
13	rs30511458	111.2	27	18	0	45	N.S.	>0.01
14	rs30406796	22.9	17	28	0	45	N.S	>0.01
14	rs30895903	59.6	25	20	0	45	N.S.	>0.01

14	rs30865397	74.0	26	19	0	45	N.S	>0.01
15	rs13482484	25.2	19	26	0	45	N.S.	>0.01
15	rs13482528	38.8	20	25	0	45	N.S	>0.01
15	rs13482574	50.4	19	25	1	45	N.S.	>0.01
15	rs16820334	85.6	23	22	0	45	N.S	>0.01
15	rs16804751	97.7	25	17	3	45	N.S.	>0.01
16	rs4161352	10.8	16	29	0	45	N.S	>0.01
16	rs4165602	27.4	16	28	1	45	N.S.	>0.01
16	rs4170048	32.1	17	26	2	45	N.S	>0.01
17	rs33418817	11.5	27	17	1	45	N.S.	>0.01
17	rs33259283	28.1	27	18	0	45	N.S	>0.01
17	rs33428427	40.9	27	18	0	45	N.S.	>0.01
17	rs13483097	72.7	24	21	0	45	N.S	>0.01
17	rs13483140	85.4	21	24	0	45	N.S.	>0.01
18	rs29827614	25.5	38	7	0	45	21.3	<0.0001
18	rs29823686	38.2	37	8	0	45	18.6	<0.001
18	rs13483427	70.6	31	14	0	45	6.42	<0.01
19	rs6247194	13.9	26	19	0	45	N.S	>0.01
19	rs13483576	26.0	22	23	0	45	N.S.	>0.01
19	rs4232188	43.5	21	24	0	45	N.S	>0.01
19	rs6339594	56.3	19	26	0	45	N.S.	>0.01

Num_het: number of mice with heterozygous C3H/BALB/c genotype; Num_wt: number of mice with homozygous wild-type BALB/c/BALB/c genotype; N.S: non-significant. SNPs refer to the NCBI database (http://www.ncbi.nlm.nih.gov/)

Further fine mapping of the causative mutation was carried out using SNP markers (rs52303422: 9.5 Mb; rs52534573: 11.2 Mb; rs46961948: 11.4 Mb; rs52391350: 12.9 Mb; rs52376653: 13.6 Mb; rs31073798: 14.3 Mb; rs31158307: 14.6 Mb; rs31155567: 14.6 Mb; rs31158391: 14.6 Mb; rs31243033: 17.0 Mb; rs31247952: 17.0 Mb; rs31220775: 17.5 Mb; rs51268966: 23.4 Mb; rs52585890: 26.1 Mb) and the microsatellite markers D18Mit68 (C3H: 113 bp; BALB/c: 95 bp) (Fig. 4.1) and D18Mit70 (C3H: 124 bp; BALB/c: 108 bp) (Table 4.3). Although the SNPs were published to detect polymorphic alleles in C3H and BALB/c mice, in this study no allelic difference was seen in C3H and BALB/c mice. From the polymorphic markers used for chromosome 18, rs29827614 and D18Mit68 showed the highest χ^2 value (Tables 4.2 and 4.3).

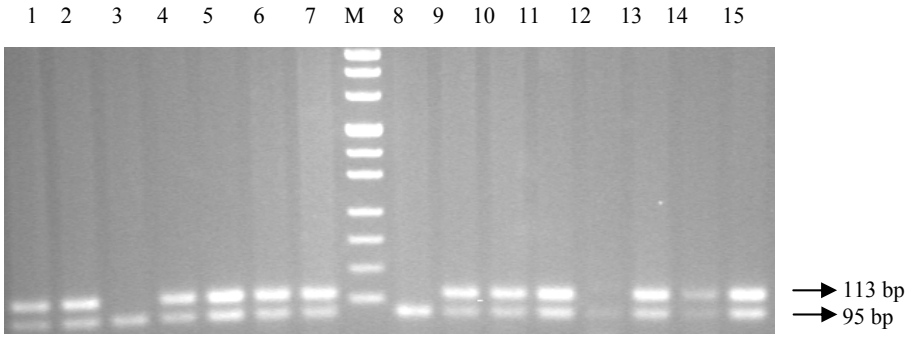

Fig. 4.1: Electrophoretic pattern of the C3H (113 bp) and BALB/c (95 bp) allele amplified using polymorphic marker D18Mit68. Lanes 1-15 are backcross animals. Lanes 3, 8, and 12 show animals which are homozygous for the BALB/c allele, the other mice show a heterozygous C3H/BALB/c genotype. Lane M is the pUC 8 marker.

Table 4.3: Fine mapping analysis of chromosome 18 in line HST014

Marker	Locus (Mb)	Num_het	Num_wt	Failed	Total	χ^2 value
D18Mit68	21.5	38	7	0	45	21.4
D18Mit70	35.0	35	10	0	45	12.3

Num_het: number of mice with heterozygous C3H/BALB/c genotype; Num_wt: number of mice with homozygous wild-type BALB/c/BALB/c genotype.

4.1.2 Identification of the causative mutation

The three candidate genes *Aqp4, Mep1b,* and *Kctd1* were chosen for sequence analysis (Table 4.4). Two phenotypically heterozygous mutant mice and two wild-type mice on the C3H genetic background were used. Genomic DNA and RNA were prepared from tails and kidneys, respectively, and cDNA was prepared from RNA to use as template in the PCR reaction. For *Aqp4*, exonic sequences as well as 3' UTR and 5' UTR regions were sequenced, whereas for *Kctd1* and *Mep1b*, cDNA transcripts were sequenced (Fig. 4.2).

Table 4.4: Candidate genes in line HST014 and their published phenotype data

Gene	Position (Mb)	Exons	Polypeptide length (aa)	Mutant phenotype (http://www.informatics.jax.org/)
Aqp4	15.5	5	323	Homozygous knockout mice exhibited decreased urine osmolality associated with reduced water permeability in inner medullary collecting ducts, increased survival rates and reduced brain edema after acute water intoxication and ischemic stroke, as well as significant hearing impairment (Kitaura et al. 2009, Ma et al. 1997).
Mep1b	21.2	15	704	Homozygous knockout mice showed 50% prenatal lethality; survivors had reduced birth weight and showed altered renal gene expression (Norman et al. 2003).
Kctd1	15.1	5	265	No mutant phenotype is published (http://www.informatics.jax.org/).

A)

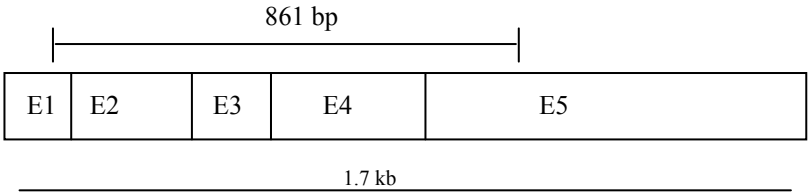

B)

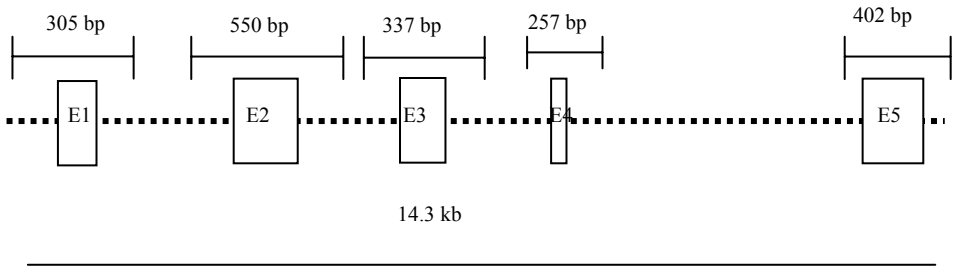

C)

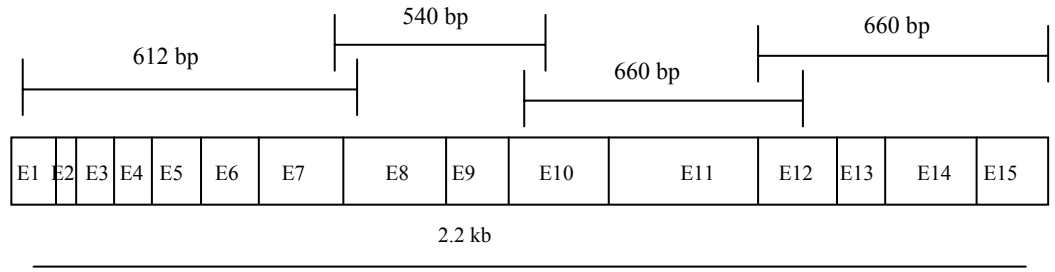

Fig. 4.2: Position and length of PCR products amplified on the candidate genes of line HST014. A) *Kctd1* cDNA. B) *Aqp4* gene. C) *Mep1b* cDNA. E: exon

Sequence analysis of *Aqp4* and *Mep1b* resulted in identical sequences in wild-type and phenotypically heterozygous mutant animals, which were also identical to the published sequences in the Ensembl database (http://www.ensembl.org/). Sequence analysis of the *Kctd1* cDNA transcript revealed a point mutation resulting in a T→A transversion at nt 80 (ENSMUST00000025992, as of March 2011), which leads to the amino acid exchange from isoleucine to asparagine at aa position 27 (Fig. 4.3). The name of line HST014 was designated as *Kctd1*^{I27N}.

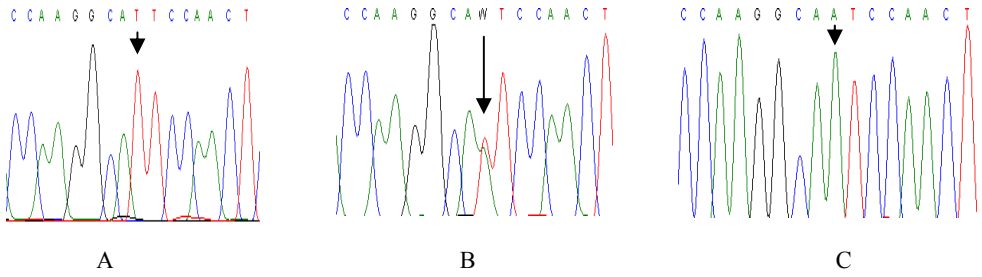

Fig. 4.3: Electropherogram of the sequence of the gene *Kctd1*. Sequence from A) a phenotypically wild-type mouse, B) a phenotypically heterozygous mutant mouse, and C) a homozygous mutant fetus (see 4.1.4). The arrow shows the position of the T to A transversion which leads to the amino acid exchange from isoleucine to asparagine at aa position 27.

4.1.3 Allelic differentiation of the *Kctd1*^{I27N} mutation by PCR-RFLP

The point mutation abolished the restriction site for the enzyme *Bsm*I. Thus, PCR products (520 bp) encompassing the mutation site amplified from the mutant allele remain unrestricted, whereas PCR products of the wild-type allele were restricted in two fragments (312 bp and 208 bp). Restricted fragments were analyzed on a 2% agarose gel (Fig. 4.4).

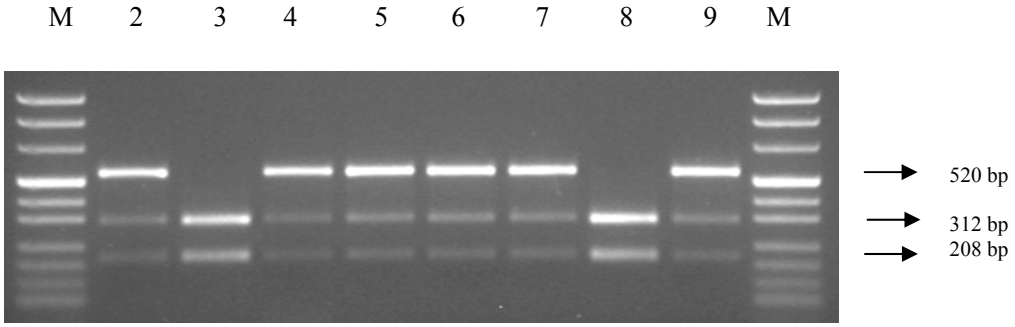

Fig. 4.4: Electrophoretic pattern of the PCR–RFLP in the line *Kctd1*^{I27N}. Lanes 2, 4, 5, 6, 7, and 9: phenotypically heterozygous mutant mice; lanes 3 and 8: phenotypically wild-type mice. Lane M is the pUC 8 marker.

4.1.4 Analysis of *Kctd1*^{I27N} homozygous mutant mice

To assess the consequences of homozygosity of the mutation, *Kctd1*^{I27N} heterozygous mutant mice were intercrossed to generate homozygous mutant animals. At three months of age, 47 offspring from four mating pairs were analyzed (Table 4.5). We did not find any homozygous mutant mice whereas heterozygous mutant mice (n = 31) and wild-type mice (n = 16) appeared in a 2:1 ratio as expected. Next, we carried out timed matings of heterozygous mutant mice to harvest fetuses at day E17.5 for the analysis. A total of 21 fetuses were

harvested from three matings and all appeared grossly normal in their morphology. Homozygous mutant, heterozygous mutant, and wild-type animals were observed according to the Mendelian ratio in the genotype analysis (Table 4.5, Fig. 4.5). Hence, homozygous mutant mice showed early postnatal mortality.

Table 4.5: Number of offspring produced from matings of *Kctd1*^{I27N} heterozygous mutant mice of line *Kctd1*^{I27N}

Time of analysis	Total	Genotype		
		Homozygous mutant	Heterozygous mutant	Wild-type
3 months	47	0 (0%)	31 (66%)	16 (34%)
Fetal (E17.5)	21	5 (24%)	10 (48%)	6 (28%)

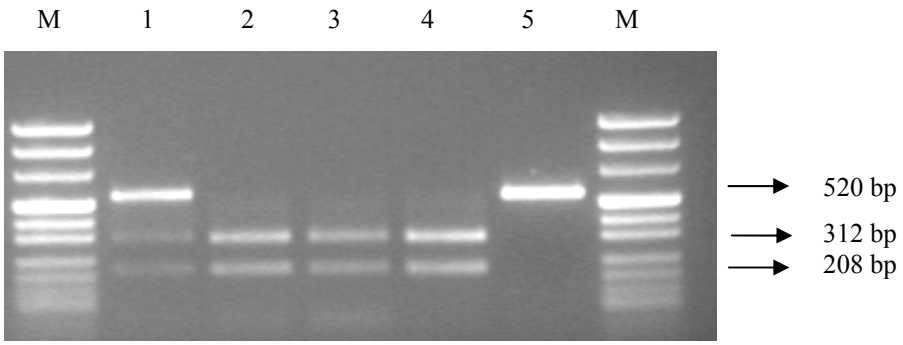

Fig. 4.5: Electrophoretic pattern of the PCR-RFLP in the line *Kctd1*^{I27N} using fetuses (E17.5). Lane 1: heterozygous mutant; lanes 2, 3, 4: wild-type; and lane 5: homozygous mutant. Lane M is the pUC 8 marker.

4.1.5 Clinical chemical analysis of *Kctd1*^{I27N} heterozygous mutant mice

The mutant line HST014 was established due to increased plasma urea levels in heterozygous mutant mice. Therefore, heterozygous mutant mice on the C3H genetic background were mated with wild-type C3H mice and heterozygous mutant offspring were used for clinical chemical analysis compared to wild-type littermates. At the age of three months, heterozygous mutant animals of both genders showed significantly increased levels of urea, creatinine-J, potassium, α-amylase, and lipase in the blood plasma. Heterozygous mutant females showed hypercalcemia (Table 4.6). Plasma urea was already found to be increased at 6 and 9 weeks of age in both sexes (Fig. 4.6).

Table 4.6: Plasma data of 12-to 14-week-old mice of line *Kctd1*^{I27N}

	Male			Female		
	Het (n = 16)	Wt (n = 15)	t-test (het vs. wt)	Het (n = 10)	Wt (n = 13)	t-test (het vs. wt)
Na (mmol/l)	148 ± 4	147 ± 3	n.s.	148 ± 4	146 ± 6	n.s.
K (mmol/l)	4.9 ± 0.4	4.4 ± 0.2	p<0.001	4.9 ± 0.4	4.4 ± 0.4	p<0.01
Ca (mmol/l)	2.3 ± 0.1	2.2 ± 0.1	n.s.	2.4 ± 0.1	2.3 ± 0.1	p<0.001
Cl (mmol/l)	112 ± 5	112 ± 2	n.s.	114 ± 4	113 ± 6	n.s.
Pi (mmol/l)	1.6 ± 0.2	1.5 ± 0.3	n.s.	1.8 ± 0.4	1.8 ± 0.3	n.s.
Total protein (g/dl)	5.2 ± 0.2	5.1 ± 0.3	n.s.	5.2 ± 0.2	5.2 ± 0.3	n.s.
Creatinine-J (µmol/l)	29 ± 3	27 ± 2	p<0.05	33 ± 5	30 ± 2	p<0.05
Creatinine-E (µmol/l)	13 ± 3	12 ± 5	n.s.	14 ± 4	12 ± 4	n.s.
Urea (mg/dl)	85 ± 12	50 ± 6	p<0.001	88 ± 13	47 ± 8	p<0.001
Uric acid (mg/dl)	5.4 ± 1	4.9 ± 1	n.s.	4.8 ± 1.3	4.4 ± 1.0	n.s.
Cholesterol (mg/dl)	127 ± 10	125 ± 8	n.s.	109 ± 9	107 ± 7	n.s.
Triglycerides (mg/dl)	253 ± 66	233 ± 69	n.s.	222 ± 53	187 ± 52	n.s.
CK (U/l)	292 ± 314	151 ± 91	n.s.	194 ± 213	232 ± 220	n.s.
ALT (U/l)	93 ± 141	50 ± 23	n.s.	41 ± 13	54 ± 46	n.s.
AST (U/l)	66 ± 23	63 ± 13	n.s.	59 ± 19	66 ± 21	n.s.
AP (U/l)	139 ± 10	135 ± 15	n.s.	167 ± 10	163 ± 18	n.s.
Amylase (U/l)	2322 ± 203	2152 ± 124	p<0.01	2207 ± 295	1812 ± 88	p<0.001
Glucose (mg/dl)	108 ± 32	98 ± 27	n.s.	122 ± 46	124 ± 53	n.s.
Albumin (g/dl)	2.4 ± 0.1	2.4 ± 0.1	n.s.	2.6 ± 0.1	2.7 ± 0.1	n.s.
Ferritin (µg/l)	23 ± 8	20 ± 4	n.s.	24 ± 5	24 ± 5	n.s.
Transferrin (mg/dl)	141 ± 13	140 ± 12	n.s.	144 ± 15	141 ± 14	n.s.
Lipase (U/l)	54 ± 7	43 ± 9	p<0.001	61 ± 4	46 ± 8	p<0.01
C-reactive protein (mg/l)	1.4 ± 0.8	1.4 ± 0.6	n.s.	1.1 ± 0.4	1.5 ± 1.1	n.s.
Lactate (mmol/l)	11 ± 2	11 ± 1	n.s.	12 ± 3	12 ± 2	n.s.

Data represents the means ± SD; SD: standard deviation. Student's t-test, p<0.05, p<0.01, and p<0.001.
n: number of the animals analyzed. ns: non-significant. Het: heterozygous mutant mice; Wt: wild-type mice.
CK: creatine kinase; ALT: alanine aminotransferase; AST: aspartate aminotransferase; AP: alkaline phosphatase.

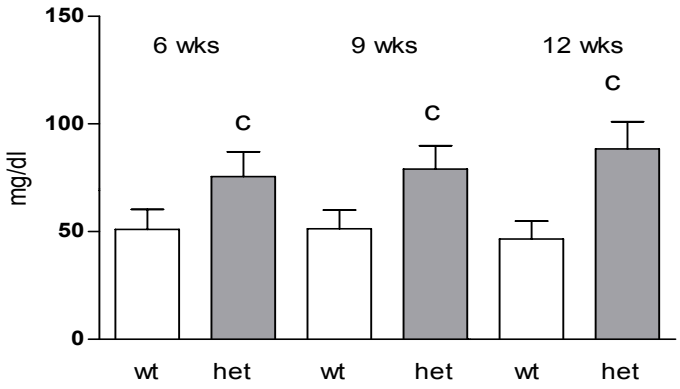

Fig: 4.6: Plasma urea level in females at different ages. wt: wild-type; het: heterozygous mutant; wks: weeks. [C]Student's t-test vs wild-type: $p<0.001$. Data represents mean ± SD. 10-26 mice are analyzed per genotype.

4.1.6 Urine analysis of *Kctd1*^{I27N} heterozygous mutant mice

Metabolic cage analysis was carried out with heterozygous mutant mice and age-matched wild-type littermate controls at the age of 14-15 weeks. Heterozygous mutant males showed a significant increase in water intake and mild polyuria as well as distinct hypercalciuria. Heterozygous mutant females also showed distinct hypercalciuria as well as a moderate increase in water intake and urine volume. Creatinine excretion measured with the enzymatic method (creatinine-E) was significantly reduced in heterozygous mutant females. After 24 h water deprivation, heterozygous mutant mice showed no significant differences (Table 4.7).

Table 4.7: Urine data of 14-to 15-week-old mice of line *Kctd1*^{I27N} under basal conditions and after deprivation of drinking water for 24 h in metabolic cages

	Male			Female		
	Het (n = 11)	Wt (n = 11)	t-test (het vs. wt)	Het (n = 11)	Wt (n = 11)	t-test (het vs. wt)
Body weight (g)	26.6 ± 2.4	26.8 ± 2.2	n.s.	23.0 ± 1.0	24.4 ± 1.8	p<0.05
Drinking water ad libitum						
Water intake (ml/day)	7.0 ± 2.2	5.5 ± 0.8	p<0.05	6.4 ± 2.1	5.7 ± 1.0	n.s.
Food intake (g/day)	4.0 ± 1.0	4.7 ± 0.7	n.s.	5.5 ± 0.5	5.4 ± 0.6	n.s.
Feaces exretion (g/day)	1.8 ± 0.4	2.0 ± 0.3	n.s.	2.2 ± 0.5	2.2 ± 0.4	n.s.
Urine volume (ml/day)	1.9 ± 0.7	1.3 ± 0.6	p<0.05	1.7 ± 1.4	1.3 ± 0.4	n.s.
Na (µmol/day)	259 ± 53	260 ± 99	n.s.	292 ± 72	275 ± 76	n.s.
K (µmol/day)	704 ± 127	707 ± 256	n.s.	744 ± 181	794 ± 212	n.s.
Ca (µmol/day)	7.0 ± 2.5	2.8 ± 0.8	p<0.001	8.7 ± 3.0	3.3 ± 0.9	p<0.001
Cl (µmol/day)	450 ± 90	471 ± 148	n.s.	558 ± 111	556 ± 119	n.s.
Mg (µmol/day)	34 ± 8	29 ± 10	n.s.	39 ± 10	34 ± 11	n.s.
Pi (µmol/day)	183 ± 90	118 ± 58	n.s.	162 ± 64	152 ± 76	n.s.
Creatinine-J (µmol/day)	6.2 ± 1.5	5.8 ± 2.0	n.s.	5.1 ± 1.3	5.6 ± 1.4	n.s.
Creatinine-E (µmol/day)	3.5 ± 0.9	3.4 ± 1.2	n.s.	2.6 ± 0.6	3.3 ± 0.7	p<0.05
Urea (mmol/day)	2.3 ± 0.4	2.2 ± 0.7	n.s.	2.5 ± 0.6	2.7 ± 0.6	n.s.
Uric acid (nmol/day)	750 ± 283	940 ± 338	n.s.	881 ± 170	1144 ± 404	n.s.
Glucose (µmol/day)	3.6 ± 1.2	3.2 ± 1.2	n.s.	5.0 ± 3.0	4.3 ± 1.1	n.s.
Total protein (mg/day)	15 ± 5	14 ± 8	n.s.	4.4 ± 1.6	5.3 ± 1.8	n.s.
Albumin (nmol/day)	2.5 ± 0.7	3.0 ± 1.7	n.s.	3.0 ± 1.2	2.8 ± 0.9	n.s.
Deprivation of drinking water for 24 h						
Loss of body weight (%)	10.0 ± 1.8	9.5 ± 1.5	n.s.	12.4 ± 2.7	10.6 ± 1.7	n.s.
Food intake (g/day)	3.4 ± 1.0	3.0 ± 0.5	n.s.	3.1 ± 0.9	3.4 ± 0.3	n.s.
Urine volume (ml/day)	0.7 ± 0.4	0.7 ± 0.3	n.s.	0.5 ± 0.4	0.4 ± 0.2	n.s.
Feaces exretion (g/day)	1.0 ± 0.2	0.9 ± 0.2	n.s.	1.0 ± 0.1	1.0 ± 0.3	n.s.

Values are means ± SD. SD: standard deviation. Student's t-test, p<0.05, p<0.01, p<0.001.
ns: non-significant; het: heterozygous mutant; wt: wild-type. n: animals analyzed.
Age of mice analyzed: 14–15 weeks.

4.1.7 Morphological analysis of *Kctd1*^{I27N} heterozygous mutant mice

Morphological analysis including determination of body and organ weights was performed on four month old *Kctd1*^{I27N} heterozygous mutants of both sexes and wild-type littermates as controls. Heterozygous mutants of both sexes were viable and fertile, and no grossly apparent phenotype was observed. Heterozygous mutant females showed a decreased body weight and kidney weight. However, the relative kidney weight was unaltered. Further, the relative brain weight was increased in the heterozygous mutant females. The absolute (Table 4.8) and relative weights of the other organs (data not shown) of heterozygous mutants of both genders were not significantly altered. Kidneys from heterozygous mutants were light microscopically indistinguishable from those of wild-type littermates (not shown).

Table 4.8: Absolute body weight and organ weights of 4-month-old mice of line *Kctd1*^{I27N}

	Male			Female		
			t-test			t-test
	Het (n = 8)	Wt (n = 8)	(het vs. wt)	Het (n = 9)	Wt (n = 9)	(het vs. wt)
Body weight (g)	28.2 ± 2.4	27.3 ± 1.9	n.s.	23.6 ± 0.6	25.4 ± 1.5	p<0.01
Nose-to-rump length (cm)	9.4 ± 0.2	9.4 ± 0.2	n.s.	9.2 ± 0.4	9.2 ± 0.4	n.s.
Brain (mg)	457 ± 13	449 ± 20	n.s.	476 ± 23[a]	459 ± 21	n.s.
Liver (g)	1.5 ± 0.2	1.5 ± 0.1	n.s.	1.2 ± 0.1	1.3 ± 0.1	n.s.
Kidney (mg)	522 ± 60	508 ± 60	n.s.	314 ± 12	348 ± 18	p<0.001[b]
Thymus (mg)	8.2 ± 3.2	7.5 ± 1.9	n.s.	5.0 ± 1.1	4.9 ± 1.6	n.s.
Adrenal gland (mg)	8.7 ± 1.2	8.5 ± 3.4	n.s.	11.0 ± 2.0	10.3 ± 2.8	n.s.
Lung (mg)	182 ± 18	168 ± 19	n.s.	163 ± 11	172 ± 11	n.s.
Heart (mg)	122 ± 8	121 ± 18	n.s.	117 ± 11	112 ± 8	n.s.
Testis (mg)	175 ± 18	169 ± 11	n.s.			
Uterus (mg)				136 ± 23	144 ± 33	n.s.
Urinary bladder (mg)	28.5 ± 4.7	34.4 ± 16.0	n.s.	21.8 ± 2.9	22.2 ± 3.8	n.s.
Spleen (mg)	78 ± 9	79 ± 8	n.s.	114 ± 35	118 ± 18	n.s.
Carcass (g)	20 ± 2.3	19 ± 1.5	n.s.	17 ± 0.4	18 ± 1.3	n.s.

Data represent means ± SD. SD: standard deviation. Student's t-test, $p<0.05$, $p<0.01$, and $p<0.001$.
Het: heterozygous mutant; wt: wild-type; n.s: non-significant.; n: animals analyzed.
a: the relative brain weight is significantly increased in heterozygous mutant females ($p<0.05$).
b: the relative kidney weight is unaltered.

4.2 Line HST011

4.2.1 Re-analysis of line HST011 showed erroneous linkage analysis

Line HST011 was established in the screen for recessive mutations within the Munich ENU mouse mutagenesis project. Phenotypically homozygous mutant animals showed increased plasma urea levels with small kidneys. Linkage analysis was already carried out previously, independent from this study (see 3.1.2). Genetic analysis revealed linkage of the causative mutation to chromosome 7 ($\chi^2 = 15.5$) and chromosome 1 ($\chi^2 = 9.9$; Table 4.9).

Table 4.9: Data from the previous linkage analysis of line HST011 carried out independently from this study

Chromosome	rSNP	Locus (Mb)	Num_hom	Num_het	Num_wt	Total	χ^2 value	P value
1	rs13475764	23.5	21	16	10	47	9.9	>0.001
1	rs13475818	38.1	21	16	10	47	9.9	>0.001
7	rs4226783	100.0	20	23	4	47	10.9	>0.001
7	rs13479476	124.0	22	22	3	47	15.5	>0.0001

Num_hom: number of mice with homozygous C3H/C3H genotype; num_het: number of mice with heterozygous C3H/BALB/c genotype; num_wt: number of mice with homozygous BALB/c/BALB/c genotype.

Based on these results, analysis of line HST011 in this study started with the fine mapping of the causative mutation. As the highest linkage was revealed for chromosome 7, additional polymorphic markers were examined for the defined region (Table 4.10). However, no clear linkage of the causative mutation was observed.

Table 4.10: Polymorphic markers used for fine mapping in line HST011

Marker	Locus (Mb)	Num_hom	Num_het	Num_wt	Failed	Total
D7Mit90	87.5	11	28	5	0	44
D7Mit323	108.0	18	18	8	0	44
D7Mit68	132.4	22	19	3	0	44
D7Mit259	151.9	16	21	7	0	44

Num_hom: number of mice with homozygous C3H/C3H genotype; num_het: number of mice with heterozygous C3H/BALB/c genotype; num_wt: number of mice with homozygous BALB/c/BALB/c genotype.

Simultaneously, based on mutant phenotype and linked chromosomal region, three candidate genes were selected for sequence analysis (Table 4.11). Two phenotypically homozygous mutant animals and two wild-type animals on the C3H genetic background were used. Genomic DNA and RNA were prepared from tail and kidney, respectively, and cDNA was prepared from RNA for cDNA sequencing. For *Umod*, cDNA and 5' UTR were sequenced, and for *Aqp11* and *Wnt11* exonic sequences were analyzed. Sequences of all three genes were identical in phenotypically mutant animals and wild-type animals.

Table 4.11: Candidate genes for line HST011 on chromosome 7

Gene	Position (Mb)	Exons	Polypeptide length (aa)	Mutant phenotype (http://www.informatics.jax.org/)
Umod	126.6	11	642	Knock-out homozygous mutant mice exhibited increased susceptibility to bladder infection and abnormal kidney function. ENU-induced homozygous mutants exhibited abnormal kidney function and decreased metabolic rate, body weight, and bone density (Bates et al. 2004, Kemter et al. 2009, Mo et al. 2004).
Wnt11	105.9	7	354	Knock-out homozygous mutants showed high embryonic lethality, and born mutants died within the first 2 days. The kidneys were small and exhibited delayed development (Majumdar et al. 2003).
Aqp11	104.8	3	271	Homozygous mutant mice displayed premature death, kidney failure, and polycystic kidneys with cysts originating from the proximal tubules, and growth retardation (Morishita et al. 2005).

After that, the breeding data of the backcross animals used in the previous linkage analysis was re-analyzed. It was revealed that more phenotypically mutant G2 animals appeared than expected according to the Mendelian ratio (Table 4.12). It was assumed that an erroneous mating during the backcross breeding might have been occurred. In the mouse facility, additional ENU-induced mutant lines exhibiting increased plasma urea levels were maintained including the *Umod*^{C93F} mutant line with the causative mutation found on chromosome 7 (Prückl 2011). Therefore, the G2 backcross animals were genotyped for this point mutation by

using allele-specific PCR strategy. Some backcross animals were found with the *Umod*^{C93F} mutant allele (Fig 4.7). This clearly showed that a mutant mouse from the *Umod*^{C93F} mutant line was erroneously used for the backcross mating of line HST011.

The subsequent analysis of the original line HST011 on the C3H genetic background did not reveal the *Umod*^{C93F} mutant allele in these mice.

Table 4.12: Observed phenotype of the 276 G2 backcross animals of line HST011

	Phenotypically homozygous mutant	Phenotypically wild-type (heterozygous mutant and wild-type)
Number of G2 backcross animals (%)	121 (44%)	155 (56%)
Expected phenotype ratio	25%	75%

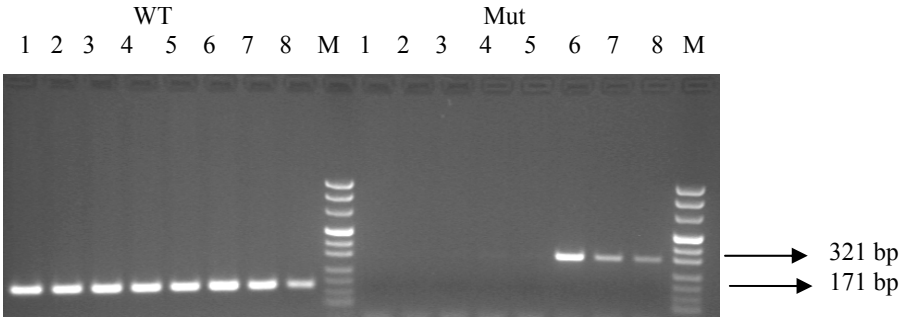

Fig. 4.7: Allele-specific PCR for the *Umod*^{C93F} mutation. Samples from eight G2 backcross animals of line HST011 are shown. Lanes 1-8 WT show the result for the wild-type allele (171 bp) whereas lanes 1-8 Mut show the result for the mutant allele (321 bp). The samples 1-5 are homozygous wild-type and samples 6, 7 and 8 are heterozygous for the *Umod*^{C93F} mutation. Lane M is the pUC8 marker.

4.2.2 Re-mapping of the causative mutation to chromosome 1

The phenotypically mutant G2 animals were screened for the *Umod*^{C93F} mutation. Animals carrying the mutant allele were excluded from the analysis. Linkage analysis with this reduced pool of phenotypically mutant G2 animals showed a strong linkage of the causative mutation to a single locus on chromosome 1 (analogous to the data shown in Table 4.12). Therefore, fine mapping was carried out with phenotypically mutant G2 animals using additional polymorphic markers for chromosome 1 (Table 4.13).

Table 4.13: Polymorphic markers of chromosome 1 used for fine mapping

Marker	Locus (Mb)	Num_hom	Num_het	Num_wt	Failed	Total
D1Mit64	12.8	14	8	0	0	22
D1Mit432	24.3	12	4	4	4	24
D1Mit411	33.2	10	6	8	0	24
D1Mit212	40.0	17	4	1	0	22
D1Mit156	65.8	9	13	6	0	28
D1Mit415	88.3	9	12	6	1	28

Num_hom: number of mice with homozygous C3H/C3H genotype; num_het: number of mice with heterozygous C3H/BALB/c genotype; num_wt: number of mice with homozygous BALB/c/BALB/c genotype.

Phenotypically homozygous mutant G2 animals should have the homozygous C3H/C3H genotype at the chromosomal site of the causative mutation. The highest number of animals having a homozygous C3H/C3H genotype were found at 40.0 Mb, and it was revealed with marker D1Mit212 (Fig. 4.8).

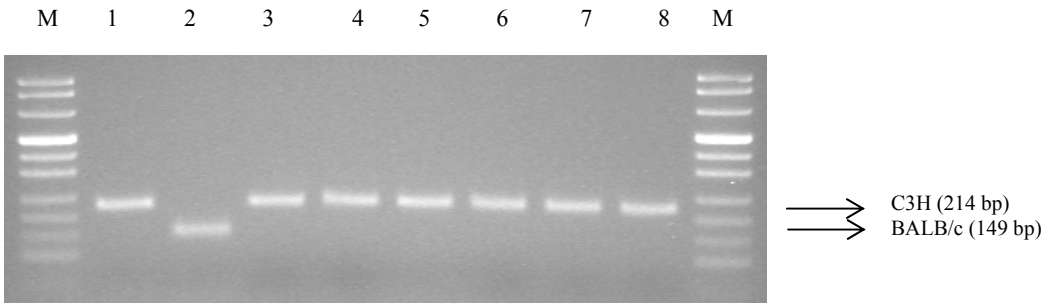

Fig. 4.8: Electrophoretic pattern of the C3H and BALB/c allele amplified by marker D1Mit212. Lane 1: wild-type C3H; lane 2: wild-type BALB/c; lanes 3-8: phenotypically homozygous mutant G2 mice. Lane M is the pUC8 marker.

4.2.3 Sequence analysis of the gene *Pou3f3*

The candidate gene *Pou3f3* was selected for the sequence analysis, as it is located at 42.7 Mb on chromosome 1, and a published mutant phenotype has been described with increased plasma urea and potassium levels associated with renal hypoplasia (http://www.informatics.jax.org/). *Pou3f3* consists of a single exon (3062 bp) which codes for a 497 aa polypeptide (Fig. 4.9).

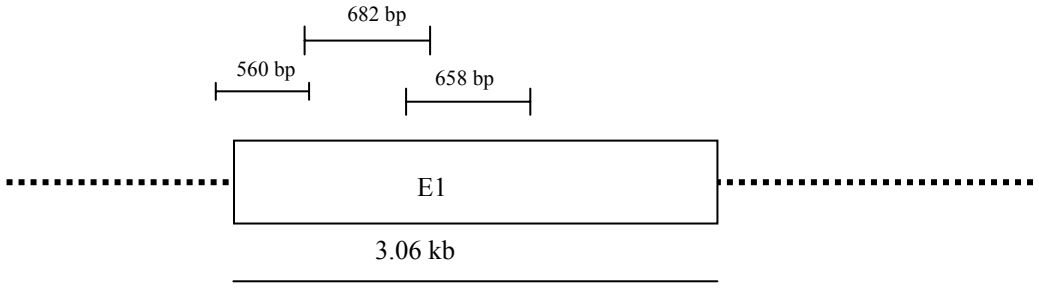

Fig. 4.9: Position and length of PCR products amplified on the candidate gene *Pou3f3* of line HST011. E: exon

Two phenotypically homozygous mutant mice and two wild-type mice were analyzed for the exonic sequence. Sequence analysis revealed a T→C point mutation at nt 1268 (ENSMUST00000054883, Fig. 4.10). The resulting causative mutation leads to the amino acid exchange from leucine to proline at aa position 423. The name of line HST011 was designated as *Pou3f3*^{L423P}.

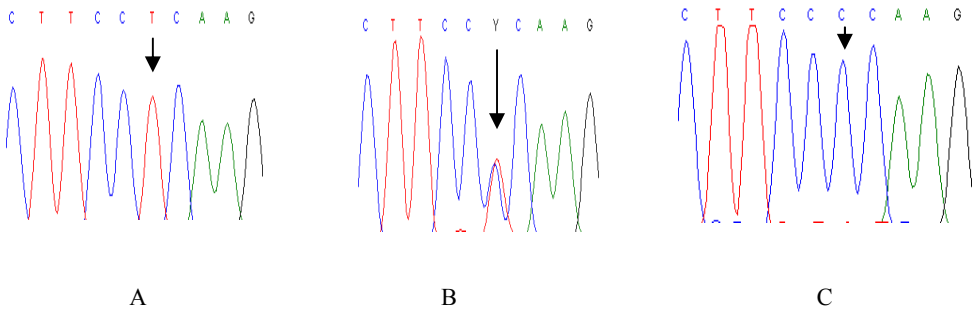

Fig. 4.10: Electropherogram of the sequence of the gene *Pou3f3*. Sequence from A) a phenotypically wild-type mouse, B) a heterozygous mutant mouse, and C) a phenotypically homozygous mutant mouse. The arrow shows the position of the T to C transition which leads to the amino acid exchange from leucine to proline at aa position 423.

4.2.4 Allelic differentiation of the *Pou3f3*^{L423P} mutation by PCR-RFLP

The point mutation in the *Pou3f3*^{L423P} mutant line abolished the restriction site for the enzyme *Sml*I. Therefore, PCR products (460 bp) derived from the wild-type allele were restricted into two fragments (353 bp and 107 bp), whereas PCR products amplified from the mutant allele remained unrestricted. *Sml*I digested PCR products were analyzed on a 2% agarose gel electrophoresis (Fig. 4.11).

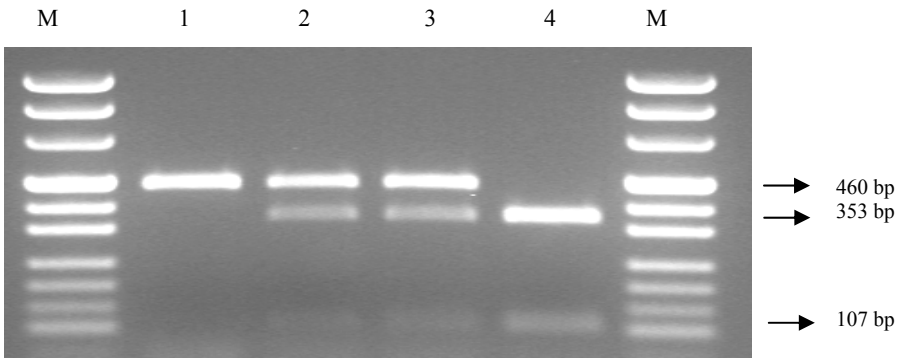

Fig. 4.11: Electrophoretic pattern of the PCR–RFLP in the line *Pou3f3*^{L423P}. Lane 1: phenotypically homozygous mutant mouse; lanes 2 and 3: heterozygous mutant mice; lane 4: wild-type mice. Lane M is the pUC 8 marker.

4.2.5 Clinical chemical analysis of *Pou3f3*^{L423P} homozygous mutant mice

The recessive mutant line HST011 was established due to increased plasma urea levels in homozygous mutant mice. Heterozygous mutant mice on the C3H genetic background were intercrossed to get homozygous mutant mice. Homozygous mutant offspring were used for clinical chemical analysis compared to littermate controls. Homozygous mutant mice of both genders showed increased values of urea, potassium, and lipase compared to heterozygous mutant and wild-type littermates. In addition, homozygous mutant males showed increased levels of AP, and decreased levels of sodium, triglycerides, and cholesterol. Homozygous mutant females showed increased cholesterol, and decreased total protein levels (Table 4.14).

Table 4.14: Plasma data of 12-to 14-week-old mice of line *Pou3f3*^{L423P}

	Male						Female					
	Hom (n = 10)	Het (n = 17)	Wt (n = 5)	t-test hom vs. het	t-test hom vs. wt	t-test het vs. wt	Hom (n = 6)	Het (n = 8)	Wt (n = 8)	t-test hom vs. het	t-test hom vs. wt	t-test het vs. wt
Na (mmol/l)	147 ± 2.8	148 ± 2.4	150 ± 1.4	n.s.	p<0.05	p<0.05	145 ± 6.9	145 ± 2.4	145 ± 3.4	n.s.	n.s.	n.s.
K (mmol/l)	4.4 ± 0.3	3.9 ± 0.4	3.8 ± 0.3	p<0.01	p<0.01	n.s.	4.2 ± 0.2	3.8 ± 0.3	3.9 ± 0.3	p<0.01	p<0.05	n.s.
Ca (mmol/l)	2.3 ± 0.1	2.2 ± 0.1	2.2 ± 0.1	n.s.	n.s.	n.s.	2.3 ± 0.1	2.3 ± 0.1	2.3 ± 0.1	n.s.	n.s.	n.s.
Cl (mmol/l)	108 ± 2	109 ± 3	109 ± 2	n.s.	n.s.	n.s.	112 ± 6	109 ± 3	108 ± 3	n.s.	n.s.	n.s.
Pi (mmol/l)	2.0 ± 0.2	1.9 ± 0.2	1.8 ± 0.2	n.s.	n.s.	n.s.	2.0 ± 0.2	1.7 ± 0.3	1.9 ± 0.3	n.s.	n.s.	n.s.
Total protein (g/l)	51 ± 1.9	52 ± 1.7	52 ± 2.0	n.s.	n.s.	n.s.	49 ± 1.6	51 ± 1.5	51 ± 1.1	n.s.	p<0.05	n.s.
Creatinine-J (µmol/l)	27 ± 1.3	28 ± 2.6	28 ± 1.7	n.s.	n.s.	n.s.	28 ± 1.2	28 ± 2.6	28 ± 0.9	n.s.	n.s.	n.s.
Creatinine-E (µmol/l)	10 ± 0.8	9 ± 1.4	9 ± 1.3	n.s.	n.s.	n.s.	11 ± 2.0	10 ± 0.7	10 ± 0.8	n.s.	n.s.	n.s.
Urea (mg/dl)	87 ± 7	46 ± 7	50 ± 8	p<0.001	p<0.001	n.s.	82 ± 7	38 ± 6	42 ± 4	p<0.001	p<0.001	n.s.
Uric acid (mg/dl)	2.8 ± 1.3	2.6 ± 1.5	2.8 ± 1.3	n.s.	n.s.	n.s.	2.0 ± 0.8	2.2 ± 1.1	2.9 ± 1.3	n.s.	n.s.	n.s.
Cholesterol (mmol/l)	3.6 ± 0.2	4.0 ± 0.5	4.0 ± 0.4	p<0.05	p<0.05	n.s.	3.3 ± 0.1	3.3 ± 0.3	3.1 ± 0.2	n.s.	p<0.05	n.s.
Triglycerides (mmol/l)	1.5 ± 0.4	1.9 ± 0.6	2.4 ± 0.6	p<0.05	p<0.01	n.s.	1.6 ± 0.7	1.7 ± 1.1	2.1 ± 0.7	n.s.	n.s.	n.s.
CK (U/l)	96 ± 83	79 ± 55	100 ± 50	n.s.	n.s.	n.s.	163 ± 87	96 ± 94	113 ± 65	n.s.	n.s.	n.s.
ALT (U/l)	34 ± 15	43 ± 23	26 ± 5	n.s.	n.s.	n.s.	25 ± 8	25 ± 4	29 ± 8	n.s.	n.s.	n.s.
AST (U/l)	48 ± 10	48 ± 21	44 ± 5	n.s.	n.s.	n.s.	54 ± 7	48 ± 9	53 ± 10	n.s.	n.s.	n.s.
AP (U/l)	141 ± 13	112 ± 15	104 ± 14	p<0.001	p<0.001	n.s.	152 ± 10	128 ± 21	142 ± 28	p<0.05	n.s.	n.s.
a-amylase (U/l)	576 ± 47	532 ± 84	535 ± 61	n.s.	n.s.	n.s.	591 ± 69	502 ± 81	486 ± 31	n.s.	n.s.	n.s.
Glucose (mg/dl)	121 ± 17	134 ± 15	137 ± 21	n.s.	n.s.	n.s.	121 ± 17	128 ± 13	127 ± 16	n.s.	n.s.	n.s.
Albumin (g/dl)	2.6 ± 0.2	2.7 ± 0.2	2.7 ± 0.2	n.s.	n.s.	n.s.	2.7 ± 0.2	2.8 ± 0.1	2.8 ± 0.1	n.s.	n.s.	n.s.
Ferritin (µg/l)	52 ± 12	85 ± 24	76 ± 2	p<0.05	n.s.	n.s.	78 ± 27	103 ± 8	87 ± 9	n.s.	n.s.	n.s.
Transferrin (mg/dl)	155 ± 2	159 ± 5	157 ± 5	n.s.	n.s.	n.s.	158 ± 3	162 ± 2	161 ± 3	n.s.	n.s.	n.s.
Lipase (U/l)	56 ± 3	48 ± 5	50 ± 1	p<0.01	p<0.05	n.s.	58 ± 3	52 ± 3	53 ± 3	p<0.05	p<0.05	n.s.
C-reactive protein (mg/l)	0.2 ± 0.4	1.1 ± 0.8	0.7 ± 0.6	p<0.05	n.s.	n.s.	0.8 ± 0.4	0.8 ± 0.5	1.1 ± 0.9	n.s.	n.s.	n.s.
Lactate (mmol/l)	10 ± 1.2	11 ± 2.8	11 ± 1.1	n.s.	n.s.	n.s.	10 ± 1.3	10 ± 1.5	10 ± 1.0	n.s.	n.s.	n.s.
LDL (mg/dl)	117 ± 48	147 ± 58	102 ± 6	n.s.	n.s.	n.s.	120 ± 22	124 ± 41	139 ± 66	n.s.	n.s.	n.s.

Data represents the means ± SD; SD: standard deviation. Student's t-test, p<0.05, p<0.01, and p<0.001.
n: number of the animals analyzed. ns: non-significant. Hom: homozygous mutant; Het: heterozygous mutant; Wt: wild-type.
CK: creatine kinase; ALT: alanine aminotransferase; AST: aspartate aminotransferase; AP: alkaline phosphatase; LDL: low density lipoprotein

4.2.6 Urine analysis of *Pou3f3*^{L423P} homozygous mutant mice

Metabolic cage analysis was performed with homozygous mutant mice compared to age-matched heterozygous mutant and wild-type littermate controls. Animals were analyzed at the age of 14-15 weeks. Homozygous mutant males showed mild polyuria as well as decreased daily uric acid excretion. Homozygous mutant females showed decreased uric acid excretion and mild glycosuria. After 24 h water deprivation, homozygous mutant mice of both sexes showed increased loss of the body weight, and they consumed significantly less food (Table 4.15).

Table 4.15: Urine data of 14-to 15-week-old mice of line *Pou3f3*^{L423P} under basal conditions and after deprivation of drinking water for 24 h in metabolic cages

	Male			Female		
			t-test			t-test
	Hom (n = 8)	Wt + het (n = 8)	hom vs. wt +het	Hom (n = 4)	Wt + het (n = 10)	hom vs. wt + het
Body weight (g)	20.4 ± 1.4	26.3 ± 3.6	p<0.001	18.2 ± 2.2	23.3 ± 2.7	p<0.01
Drinking water ad libitum						
Water intake (ml/day)	5.9 ± 3.0	4.3 ± 0.7	n.s.	5.5 ± 1.7	4.9 ± 2.3	n.s.
Food intake (g/day)	3.5 ± 1.2	3.9 ± 0.6	n.s.	3.6 ± 0.7	4.2 ± 0.7	n.s.
Feaces exretion (g/day)	1.6 ± 0.8	1.7 ± 0.5	n.s.	2.3 ± 0.8	2.0 ± 0.6	n.s.
Urine volume (ml/day)	1.5 ± 0.7	0.9 ± 0.3	p<0.05	1.6 ± 0.5	1.0 ± 0.6	n.s.
Na (µmol/day)	125 ± 47	169 ± 36	n.s.	170 ± 69	231 ± 67	n.s.
K (µmol/day)	375 ± 114	422 ± 149	n.s.	505 ± 117	600 ± 232	n.s.
Ca (µmol/day)	1.5 ± 0.5	1.4 ± 0.6	n.s.	3.0 ± 0.8	2.0 ± 0.9	n.s.
Cl (µmol/day)	217 ± 78	274 ± 73	n.s.	315 ± 112	395 ± 118	n.s.
Mg (µmol/day)	9 ± 7	15 ± 9	n.s.	23 ± 13	22 ± 9	n.s.
Pi (µmol/day)	50 ± 54	63 ± 47	n.s.	77 ± 71	99 ± 59	n.s.
Creatinine-J (µmol/day)	3.5 ± 1.0	4.0 ± 1.0	n.s.	3.8 ± 1.1	4.9 ± 1.3	n.s.
Creatinine-E (µmol/day)	2.1 ± 0.5	2.5 ± 0.6	n.s.	2.5 ± 0.7	3.1 ± 0.9	n.s.
Urea (mmol/day)	1.2 ± 0.3	1.3 ± 0.4	n.s.	1.6 ± 0.4	1.8 ± 0.6	n.s.
Uric acid (nmol/day)	329 ± 94	587 ± 154	p<0.01	522 ± 84	977 ± 208	p<0.01
Glucose (µmol/day)	1.5 ± 1.1	2.1 ± 1.1	n.s.	5.0 ± 2.5	3.1 ± 0.8	p<0.05
Total protein (mg/day)	5.0 ± 1.7	7.3 ± 3.7	n.s.	0.9 ± 0.3	2.9 ± 2.1	n.s.
Albumin (nmol/day)	1.4 ± 0.3	1.9 ± 0.6	n.s.	2.0 ± 0.2	2.2 ± 0.7	n.s.
Deprivation of drinking water for 24 h						
Loss of body weight (%)	13.2 ± 2.2	9.6 ± 1.4	p<0.01	13.4 ± 1.2	9.7 ± 1.3	p<0.001
Food intake (g/day)	1.2 ± 0.4	2.3 ± 0.3	p<0.001	1.8 ± 0.2	2.3 ± 0.3	p<0.01
Urine volume (ml/day)	0.6 ± 0.3	0.5 ± 0.2	n.s.	0.7 ± 0.1	0.5 ± 0.2	n.s.
Feaces exretion (g/day)	0.4 ± 1.0	0.8 ± 0.2	p<0.001	0.8 ± 0.1	0.9 ± 0.2	n.s.

Values are means ± SD. SD: standard deviation. Student's t-test, p<0.05, p<0.01, p<0.001.
Hom: homozygous mutant; het: heterozygous mutant; Wt: wild-type.
n: the number of animals analyzed; ns: non-significant. Age of mice analyzed: 14–15 weeks.

4.2.7 Morphological analysis of *Pou3f3*^{L423P} homozygous mutant mice

Morphological analysis including body and organ weights was carried out on four-month-old homozygous mutant, heterozygous mutant, and wild-type littermates with a small group size of n = 3-5. Homozygous mutant animals of both sexes showed significantly decreased body and carcass weights as well as a decreased nose-to-rump length (Table 4.16). An absolute weight of most organs was significantly reduced in homozygous mutants compared to heterozygous mutant and wild-type control mice. In comparison to wild-type mice, homozygous mutants of both sexes showed decreased relative kidney and liver weights (Table 4.17, Fig. 4.12). Kidneys from homozygous mutants were, except of the small size; light microscopically indistinguishable from those of control littermates (not shown).

Fig. 4.12: Representative macroscopic appearance of the kidneys of a four-month-old *Pou3f3*^{L423P} homozygous mutant mouse and a sex-matched wild-type littermate.

Table 4.16: Absolute body weight and organ weights of 4-month-old mice of line *Pou3f3*^{L423P}

	Male			t-test			Female			t-test		
	Hom (n = 5)	Het (n = 4)	Wt (n = 3)	hom vs. het	hom vs. wt	het vs. wt	Hom (n = 4)	Het (n = 3)	Wt (n = 3)	hom vs. het	hom vs. wt	het vs. wt
Body weight (g)	23.6 ± 2.0	32.1 ± 4.1	31.7 ± 1.4	p<0.01	p<0.001	n.s.	20.8 ± 1.6	29.4 ± 0.6	31.0 ± 5.7	p<0.001	p<0.05	n.s.
Nose-to-rump length (cm)	8.8 ± 0.3	9.8 ± 0.3	9.8 ± 0.4	p<0.01	p<0.01	n.s.	8.8 ± 0.2	9.5 ± 0.2	9.9 ± 0.3	p<0.01	p<0.01	n.s.
Brain (mg)	395 ± 12	444 ± 8	465 ± 8	p<0.001	p<0.001	n.s.	400 ± 26	456 ± 10	473 ± 3	p<0.01	p<0.01	n.s.
Liver (g)	1.1 ± 0.1	1.5 ± 0.2	1.5 ± 0.1	p<0.01	p<0.001	n.s.	0.9 ± 0.1	1.3 ± 0.1	1.5 ± 0.3	p<0.001	p<0.001	n.s.
Kidney (mg)	353 ± 40	558 ± 104	531 ± 45	p<0.01	p<0.01	n.s.	202 ± 28	333 ± 6	340 ± 51	p<0.001	p<0.01	n.s.
Lung (mg)	142 ± 8	183 ± 22	182 ± 7	p<0.01	p<0.001	n.s.	148 ± 15	180 ± 8	188 ± 29	p<0.05	p<0.05	n.s.
Heart (mg)	108 ± 12	131 ± 13	135 ± 16	p<0.05	p<0.05	n.s.	84 ± 8	120 ± 11	119 ± 22	p<0.01	p<0.05	n.s.
Testis (mg)	130 ± 15	152 ± 24	167 ± 18	n.s.	p<0.05	n.s.						
Uterus (mg)							84 ± 18	101 ± 34	112 ± 27	n.s.	n.s.	n.s.
Urinary bladder (mg)	27 ± 4.5	26 ± 5.5	23 ± 2.0	n.s.	n.s.	n.s.	21 ± 3.8	23 ± 5.0	22 ± 1.0	n.s.	n.s.	n.s.
Spleen (mg)	76 ± 13	85 ± 10	81 ± 3.0	n.s.	n.s.	n.s.	87 ± 5	115 ± 16	117 ± 27	p<0.05	n.s.	n.s.
Carcass (g)	17.7 ± 1.3	24.0 ± 3.4	23.8 ± 1.5	p<0.01	p<0.001	n.s.	15.4 ± 1.5	21.9 ± 1.1	22.5 ± 4.6	p<0.01	p<0.05	n.s.

Data presents mean ± SD. SD: standard deviation. Student's t-test, p<0.05, p<0.01, and p<0.001.
n: animals analyzed; hom: homozygous mutant; het: heterozygous mutant; wt: wild-type. n.s: non-significant.

Table 4.17: Relative organ weights of 4-month-old mice of line *Pou3f3*^{L423P}

	Male						Female					
				t-test						t-test		
	Hom (n = 5)	Het (n = 4)	Wt (n = 3)	hom vs. het	hom vs. wt	het vs. wt	Hom (n = 4)	Het (n = 3)	Wt (n = 3)	hom vs. het	hom vs. wt	het vs. wt
Brain (mg)	1.7 ± 0.2	1.4 ± 0.2	1.5 ± 0.1	p<0.05	n.s.	n.s.	1.9 ± 0.1	1.6 ± 0.0	1.6 ± 0.3	p<0.001	n.s.	n.s.
Liver (g)	4.3 ± 0.2	4.7 ± 0.3	4.8 ± 0.1	n.s.	p<0.01	n.s.	4.2 ± 0.1	4.5 ± 0.7	4.7 ± 0.1	n.s.	p<0.05	n.s.
Kidney (mg)	1.5 ± 0.2	1.7 ± 0.1	1.7 ± 0.1	p<0.05	p<0.05	n.s.	1.0 ± 0.1	1.1 ± 0.0	1.1 ± 0.1	p<0.05	p<0.05	n.s.
Lung (mg)	0.6 ± 0.04	0.6 ± 0.02	0.6 ± 0.01	n.s.	n.s.	n.s.	0.7 ± 0.05	0.6 ± 0.03	0.6 ± 0.03	p<0.05	p<0.05	n.s.
Heart (mg)	0.5 ± 0.02	0.4 ± 0.02	0.4 ± 0.05	p<0.05	n.s.	n.s.	0.4 ± 0.02	0.4 ± 0.05	0.4 ± 0.04	n.s.	n.s.	n.s.
Urinary bladder (mg)	0.11 ± 0.01	0.08 ± 0.01	0.07 ± 0.01	p<0.01	p<0.01	n.s.	0.10 ± 0.01	0.08 ± 0.02	0.07 ± 0.01	n.s.	p<0.05	n.s.

Data presents mean ± SD. SD: standard deviation. Student's t-test, p<0.05; p<0.01; p<0.001.
Hom: homozygous mutant; het: heterozygous mutant; wt: wild-type. n.s: non-significant; n: animals analyzed.

4.3 Line HST015

4.3.1 Linkage analysis of the causative mutation

Phenotypically heterozygous mutant mice on the C3H genetic background showed a significantly reduced breeding capacity. However, by mating phenotypically heterozygous mutant mice with albino BALB/c mice, we were able to get G1 hybrid mice. G1 offspring were screened for increased plasma urea levels (>70 mg/dl for males and >65 mg/dl for females as cut-off values) at the age of 12 and 15 weeks. Phenotypically mutant G1 animals were mated with BALB/c mice to produce G2 offspring. Only about 25% G2 animals showed increased plasma urea levels and this was not consistent in the second measurement, however they showed decreased body weight and/or aggressive and/or hyperactive behaviour. Phenotypically mutant G2 backcross mice were further mated with BALB/c mice to get G3 offspring. Some phenotypically mutant G2 mice were failed to produce offspring and we also observed that more pigmented G3 mice showed increased plasma urea levels as compared to albino G3 mice (Table 4.18). In addition, 58 G2 mice were also analyzed for coat color and mutant phenotype defined as increased plasma urea levels. Out of 58 G2 mice, 15 pigmented mice were phenotypically mutant and 10 pigmented mice were wild-type (χ^2 value = 4.0), whereas 9 albino mice were phenotypically mutant and 24 albino mice were wild-type (χ^2 value = 21.1). Thus, it was assumed that it might be a linkage between coat color and mutant phenotype. BALB/c mice show an albino coat color due to the recessive mutation *Tyr*$^{c/c}$ on chromosome 7 (94.5 Mb).

To verify the linkage, we re-analyzed data from the ENU-induced mutant line HST001 with increased plasma urea levels as primary phenotype and the causative dominant mutation *Umod*^{C93F} on chromosome 7 (126.6 Mb) as the linkage analysis was also carried out with G2 backcross mice produced with the BALB/c inbred strain (Prückl 2011). By analyzing the coat color of G2 backcross animals of line HST001, strong linkage between coat color and mutant phenotype was observed (Table 4.18).

Table 4.18: Phenotypic analysis of coat color and mutant phenotype (increased plasma urea levels) in backcross animals of line HST001 and HST015

	HST001 (G2)			HST015 (G3)		
Coat color	Phenotypically mutant	Phenotypically wild-type	χ^2 value	Phenotypically mutant	Phenotypically wild-type	χ^2 value
Pigmented	79 (89%)	23 (21%)	30	30 (83%)	6 (11%)	43
Albino	10 (11%)	86 (79%)	64	6 (17%)	48 (89%)	60
χ^2 value	60	33		43	60	

G2: Backcross animals from the second backcross generation with BALB/c mice; G3: Backcross animals from the third backcross generation with BALB/c mice

4.3.2 Fine mapping of chromosome 7

Fine mapping was carried out using polymorphic markers of chromosome 7 (Table 4.19). Twenty four phenotypically mutant G2-G3 backcross animals were analyzed. The markers D7Mit276 and D7Mit90 showed the heterozygous C3H/BALB/c genotype in all mice examined.

Table 4.19: Fine mapping analysis of chromosome 7 in line HST015

Marker	Locus (Mb)	Heterozygous C3H/BALB/c	BALB/c/BALB/c	Total
D7Mit230	56.7	22	2	24
D7Mit276	69.4	24	0	24
D7Mit90	87.5	24	0	24
D7Mit323	108.0	22	2	24
D7Mit40	123.9	19	5	24
D7Mit68	132.4	17	7	24

4.3.3 Candidate gene analysis

The two candidate genes *Tomt* and *Chd2* were selected for sequence analysis (Table 4.20). Genomic DNA and RNA was extracted from two phenotypically heterozygous mutant mice (one on the C3H genetic background and one on the mixed C3H×BALB/c genetic background) and two phenotypically wild-type mice on the C3H genetic background. For *Tomt*, the exonic regions were sequenced,

whereas for *Chd2* cDNA transcript sequencing is going on (Fig. 4.13). Sequence analysis of *Tomt* resulted in the identical sequence in phenotypically heterozygous mutant mice and wild-type mice.

Table 4.20: Candidate genes in line HST015 and their published phenotype data

Gene	Position (Mb)	Exons	Polypeptide length (aa)	Mutant phenotype (http://www.informatics.jax.org/
Tomt	109.0	4	258	ENU-induced homozygous mutants exhibited marked hyperactivity, bidirectional circling and head-tossing. These behaviours were suppressed during sleep and nursing. Homozygous mutant males exhibited increased male to male aggression (Du et al. 2008).
Chd2	80.5	39	1827	Gene trapped homozygous mutant mice exhibited early postnatal lethality associated with fetal growth retardation. Heterozygous mutant mice exhibited postnatal lethality and premature death after weaning associated with growth retardation and multi-organ defects (Marfella et al. 2006).

A)

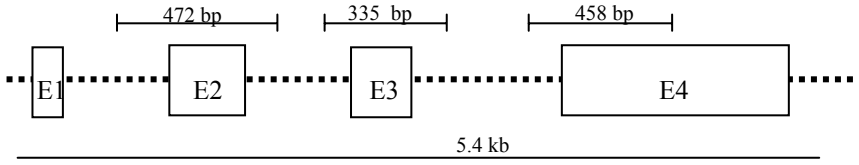

B)

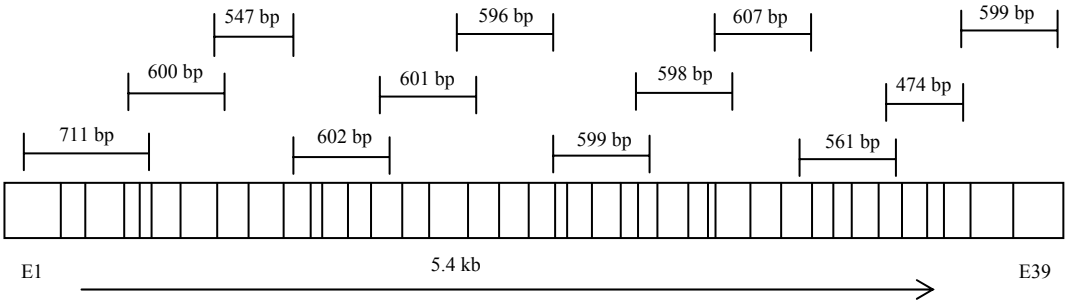

Fig. 4.13: Position and length of PCR products amplified on the candidate genes of line HST015. A*) Tomt* gene and B) *Chd2* cDNA. E: exon

4.3.4 Clinical chemical analysis of phenotypically heterozygous mutant mice

After rederivation of line HST015 in the mouse facility of the Moorversuchsgut by IVF, phenotypically heterozygous mutant mice showed reduced fertility. To avoid physical stress for the animals, only small amounts of blood were taken and used in the analysis especially of parameters which are predictive for the kidney function. Phenotypically heterozygous mutant mice on the C3H genetic background were defined by increased levels of plasma urea in both sexes. Plasma levels of total protein and uric acid were significantly decreased in phenotypically heterozygous mutant mice as compared to littermate controls. Phenotypically heterozygous mutant females showed increased creatinine-J levels (Table 4.21).

Table 4.21: Plasma data of 12-to14-week-old mice on the C3H genetic background of line HST015

	Male			Female		
	Ph. het (n = 7)	Ph. wt (n = 14)	t-test (het vs. wt)	Ph. het (n = 9)	Ph. wt (n = 13)	t-test (het vs. wt)
Total protein (g/dl)	5.2 ± 0.2	5.6 ± 0.3	p<0.01	5.3 ± 0.3	5.6 ± 0.3	p<0.05
Creatinine-J (µmol/l)	32 ± 2.1	33 ± 2.2	n.s.	34 ± 2.3	32 ± 1.8	p<0.05
Urea (mg/dl)	89 ± 22	59 ± 6	p<0.001	81 ± 9	48 ± 9	p<0.001
Uric acid (mg/dl)	2.3 ± 1.2	4.9 ± 1.2	p<0.001	1.5 ± 0.6	3.5 ± 1.2	p<0.001

Data represents the means ± SD; SD: standard deviation. Student's t-test, p<0.05, p<0.01, and p<0.001.
n: number of the animals analyzed. ns: non-significant.
Ph. het: phenotypically heterozygous mutant mice; Ph. wt: phenotypically wild-type mice.

4.3.5 Phenotypical analysis of backcross mice

Mice on the mixed C3H×BALB/c genetic background were phenotypically analyzed (58 G2 and 80 G3 mice) for increased plasma urea levels. Using >70 mg/dl for males and >65 mg/dl for females as cut-off values, the 138 G2-G3 backcross mice were classified in 60 (43%) heterozygous mutant mice and 78 (57%) wild-type mice. In addition, we observed growth retarded pups at birth. Therefore, we measured the body weight at the age of 3 months in both groups classified by the increased plasma urea levels. Phenotypically heterozygous mutant mice exhibited growth retardation. We also carried out sections of phenotypically heterozygous mutant females and found that some females had increased ovaries and uteri (Fig. 4.14).

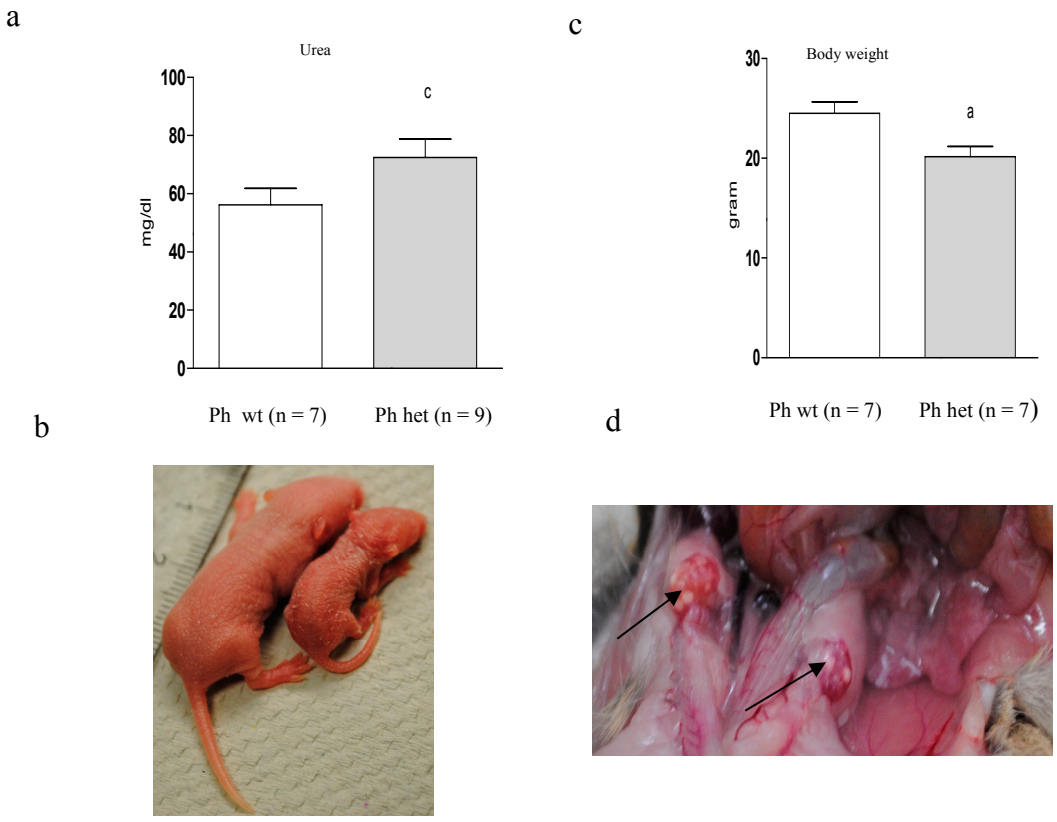

Fig. 4.14: Analysis of G2-G3 backcross mice of line HST015 on the mixed C3H×BALB/c genetic background. a) Classification into phenotypically heterozygous mutants and wild-type mice according to their plasma urea levels. b) One of the one-day-old pups is showing growth retardation. c) Body weight of three-month-old female mice which were classified into phenotypically heterozygous mutants and wild-type mice according to the plasma urea levels (see a). d) Ovaries from a phenotypically heterozygous mutant female (arrow). Data represents the mean ± SD. Student's, t-test $p<0.05^{a}$, $p<0.001^{c}$. Ph wt: phenotypically wild-type; Ph het: phenotypically heterozygous mutant; n: number of animals analyzed.

4.4 Line CLP001

4.4.1 Sequence analysis of the gene *Gsdma3*

Linkage analysis and fine mapping was already carried out independent of this study, and the causative mutation was mapped to a defined region around 100 Mb on chromosome 11. *Gsdma3* was chosen for the sequence analysis (Fig. 4.15; http://www.informatics.jax.org/).

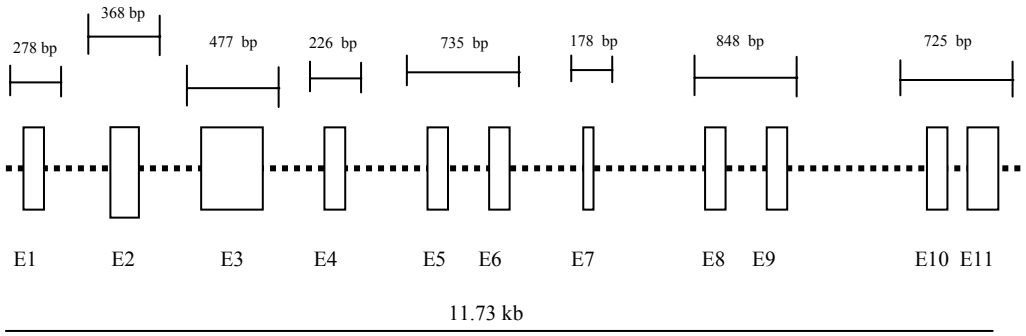

Fig. 4.15: Position and length of PCR products amplified on the gene *Gsdma3*. E: exon

Sequence analysis revealed a T→A transversion at nt 1158 (ENSMUST00000073295), which leads to the amino acid exchange from isoleucine to asparagine at aa position 359 (Fig. 4.16). The name of line CLP001 was designated as *Gsdma3*^{I359N}.

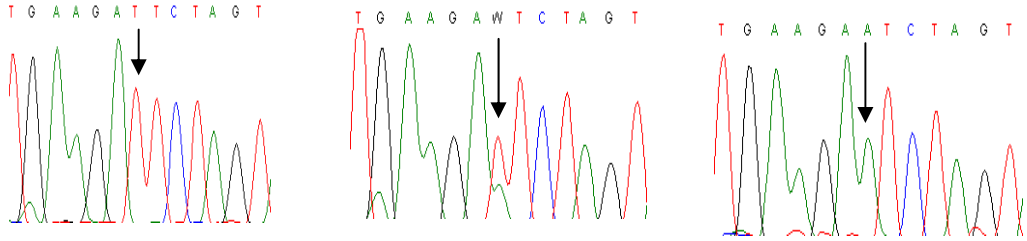

Fig. 4.16: Electropherogram of the sequence of *Gsdma3*. Sequence from A) a wild-type mouse, B) a phenotypically heterozygous mutant mouse, and C) a phenotypically homozygous mutant mouse. The arrow shows the position of the T to A transversion which leads to the amino acid exchange from isoleucine to asparagine at aa position 359.

4.4.2 Allelic differentiation of the *Gsdma3*^{I359N} mutant mice by ARMS-PCR

Allelic differentiation was carried out by the amplification refractory mutation system PCR (ARMS-PCR; see 3.3.4.2). The allele-specific reverse primer INT1 (5’ tttctccaaggattttactaaaa 3’) and the forward primer EXT1 (5’ caaatgagcatatgaatgaatag 3’) were used for amplifying the wild-type allele (230 bp). For the amplification of the mutant allele (144 bp), the allele-specific forward primer INT2 (5’ ctaactgaagaacaactgaataa 3’) and the reverse primer EXT2 (5’ atgttcccacaagttctagcg 3’) were used. A 374 bp long fragment was amplified from both external primers (Fig. 4.17a and b).

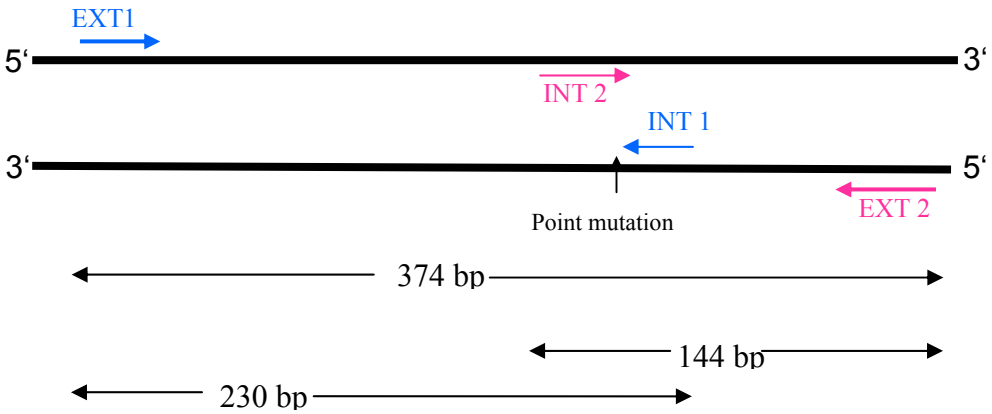

Fig. 4.17a: Scheme of the ARMS-PCR. The mutant allele-specific primer INT2 amplifies the 144 bp PCR product with primer EXT2. Primer INT1 (wild-type allele-specific) amplifies the 230 bp wild-type PCR product. In addition, a 374 bp long PCR product is derived from primers EXT1 and EXT2.

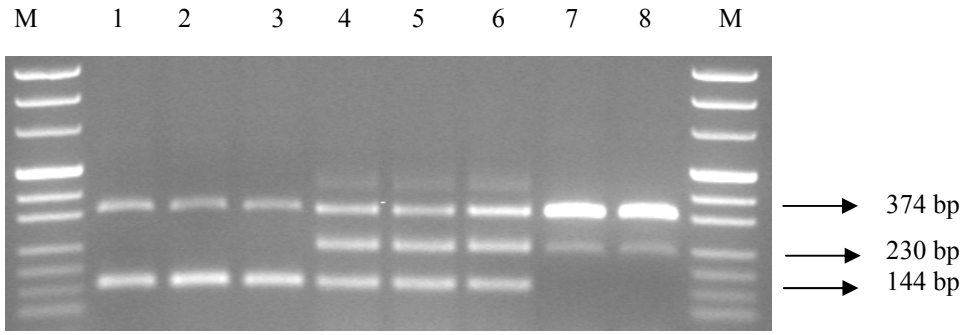

Fig. 4.17b: Electrophoretic pattern of the allele-specific PCR in line *Gsdma3*^{I359N}. Lanes 1, 2, 3: homozygous mutant mice; lanes 4, 5, 6: heterozygous mutant mice; lanes 7, 8: wild-type mice. Lane M is the pUC 8 marker.

4.4.3 Analysis of alopecia in *Gsdma3*^{I359N} mutant mice

Gsdma3^{I359N} heterozygous mutant mice exhibited alopecia. Therefore, the onset and the course of hair loss were studied in homozygous mutants and heterozygous mutants compared with wild-type littermates. In heterozygous mutant mice, hair loss started from 3 weeks of age from the neck and complete hair loss appeared at 6 weeks of age. Following this, regeneration of hair growth started resulting in a complete loose and spare hair coat at 8 weeks of age. Hair loss again started from 9 weeks of age resulting in complete baldness at 14 weeks of age. Homozygous mutant mice showed a pattern of hair loss which is similar to the heterozygous mutants. However, after regeneration of the spare and loose hair coat, the second

cycle of hair loss was more pronounced resulting in complete baldness at 10-11 weeks of age (Fig 4.18).

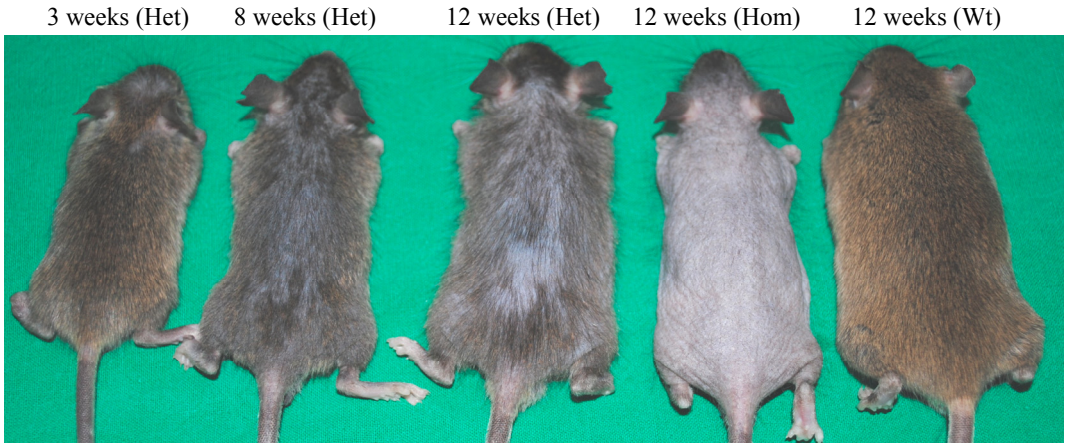

Fig. 4.18: Course of the hair loss in line *Gsdma3*^{I359N}. Hair loss starts from the neck at 3 weeks of age. At 8 weeks of age, loose and spare hair is visible after the regeneration in homozygous mutant and heterozygous mutant animals. Complete baldness appears again in homozygous mutant animals at 10-11 weeks of age and in heterozygous mutants at 14 weeks of age. Hom: homozygous mutant mice; het: heterozygous mutant mice; wt: wild-type mice.

4.4.4 Clinical chemical analysis of *Gsdma3*^{I359N} mutant mice

Clinical chemical blood analysis was carried out using homozygous mutant, heterozygous mutant and wild-type mice on the C3H genetic background. Compared to wild-type controls, homozygous mutant mice of both sexes showed a decreased activity of alkaline phosphatase (Table 4.22).

4.4.5 Morphological analysis of *Gsdma3*^{I359N} mutant mice

Morphological analysis of body and organ weights was also carried out. Homozygous mutant and heterozygous mutant animals were viable and fertile. Homozygous mutant males exhibited a decreased absolute and relative weight of the testis as well as an increased absolute and relative weight of the spleen compared to wild-type littermates. Homozygous mutant and heterozygous mutant females showed an increased absolute and relative weight of the heart compared to wild-type littermates (Table 4.23).

Table 4.22: Plasma data of 12-to 14-week-old mice of line *Gsdma3*^{I359N}

	Male						Female					
	Hom (n = 6)	Het (n = 8)	Wt (n = 8)	t-test hom vs. het	t-test hom vs. wt	t-test het vs. wt	Hom (n = 8)	Het (n = 11)	Wt (n = 9)	t-test hom vs. het	t-test hom vs. wt	t-test het vs. wt
Na (mmol/l)	146 ± 3	146 ± 5	148 ± 4	n.s.	n.s.	n.s.	146 ± 5	147 ± 9	147 ± 11	n.s.	n.s.	n.s.
K (mmol/l)	4.5 ± 0.5	4.4 ± 0.4	4.5 ± 0.4	n.s.	n.s.	n.s.	4.3 ± 0.4	4.3 ± 0.5	4.2 ± 0.7	n.s.	n.s.	n.s.
Ca (mmol/l)	2.3 ± 0.1	2.3 ± 0.1	2.2 ± 0.1	n.s.	n.s.	n.s.	2.3 ± 0.1	2.3 ± 0.1	2.3 ± 0.2	n.s.	n.s.	n.s.
Cl (mmol/l)	108 ± 5	108 ± 7	110 ± 6	n.s.	n.s.	n.s.	110 ± 7	114 ± 8	116 ± 8	n.s.	n.s.	n.s.
Pi (mmol/l)	1.8 ± 0.1	2.0 ± 0.5	1.7 ± 0.4	n.s.	n.s.	n.s.	2.0 ± 0.3	2.1 ± 0.4	2.3 ± 0.4	n.s.	n.s.	n.s.
Total protein (g/l)	49 ± 2	49 ± 2	51 ± 2	n.s.	n.s.	n.s.	50 ± 2	53 ± 5	53 ± 4	n.s.	n.s.	n.s.
Creatinine-J (µmol/l)	26 ± 2	25 ± 1	27 ± 4	n.s.	n.s.	n.s.	26 ± 3	28 ± 2	27 ± 3	n.s.	n.s.	n.s.
Creatinine-E (µmol/l)	8.7 ± 1.9	9.4 ± 1.5	12.1 ± 8.7	n.s.	n.s.	n.s.	9.3 ± 1.8	8.7 ± 1.6	9.6 ± 2.5	n.s.	n.s.	n.s.
Urea (mg/dl)	45 ± 5	50 ± 5	53 ± 5	n.s.	p<0.05	n.s.	43 ± 6	49 ± 8	46 ± 7	n.s.	n.s.	n.s.
Uric acid (mg/dl)	4.0 ± 1.7	4.9 ± 2.6	4.9 ± 1.5	n.s.	n.s.	n.s.	2.5 ± 2.0	3.4 ± 2.4	2.9 ± 1.7	n.s.	n.s.	n.s.
Cholesterol (mmol/l)	3.6 ± 0.1	3.3 ± 0.3	3.5 ± 0.2	p<0.05	n.s.	n.s.	2.9 ± 0.2	2.8 ± 0.2	3.0 ± 0.3	n.s.	n.s.	n.s.
Triglycerides (mmol/l)	2.1 ± 0.6	1.9 ± 0.7	2.1 ± 0.6	n.s.	n.s.	n.s.	1.1 ± 0.3	1.8 ± 0.7	1.8 ± 0.8	p<0.05	p<0.05	n.s.
CK (U/l)	91 ± 47	231 ± 269	330 ± 425	n.s.	n.s.	n.s.	333 ± 427	230 ± 244	215 ± 136	n.s.	n.s.	n.s.
ALT (U/l)	29 ± 10	43 ± 24	39 ± 17	n.s.	n.s.	n.s.	46 ± 23	52 ± 24	54 ± 34	n.s.	n.s.	n.s.
AST (U/l)	55 ± 15	62 ± 27	55 ± 18	n.s.	n.s.	n.s.	80 ± 35	66 ± 22	56 ± 14	n.s.	n.s.	n.s.
AP (U/l)	91 ± 6	98 ± 18	129 ± 24	n.s.	p<0.01	p<0.05	124 ± 6	126 ± 20	152 ± 28	n.s.	p<0.05	n.s.
Amylase (U/l)	ND	1885 ± 166	2046 ± 139	ND	ND	n.s.	1765 ± 35	1832 ± 109	1842 ± 199	n.s.	n.s.	n.s.
Glucose (mg/dl)	135 ± 25	127 ± 28	119 ± 19	n.s.	n.s.	n.s.	125 ± 15	131 ± 25	137 ± 27	n.s.	n.s.	n.s.
Albumin (g/dl)	2.5 ± 0.2	2.4 ± 0.2	2.3 ± 0.1	n.s.	p<0.05	n.s.	2.6 ± 0.1	2.6 ± 0.2	2.5 ± 0.4	n.s.	n.s.	n.s.
Ferritin (µg/l)	77 ± 10	68 ± 33	57 ± 43	n.s.	n.s.	n.s.	89 ± 39	44 ± 34	44 ± 41	p<0.05	p<0.05	n.s.
Transferrin (mg/dl)	156 ± 2.2	150 ± 4.5	153 ± 6.5	p<0.01	n.s.	n.s.	160 ± 1.7	155 ± 4.4	159 ± 4.4	p<0.01	n.s.	n.s.
Lipase (U/l)	43 ± 5	49 ± 13	53 ± 12	n.s.	n.s.	n.s.	52 ± 4	52 ± 8	57 ± 10	n.s.	n.s.	n.s.
C-reactive protein (mg/l)	1.4 ± 0.7	2.0 ± 2.2	0.6 ± 0.6	n.s.	n.s.	n.s.	1.6 ± 0.7	1.4 ± 1.0	1.4 ± 1.2	n.s.	n.s.	n.s.
Lactate (mmol/l)	10 ± 1.8	11 ± 1.5	11 ± 1.3	n.s.	n.s.	n.s.	10 ± 2.0	10 ± 1.1	10 ± 1.4	n.s.	n.s.	n.s.

Data represents the means ± SD; SD: standard deviation. Student's t-test, $p<0.05$, $p<0.01$, and $p<0.001$.
n: number of the animals analyzed. ns: non-significant; ND: not done
Hom: homozygous mutant mice; Het: heterozygous mutant mice; Wt: wild-type mice.
CK: creatine kinase; ALT: alanine aminotransferase; AST: aspartate aminotransferase; AP: alkaline phosphatase.

Table 4.23: Absolute body weight and organ weights of 4-month-old mice of line *Gsdma3*^{I359N}

	Male			t-test			Female			t-test		
	Hom (n = 4)	Het (n = 6)	Wt (n = 4)	hom vs. het	hom vs. wt	het vs. wt	Hom (n = 5)	Het (n = 8)	Wt (n = 6)	hom vs. het	hom vs. wt	het vs. wt
Body weight (g)	28.4 ± 1.0	27.8 ± 3.0	26.1 ± 2.0	n.s.	n.s.	n.s.	23.3 ± 1.2	24.6 ± 2.4	23.8 ± 2.1	n.s.	n.s.	n.s.
Nose-to-rump length (cm)	9.1 ± 0.1	9.0 ± 0.5	9.2 ± 0.0	n.s.	n.s.	n.s.	9.1 ± 0.1	8.9 ± 0.4	8.9 ± 0.3	n.s.	n.s.	n.s.
Brain (mg)	431 ± 14	439 ± 17	448 ± 21	n.s.	n.s.	n.s.	449 ± 7	448 ± 14	460 ± 10	n.s.	n.s.	n.s.
Liver (g)	1.6 ± 0.3	1.7 ± 0.2	1.4 ± 0.1	n.s.	n.s.	n.s.	1.3 ± 0.1	1.4 ± 0.2	1.3 ± 0.1	n.s.	n.s.	n.s.
Kidney (mg)	571 ± 60	546 ± 76	506 ± 55	n.s.	n.s.	n.s.	350 ± 20	351 ± 29	327 ± 16	n.s.	n.s.	n.s.
Lung (mg)	179 ± 16	178 ± 27	167 ± 18	n.s.	n.s.	n.s.	176 ± 16	172 ± 11	170 ± 19	n.s.	n.s.	n.s.
Heart (mg)	128 ± 14	131 ± 15	123 ± 16	n.s.	n.s.	n.s.	115 ± 13	120 ± 6	102 ± 5	n.s.	$p<0.05$[c]	$p<0.001$[c]
Testis (mg)	164 ± 7	167 ± 18	180 ± 8	n.s.	$p<0.05$[a]	n.s.						
Uterus (mg)							129 ± 28	123 ± 22	131 ± 43	n.s.	n.s.	n.s.
Urinary bladder (mg)	25 ± 4.2	23 ± 3.7	27 ± 4.9	n.s.	n.s.	n.s.	21 ± 2.4	20 ± 2.5	20 ± 4.3	n.s.	n.s.	n.s.
Spleen (mg)	103 ± 16	95 ± 20	77 ± 11	n.s.	$p<0.05$[b]	n.s.	138 ± 53	131 ± 32	118 ± 19	n.s.	n.s.	n.s.
Carcass (g)	20.7 ± 1.4	20.9 ± 1.5	18.4 ± 1.8	n.s.	n.s.	n.s.	17.1 ± 1.5	18.0 ± 1.8	17.6 ± 1.1	n.s.	n.s.	n.s.

Data represent means ± SD. SD: standard deviation. Student's t-test, $p<0.05$, $p<0.01$, and $p<0.001$.
n: animals analyzed; hom: homozygous mutant; het: heterozygous mutant; wt: wild-type; n.s: non-significant.
a: the relative testis weight of the homozygous mutant males is signifcantly decreased ($p<0.05$).
b: the relative spleen weight is significantly increased in homozygous mutant males ($p<0.05$).
c: the relative heart weight is significantly increased in homozygous mutant and heterozygous mutant females ($p<0.05$).

4.5 Generation of congenic lines

Congenic lines are going to be established using C57BL/6 and BALB/c mice as recipient genetic background for the lines HST014, HST011, and HST015 (Table 4.24). The production of the congenic lines is continuing. In the lines HST014 and HST011, the causative mutation is used to select the mice for the breeding of the next backcross generation. In line HST015, mice showing increased plasma urea levels are used for the breeding of the next backcross generation.

Table 4.24: Backcross generations produced for the lines HST014, HST011 and HST015

Line	Generation	
	C57BL/6	BALB/c
HST014	3	6
HST011	3	2
HST015	0	5

V. DISCUSSION

The goal of the present study was to examine four ENU-induced mutant mouse lines for the causative mutation and the basal clinical chemical and morphological phenotypes. Three lines harbour a dominant mutation (HST014, HST015, and CLP001) and a fourth line harbours a recessive mutation (HST011 = UREHR2). The mutant lines were maintained on the C3H genetic background. Breeding data revealed that the aberrant phenotype of each line is caused by a mutation of a single genomic locus.

ENU is a potent mutagen and induces primarily point mutations in the spermatogonial stem cells (Russell et al. 1979). Search for published ENU-induced mutants (as of 31.03.2011) in the "phenotypes and alleles" section of the MGI database (http://www.informatics.jax.org/searches/allele_form.shtml) revealed 2,282 alleles and 1,823 genes/markers. Among them, 73 alleles and 61 genes/markers are described for influencing the renal or urinary system as primary or secondary phenotype. In the phenotype-driven Munich ENU mouse mutagenesis project, the generation of several mutant lines using increased plasma urea levels as primary phenotype with dominant or recessive mutation has been described on the C3H inbred genetic background (Aigner et al. 2007). The lines described includes line HST011 (= UREHR2).

5.1 Line HST014 exhibiting the mutation *Kctd1*^{I27N}

Line HST014 was established in the screen for dominant mutations showing increased plasma urea levels. Linkage analysis revealed the causative mutation on the proximal region of chromosome 18. Sequence analysis of the candidate gene *Kctd1* (15.1 Mb) revealed a T to A transversion which leads to the amino acid exchange from isoleucine to asparagine at position 27. The probability of the existence of confounding nonsegregating mutations in the chromosomal region of 1 bp to 20 Mb of chromosome 18 is significantly low ($p<0.01$) ((http://zeon.well.ox.ac.uk/git-bin/enuMutRat; Keays et al. 2007). We calculated the mutation rate in this region because the highest linkage was found at 21.5 Mb (D18Mit68) and data showed that the candidate region is clearly proximal to 21.5 Mb.

Kctd1 is a member of the potassium channel tetramerization domain containing

(*Kctd*) gene family. The name is based on the fact that the N-termini of KCTD proteins and some voltage-gated K^+ (Kv) channels are homologous (Lee et al. 1994, Shen et al. 1993). The KCTD1 protein contains a N-terminal BTB (broad-complex, tramtrack, and bric-a-brac) domain. The zinc finger proteins BTB are protein–protein interaction modules that mediate both self-association and interaction with non-BTB partners. BTB domain containing proteins show significant conservation of the core fold. The domain mediates the homodimeric and homotetrameric assembly of transcription factors and Kv channels, respectively (Stogios et al. 2005). KCTD proteins have been anticipated to bind to and regulate Kv channels (Abbott and Goldstein 1998). However, the biological function of KCTD proteins remains unclear. Expression studies revealed high levels in fetal tissues and low levels in adults which may implicate their role during development (Gamse et al. 2005). The KCTD proteins have been demonstrated to participate in a wide variety of cellular functions including transcription regulation, cellular proliferation, apoptosis, cell morphology, ion channel assembly, and protein degradation through ubiquitination. The KCTD1 protein is expressed in the mammary gland, kidney, brain, and ovary (Ding et al. 2008). We also found mRNA expression in the kidney. It has been suggested that KCTD1 is a nuclear protein and functions as a transcriptional repressor by mediating protein-protein interactions through a BTB domain for the AP-2 family by inhibiting its transactivation (Ding et al. 2009).

The well curated MGI database (http://www.informatics.jax.org) harbouring knockout as well as mutant mouse alleles includes no information about published *Kctd1* mouse mutants. Thus, this is the first report about a *Kctd1* mutant allele in mice. *Kctd1*^{I27N} heterozygous mutant mice were mated to produce homozygous mutant mice. At 3 month of age, we could not detect homozygous mutant offspring. The analysis of fetuses at the stage E17.5 showed the expected number of homozygous mutant animals. Thus, homozygous mutant animals showed early postnatal mortality. Further experiments have to be carried out to assess the time point and the cause of the early postnatal mortality in homozygous mutant mice. These data supports the role of KCTD1 in mammalian development. The clinical chemical blood analysis as well as metabolic cage analysis of three-month-old heterozygous mutant mice revealed signs of impaired kidney functions like increased urea, creatinine, and potassium levels as well as increase in water

intake, mild polyuria, and distinct hypercalciuria.

However, there is no report available about the renal function of KCTD1. One of the regimes of the reabsorption of the glomerular filtrate is located in the TALH cells where up to 20% of the glomerular filtrate is reabsorbed. Numerous ion transporters, such as NKCC2, ROMK, Na^+/H^+ exchanger (NHE3), KCC4, and ClC-Kb are expressed in TALH (Gamba 2005). TALH dysfunction leads to the impairment of urine concentration ability and reabsorption of ions as it has been observed in another ENU-induced mutant line showing nephropathy (Kemter et al. 2010) or with impaired androgen hormones (Hsu et al. 2010). These data suggest the role of KCTD1 protein in renal physiology. However, the cell-specific expression of KCTD1 in the kidney has yet to be analyzed.

Kctd1 inhibits the transactivation of the AP-2 family (Ding et al. 2009). Transcription factor AP-2 beta (a member of the AP-2 family) homozygous knockout mice have been described showing neonatal or postnatal lethality with renal kidney cysts, depending on the strain background. Homozygous knockout mice on the congenic 129P2 genetic background had tremors, polydactyly, defective tubular secretory function and ion homeostasis, hypocalcemia, phosphatemia, hyperuremia, and terminal renal failure (Moser et al. 1997, 2003). Using the *Kctd1* mutation on the C3H genetic background, the generation of congenic lines on the BALB/c and C57BL/6 genetic background is underway, to analyze the mutant phenotype on different genetic backgrounds. *Kctd1* mutations in humans are also not reported so far (http://www.ncbi.nlm.nih.gov/omim).

5.2 Line HST011 exhibiting the mutation *Pou3f3*^{L423P}

Phenotypically mutant mice of line HST011 (= UREHR2) showed the recessive inheritance of increased plasma urea values. Re-analysis of the linkage data detected the causative mutation on chromosome 1. Sequence analysis of the gene *Pou3f3* (42.7 Mb) revealed a T→C missense mutation which leads to the amino acid exchange from leucine to proline at position 423, hence the name of line HST011 was designated as *Pou3f3*^{L423P}. The probability of the existence of confounding nonsegregating mutations in the determined chromosomal region of 33.2-65.8 Mb of chromosome 1 is low ($p<0.05$) ((http://zeon.well.ox.ac.uk/git-bin/enuMutRat; Keays et al. 2007).

Pou3f3 (*Brn1*, brain-1) is a member of the class III POU domain transcription

factors. POU transcription factors carry a common DNA binding motif called POU domain and regulate a variety of developmental processes (Finney et al. 1988, Herr et al. 1988). The POU domain contains the well-characterized DNA-binding motif called as homeodomain. The homeodomains are involved in the transcriptional regulation of developmental processes (Phillips and Luisi 2000). *Pou3f3* is an intronless gene and is GC rich (74%) throughout the coding region (Sumiyama et al. 1996). *Pou3f3* is expressed in the central nervous system (He et al. 1989, McEvilly et al. 2002) and the kidney (Nakai et al. 2003) during embryonic development.

Upon searching the MGI database (http://www.informatics.jax.org) for *Pou3f3* mutant phenotypes, two *Pou3f3* knockout mutant mouse lines are found. The first knockout mouse line was established by replacing the gene sequences which encode the first 476 amino acids with a PGK-neo cassette via homologous recombination on an unspecified genetic background (McEvilly et al. 2002). The second knockout line was also established by using a PGK-neo cassette for replacing the 1.2 kb coding region (Nakai et al. 2003). Functional studies were performed on the mixed genetic background of 129S4/SvJae×C57BL/6J mice. Heterozygous mutant mice were phenotypically normal in both knockout lines. Our heterozygous mutant mice also show a grossly normal phenotype. Homozygous knockout mice showed neonatal mortality. In contrast, *Pou3f3*^{L423P} homozygous mutant mice are viable and fertile; however they exhibit reduced body weight and a smaller size. Nakai et al. (2003) showed that one-day-old homozygous knockout mice have increased plasma urea and potassium levels with renal hypoplasia. *Pou3f3*^{L423P} homozygous mutant mice show the same symptoms. The homozygous knockout mice showed developmental defects in the forebrain and the loop of Henle (McEvilly et al. 2002, Nakai et al. 2003). Therefore, further studies have to be carried out to assess potential developmental defects in brain and kidney of line *Pou3f3*^{L423P}.

Pou3f3^{L423P} homozygous mutant mice show impaired renal functions with moderate polyuria and reduced excretion of uric acid. Nakai et al. (2003) observed decreased expression levels of *Umod*, *Ptger3*, *Nkcc2*, *Kcnj1,* and *Bsnd* in homozygous as well as heterozygous knockout mice. *Umod* associated kidney diseases have been described to exhibit reduced uric acid excretion (Bleyer et al. 2003, Kemter et al. 2009, 2010). The data support the role of *Pou3f3* in the

regulation of *Umod* and *Nkcc2*. The absence of hyperuricemia in mice with reduced renal excretion of uric acid might be due to the uricase activity present in rodents (Choi et al. 2005). In humans, up to now no mutations are reported for *Pou3f3* (http://www.ncbi.nlm.nih.gov/omim).

5.3 Line HST015 established by increased plasma urea levels

Line HST015 harbouring a dominant mutation was initially established by increased plasma urea levels on the C3H genetic background. Linkage analysis using albino BALB/c inbred mice revealed the linkage of the mutant phenotype to the pigmented coat color of phenotypically mutant backcross mice. The albino coat color in BALB/c mice appears due to the recessive mutation *Tyr*$^{c/c}$ (94.5 Mb) on chromosome 7 (Detlefsen 1921). Therefore, the causative mutation in line HST015 was determined to be on chromosome 7 which was confirmed by the use of polymorphic markers on chromosome 7. Further breeding of backcrossed mice of the line HST015 showed a low number of mice with clear appearance of increased plasma urea levels. However, additional mutant phenotypes like decreased body weight as well as aggressive and/or hyperactive behaviour were observed. The reason for these phenotypic variations is not clear. The causative mutation of line HST015 is not yet identified.

5.4 Line CLP001 exhibiting the mutation *Gsdma3*^{I359N}

The mutant phenotype of alopecia in line CLP001 was mapped to a defined region around 100 Mb on chromosome 11. Sequence analysis of the gene *Gsdma3* (98.4 Mb) revealed a T→A transversion which leads to the amino acid exchange from isoleucine to asparagine at position 359. Thus, the name of the line was designated as *Gsdma3*^{I359N}.

Gsdma3 is a member of the Gsdma gene family (Runkel et al. 2004). It has two variants: *Gsdma3*-001 is composed of 11 exons which code for a 464 aa polypeptide. *Gsdma3*-002 is composed of 10 exons which code for a 455 aa polypeptide. It is predominantly expressed in skin and gastric tissues (Tanaka et al. 2007).

Upon searching the MGI database (http://www.informatics.jax.org) for mutant phenotypes, 2 targeted, 3 spontaneous and 4 ENU-induced alleles are found. Targeted alleles were generated by insertion of the L1L2_Bact_P vector

(http://www.informatics.jax.org). However, only cell lines are available to date. The spontaneous dominant mutation “defolliculated” (dfl) was observed in BABL/c mice which affects the skin and vision. A B2 element is inserted in exon 7 near the 3' splice site at nucleotide 861 of the mRNA which leads to an in-frame stop codon and changes Ile at residue 260 to 260-ArgAspTrp-262 as well as inserting a 15 bp duplication of the mRNA sequence from nucleotide 846 to 860. Heterozygous mutant mice showed alopecia with corneal opacity (Porter et al. 2002). The second spontaneous mutation occurred in C3H mice with semidominant inheritance. The mutation is characterized by a 6 bp insertion (AAGCGG) in exon 12 starting at nucleotide 1314 which results in a duplication of the codons 411 and 412 (GAA GCG, glutamic acid, alanine) to Glu Ala Glu Ala at 411–414. Mutant mice showed abnormal coat appearance (Runkel et al. 2004). A third spontaneous mutation was observed in C57BL/10J×DBA/2J mice, which causes a G to A point mutation at nucleotide 1124 resulting in the A348T amino acid exchange. Mutant mice showed alopecia and corneal opacity (Tanaka et al. 2007).

To date, 4 different ENU-induced dominant mutations of *Gsdma3* have been identified. These include *Gsdma3*^{Bsk}, *Gsdma3*^{Fgn} (BALB/c×C3H/HeH), *Gsdma3*^{Rco2} (C3HeB/FeJ) and *Gsdma3*^{M1Btlr} (C57BL/6J). All mutations are single point mutations which result in an amino acid exchange. Mutant mice showed abnormal hair cycle and hair follicle degeneration resulting in hair loss and thickened, wrinkled skin as well as corneal opacities (Sun et al. 2009, and refs. therein). The corneal opacities in these mutants are caused by abnormalities of the sebaceous-like Meibomian gland of the inner eyelid (Porter et al. 2002*)*.

In line *Gsdma3*^{I359N}, heterozygous mutant mice also show alopecia. The onset of hair loss starts from 3 weeks of age resulting in complete hair loss at 6 weeks of age. This is followed by the regeneration of a loose and spare complete hair coat until 8 weeks of age. Hair loss starts again and results in complete baldness at 14 weeks of age in heterozygous mutants and at 10-11 weeks of age in homozygous mutants. Hair cycle morphogenesis is a developmental process in the mammal growth governed by numerous growth factors, cytokines, hormones, and other factors. The hair follicle morphogenesis is a repeated cycle of growth (anagen), regression (catagen) and rest (telogen) (Müller-Röver et al. 2001). Malfunctioning of the hair cycle leads to alopecia or hair loss and other hair related diseases. In

the two lines *Gsdma3*^{Rco2} and "defolliculated" (dfl), it was shown that the defect of the hair cycle occurred in the catagen phase at 3 weeks of age (Porter et al. 2002, Runkel et al. 2004). In line *Gsdma3*^{I359N}, the hair cycle is also disturbed in the catagen phase. However, there are also reports showing that the anagen phase is affected due to *Gdsma3* mutations (Tanaka et al. 2007). In contrast, *Gsdma3*^{I359N} mutant mice appear normal at one week of age. *Gsdma3*^{I359N} mutant mice have normal eye grossly, however microscopically analysis has yet to be done to assess the corneal defects. In humans, one *Gsdma* gene is reported to date. It is expressed in the skin, hair follicle and gastrointestinal tract. However, there are no mutations of *Gsdma* reported in humans (Sun et al. 2009).

VI. SUMMARY

Molecular genetic and phenotypic analysis of ENU-induced mutant mouse models for biomedical research

In the phenotype-driven Munich ENU mouse mutagenesis project, the mutant lines HST014, HST011, and HST015 showing increased plasma urea levels as primary phenotype as well as line CLP001 exhibiting alopecia were established. The present study examined the causative mutations and the basal clinical chemical phenotypes of these four mutant lines.

In line HST014 harbouring a dominant mutation, the causative mutation was mapped to chromosome 18. Sequence analysis of the candidate gene *Kctd1* revealed a T→A transversion which leads to the amino acid exchange from isoleucine to asparagine at codon 27. Therefore, the line was named as *Kctd1*^{I27N}. Heterozygous mutant animals were viable and fertile whereas homozygous mutant animals showed early postnatal mortality. Clinical chemical blood analysis of 12-week-old heterozygous mutant animals showed increased levels of urea, creatinine, potassium, α-amylase, and lipase. Heterozygous mutant females showed hypercalcemia as well as a decreased body weight. Heterozygous mutant animals showed a moderate increase in the water intake as well as moderate polyuria and strong hypercalciuria.

In line HST011 (= UREHR2) harbouring a recessive mutation, re-analysis of the linkage data led to the linkage of the causative mutation to chromosome 1. Sequence analysis of candidate gene *Pou3f3* revealed a T→C transition, resulting in the amino acid exchange from leucine to proline at codon 423. The line name was designated as *Pou3f3*^{L423P}. Clinical chemical blood analysis showed increased levels of urea and potassium in homozygous mutant animals of both genders. Homozygous mutant animals exhibited polyuria and decreased daily uric acid excretion. Homozygous mutant mice were viable and fertile and showed the reduction of the body weight, the nose-rump-length, and the absolute as well as relative kidney weight.

Line HST015 harbouring a dominant mutation was initially established by increased plasma urea levels. The line was subsequently maintained using additional mutant phenotypes like decreased body weight as well as aggressive

and/or hyperactive behaviour. Linkage analysis using BALB/c inbred mice revealed that the causative mutation is linked to chromosome 7. The causative mutation is not yet identified.

The dominant mutant line CLP001 showed alopecia as primary phenotype and the causative mutation was previously mapped on chromosome 11 around 100 Mb. Sequence analysis of the candidate gene *Gsdma3* revealed a T→A transversion which leads to the amino acid exchange from isoleucine to asparagine at codon 359. Thus, the name of the line was designated as *Gsdma3*^{I359N}. Heterozygous mutant mice of both sexes showed onset of hair loss from the neck from 3 weeks of age resulting in complete hair loss at 6 weeks of age which was followed by regeneration of a loose and spare hair coat at 8 weeks of age. A second cycle of hair loss started from 9 weeks resulting in complete baldness at 14 weeks of age in heterozygous mutant mice and at 10-11 weeks of age in homozygous mutants. Homozygous mutant animals were viable and fertile.

In total, the four ENU-induced mouse lines *Kctd1*^{I27N}, *Pou3f3*^{L423P}, HST015, and *Gsdma3*^{I359N} were analyzed. The established mutant lines will contribute to the understanding of the functions of the genes involved.

VII. ZUSAMMENFASSUNG

Molekulargenetische und phänotypische Untersuchung von ENU-induzierten Mausmutanten für die biomedizinische Forschung

Im Rahmen des phänotypbasierten Münchener ENU-Mausmutageneseprojektes wurden die mutanten Linien HST014, HST011 und HST015 mit erhöhten Plasmaharnstoffwerten sowie die mutante Linie CLP001 mit Alopezie als primärem Phänotyp etabliert. Ziel der Arbeit war die Suche nach der ursächlichen Mutation sowie die basale klinisch-chemische und morphologische Untersuchung dieser vier mutanten Linien.

In der dominant mutanten Linie HST014 wurde die Lage der ursächlichen Mutation auf eine definierte Region des Chromosoms 18 eingegrenzt. Die Sequenzanalyse des Kandidatengens *Kctd1* erbrachte eine T→A Transversion, die zum Austausch der Aminosäure Isoleucin zu Asparagin an Kodon 27 des Proteins führt. Somit wurde die Linie mit *Kctd1*^{I27N} bezeichnet. Heterozygot mutante Tiere beiderlei Geschlechts sind lebensfähig und fertil, wohingegen homozygot mutante Tiere eine frühzeitige postnatale Mortalität zeigen. Die klinisch-chemische Blutuntersuchung von zwölf Wochen alten heterozygoten Mutanten erbrachte erhöhte Werte für Harnstoff, Kreatinin, Kalium als auch für die Enzymaktivitäten der α-Amylase und Lipase. Heterozygot mutante weibliche Tiere zeigten auch Hyperkalzämie sowie ein verringertes Körpergewicht. Des Weiteren wiesen heterozygot mutante Mäuse einen moderaten Anstieg der täglichen Wasseraufnahme, eine moderate Polyurie und eine ausgeprägte Hyperkalzurie auf.

In der rezessiv mutanten Linie HST011 (= UREHR2) wurden die bereits vor dieser Studie vorhandenen Kopplungsdaten nochmals überprüft. Diese Überprüfung führte dazu, dass die Lage der ursächlichen Mutation auf Chromosom 1 bestimmt wurde. Die Sequenzanalyse des Kandidatengens *Pou3f3* zeigte eine T→C Transition, die zum Austausch der Aminosäure Leucin zu Prolin an Kodon 423 des Proteins führt. Somit wurde die Linie mit *Pou3f3*^{L423P} bezeichnet. Homozygot mutante Tiere beiderlei Geschlechts sind lebensfähig und fertil und zeigten als Zeichen einer gestörten Nierenfunktion erhöhte Blutwerte für Plasmaharnstoff und Plasmakalium sowie eine milde Polyurie und eine

verringerte Harnsäureausscheidung. Die morphologische Untersuchung erbrachte verringerte Werte für das Körpergewicht, die Körperlänge sowie für das relative Nierengewicht.

Die dominant mutante Linie HST015 wurde initial mit Hilfe erhöhter Plasmaharnstoffwerte als primärem Phänotyp etabliert. Für die weitere Zucht der Linie sowohl auf dem genetischen Hintergrund des C3H-Inzuchtstammes als auch bei wiederholten Verpaarungen mit BALB/c-Inzuchttieren wurden zusätzliche phänotypische Auffälligkeiten wie verringertes Körpergewicht und/oder hyperaktives bzw. aggressives Verhalten als phänotypische Merkmale mutanter Tiere neu identifiziert und verwendet. Nach Verpaarung von phänotypisch mutanten Tieren auf dem genetischen Hintergrund des pigmentierten C3H-Inzuchtstammes mit BALB/c-Albinoinzuchttieren wurde eine Kopplung der ursächlichen Mutation mit der Fellfarbe festgestellt, wodurch die Bestimmung der Lage der ursächlichen Mutation auf Chromosom 7 ermöglicht wurde und in weiteren Untersuchungen bestätigt wurde. Die Identifizierung der Mutation selbst steht noch aus.

Die dominant mutante Linie CLP001 wurde mit Alopezie als primärem Phänotyp etabliert. Schon vorhandene Kopplungsdaten zeigten die Lage der ursächlichen Mutation auf Chromosom 11 bei ca. 100 Mb an. Die Sequenzanalyse des Kandidatengens *Gsdma3* erbrachte eine T→A Transversion, die zum Austausch der Aminosäure Isoleucin zu Asparagin an Kodon 359 des Proteins führt. Somit wurde die Linie mit *Gsdma3*^{I359N} bezeichnet. Homozygot mutante Tiere beiderlei Geschlechts sind lebensfähig und fertil. Heterozygote Mutanten zeigen drei Wochen p.p. den Beginn des Haarausfalles, der sich von der Nackengegend über das ganze Fell ausbreitet. Mit einem Alter von sechs Wochen tritt eine vollständige Alopezie bei diesen Tieren auf, die von einer regenerativen Phase gefolgt wird, so dass mit acht Wochen wieder ein schütteres Fell vorhanden ist. Eine Woche später beginnt der nochmalige Haarausfall, was zur vollständigen und permanenten Alopezie mit 14 Wochen p.p. führt. Bei homozygot mutanten Tieren tritt diese permanente Alopezie bereits nach 10-11 Wochen auf.

Zusammenfassend wurden die vier ENU-induzierten Mauslinien *Kctd1*^{I27N}, *Pou3f3*^{L423P}, HST015 und *Gsdma3*^{I359N} untersucht. Die Untersuchung dieser mutanten Linien trägt zum Verständnis der Funktion der am jeweiligen Krankheitsgeschehen beteiligten Gene bei.

VIII. REFERENCES

Abbott GW, Goldstein SA (1998) A superfamily of small potassium channel subunits: form and function of the MinK-related peptides (MiRPs). *Q Rev Biophys* 31: 357–398.

Acevedo-Arozena A, Wells S, Potter P, Kelly M, Cox RD, Brown SDM (2008) ENU mutagenesis, a way forward to understand gene function. *Annu Rev Genomics Hum Genet* 9: 49–69.

Aigner B, Rathkolb B, Herbach N, Kemter E, Schessl C, Klaften M, Klempt M, Hrabé de Angelis M, Wanke R, Wolf E (2007) Screening for increased plasma urea levels in a large-scale ENU mouse mutagenesis project reveals kidney disease models. *Am J Physiol Renal Physiol* 292: F1560–F1567.

Aigner B, Rathkolb B, Herbach N, Hrabé de Angelis M, Wanke R, Wolf E (2008) Diabetes models by screen for hyperglycemia in phenotype-driven ENU mouse mutagenesis projects. *Am J Physiol Endocrinol Metab* 294: E232–E240.

Augustin M, Sedlmeier R, Peters T, Huffstadt U, Kochmann E, Simon D, Schöniger M, Garke-Mayerthaler S, Laufs J, Mayhaus M, Franke S, Klose M, Graupner A, Kurzmann M, Zinser C, Wolf A, Voelkel M, Kellner M, Kilian M, Seelig S, Koppius A, Teubner A, Korthaus D, Nehls M, Wattler S (2005) Efficient and fast targeted production of murine models based on ENU mutagenesis. *Mamm Genome* 16: 405–413.

Balling R (2001) ENU mutagenesis: analyzing gene function in mice. *Annu Rev Genomics Hum Genet* 2: 463–492.

Barbaric I, Wells S, Russ A, Dear TN (2007) Spectrum of ENU-induced mutations in phenotype-driven and gene-driven screens in the mouse. *Environ Mol Mutagen* 48: 124–142.

Bates JM, Raffi HM, Prasadan K, Mascarenhas R, Laszik Z, Maeda N, Hultgren SJ, Kumar S (2004) Tamm-Horsfall protein knockout mice are more prone to urinary tract infection:rapid communication. *Kidney Int* 65: 791–797.

Bennett BJ, Farber CR, Orozco L, Kang HM, Ghazalpour A, Siemers N, Neubauer M, Neuhaus I, Yordanova R, Guan B, Truong A, Yang WP, He A, Kayne P, Gargalovic P, Kirchgessner T, Pan C, Castellani LW, Kostem E,

Furlotte N, Drake TA, Eskin E, Lusis AJ (2010) A high-resolution association mapping panel for the dissection of complex traits in mice. *Genome Res* 20: 281–290.

Bielas JH, Heddle JA (2000) Proliferation is necessary for both repair and mutation in transgenic mouse cells. *Proc Natl Acad Sci USA* 97: 11391–11396.

Bilgüvar K, Oztürk AK, Louvi A, Kwan KY, Choi M, Tatli B, Yalnizoğlu D, Tüysüz B, Cağlayan AO, Gökben S, Kaymakçalan H, Barak T, Bakircioğlu M, Yasuno K, Ho W, Sanders S, Zhu Y, Yilmaz S, Dinçer A, Johnson MH, Bronen RA, Koçer N, Per H, Mane S, Pamir MN, Yalçinkaya C, Kumandaş S, Topçu M, Ozmen M, Sestan N, Lifton RP, State MW, Günel M (2010) Whole-exome sequencing identifies recessive WDR62 mutations in severe brain malformations. *Nature* 467: 207–210.

Bleyer AJ, Woodard AS, Shihabi Z, Sandhu J, Zhu H, Satko SG, Weller N, Deterding E, McBride D, Gorry MC, Xu L, Ganier D, Hart TC (2003) Clinical characterization of a family with a mutation in the uromodulin (Tamm-Horsfall glycoprotein) gene. *Kidney Int* 64: 36–42.

Bult CJ, Eppig JT, Kadin JA, Richardson JE, Blake JA (2008) The Mouse Genome Database (MGD): mouse biology and model systems. *Nucleic Acids Res* 36: D724–D728.

Caspary T, Anderson KV (2006) Uncovering the uncharacterized and unexpected: unbiased phenotype-driven screens in the mouse. *Dev Dyn* 235: 2412–2423.

Chen Y, Yee D, Dains K, Chatterjee A, Cavalcoli J, Schneider E, Om J, Woychik RP, Magnuson T (2000) Genotype-based screen for ENU-induced mutations in mouse embryonic stem cells. *Nat Genet* 24: 314–317.

Choi HK, Mount DB, Reginato AM (2005) Pathogenesis of gout. *Ann Intern Med* 143: 499–516.

Choi M, Scholl UI, Ji W, Liu T, Tikhonova IR, Zumbo P, Nayir A, Bakkaloğlu A, Ozen S, Sanjad S, Nelson-Williams C, Farhi A, Mane S, Lifton RP (2009) Genetic diagnosis by whole exome capture and massively parallel DNA sequencing. *Proc Natl Acad Sci USA* 106: 19096–19101.

Coffey AJ, Kokocinski F, Calafato MS, Scott CE, Palta P, Drury E, Joyce CJ,

Leproust EM, Harrow J, Hunt S, Lehesjoki AE, Turner DJ, Hubbard TJ, Palotie A (2011) The GENCODE exome: sequencing the complete human exome. *Eur J Hum Genet* 19: 1–5.

Coghill EL, Hugill A, Parkinson N, Davison C, Glenister P, Clements S, Hunter J, Cox RD, Brown SD (2002) A gene-driven approach to the identification of ENU mutants in the mouse. *Nat Genet* 30: 255–256.

Cordes SP (2005) *N*-ethyl-*N*-nitrosourea mutagenesis: boarding the mouse mutant express. *Microbiol Mol Biol Rev* 69: 426–439.

Detlefsen JA (1921) A new mutation in the house mouse. *Am Naturalist* 55: 469–473.

Ding XF, Luo C, Ren KQ, Zhang J, Zhou JL, Hu X, Liu RS, Wang Y, Gao X, Zhang J (2008) Characterization and expression of a human KCTD1 gene containing the BTB domain, which mediates transcriptional repression and homomeric interactions. *DNA Cell Biol* 27: 257–265.

Ding X, Luo C, Zhou J, Zhong Y, Hu X, Zhou F, Ren K, Gan L, He A, Zhu J, Gao X, Zhang J (2009) The interaction of KCTD1 with transcription factor AP-2alpha inhibits its transactivation. *J Cell Biochem* 106: 285–295.

Du X, Schwander M, Moresco EM, Viviani P, Haller C, Hildebrand MS, Pak K, Tarantino L, Roberts A, Richardson H, Koob G, Najmabadi H, Ryan AF, Smith RJ, Müller U, Beutler B (2008) A catechol-O-methyltransferase that is essential for auditory function in mice and humans. *Proc Natl Acad Sci USA* 105: 14609–14614.

Festing MFW (1993) *International index of laboratory animals* 6th edn. (Lion Lith Ltd, Carshalton, Surrey UK).

Finney M, Ruvkun G, Horvitz HR (1988) The C. elegans cell lineage and differentiation gene unc-86 encodes a protein with a homeodomain and extended similarity to transcription factors. *Cell* 55: 757–769.

Frazer KA, Eskin E, Kang HM, Bogue MA, Hinds DA, Beilharz EJ, Gupta RV, Montgomery J, Morenzoni MM, Nilsen GB, Pethiyagoda CL, Stuve LL, Johnson FM, Daly M J, Wade CM, Cox DR (2007) A sequence-based variation map of 8.27 million SNPs in inbred mouse strains. *Nature* 448: 1050–1053.

Fuchs H, Gailus-Durner V, Adler T, Pimentel JA, Becker L, Bolle I, Brielmeier M, Calzada-Wack J, Dalke C, Ehrhardt N, Fasnacht N, Ferwagner B, Frischmann U, Hans W, Hölter SM, Hölzlwimmer G, Horsch M, Javaheri A, Kallnik M, Kling E, Lengger C, Maier H, Mossbrugger I, Mörth C, Naton B, Nöth U, Pasche B, Prehn C, Przemeck G, Puk O, Racz I, Rathkolb B, Rozman J, Schäble K, Schreiner R, Schrewe A, Sina C, Steinkamp R, Thiele F, Willershäuser M, Zeh R, Adamski J, Busch DH, Beckers J, Behrendt H, Daniel H, Esposito I, Favor J, Graw J, Heldmaier G, Höfler H, Ivandic B, Katus H, Klingenspor M, Klopstock T, Lengeling A, Mempel M, Müller W, Neschen S, Ollert M, Quintanilla-Martinez L, Rosenstiel P, Schmidt J, Schreiber S, Schughart K, Schulz H, Wolf E, Wurst W, Zimmer A, Hrabé de Angelis M (2009) The German Mouse Clinic: A platform for systemic phenotype analysis of mouse models. *Curr Pharm Biotechnol* 10: 236–243.

Gailus-Durner V, Fuchs H, Becker L, Bolle I, Brielmeier M, Calzada-Wack J, Elvert R, Ehrhardt N, Dalke C, Franz TJ, Grundner-Culemann E, Hammelbacher S, Holter SM, Holzlwimmer G, Horsch M, Javaheri A, Kalaydjiev SV, Klempt M, Kling E, Kunder S, Lengger C, Lisse T, Mijalski T, Naton B, Pedersen V, Prehn C, Przemeck G, Racz I, Reinhard C, Reitmeir P, Schneider I, Schrewe A, Steinkamp R, Zybill C, Adamski J, Beckers J, Behrendt H, Favor J, Graw J, Heldmaier G, Hofler H, Ivandic B, Katus H, Kirchhof P, Klingenspor M, Klopstock T, Lengeling A, Muller W, Ohl F, Ollert M, Quintanilla-Martinez L, Schmidt J, Schulz H, Wolf E, Wurst W, Zimmer A, Busch DH, Hrabé de Angelis M (2005) Introducing the German Mouse Clinic: open access platform for standardized phenotyping. *Nat Methods* 2: 403–404.

Gamba G (2005) Molecular physiology and pathophysiology of electroneutral cation-chloride cotransporters. *Physiol Rev* 85: 423–493.

Gamse JT, Kuan YS, Macurak M, Brösamle C, Thisse B, Thisse C, Halpern ME (2005) Directional asymmetry of the zebrafish epithalamus guides dorsoventral innervation of the midbrain target. *Development* 132: 4869–4881.

He X, Treacy MN, Simmons DM, Ingraham HA, Swanson LW, Rosenfeld MG (1989) Expression of a large family of POU-domain regulatory genes in mammalian brain development. *Nature* 340: 35–41.

Herr W, Sturm RA, Clerc RG, Corcoran LM, Baltimore D, Sharp PA, Ingraham

HA, Rosenfeld MG, Finney M, Ruvkun G, Horvitz HR (1988) The POU domain: a large conserved region in the mammalian pit-1, oct-1, oct-2, and Caenorhabditis elegans unc-86 gene products. *Genes Dev* 2: 1513–1516.

Hrabé de Angelis M, Flaswinkel H, Fuchs H, Rathkolb B, Soewarto D, Marschall S, Heffner S, Pargent W, Wuensch K, Jung M, Reis A, Richter T, Alessandrini F, Jakob T, Fuchs E, Kolb H, Kremmer E, Schaeble K, Rollinski B, Roscher A, Peters C, Meitinger T, Strom T, Steckler T, Holsboer F, Klopstock T, Gekeler F, Schindewolf C, Jung T, Avraham K, Behrendt H, Ring J, Zimmer A, Schughart K, Pfeffer K, Wolf E, Balling R (2000) Genome-wide, large-scale production of mutant mice by ENU mutagenesis. *Nat Genet* 25: 444–447.

Hsu YJ, Dimke H, Schoeber JP, Hsu SC, Lin SH, Chu P, Hoenderop JG, Bindels RJ (2010) Testosterone increases urinary calcium excretion and inhibits expression of renal calcium transport proteins. *Kidney Int* 77: 601–608.

Justice MJ, Jenkins NA, Copeland NG (1992) Recombinant inbred mouse strain: models for disease study. *Trends Biotech* 10: 120–126.

Justice MJ, Noveroske JK, Weber JS, Zheng B, Bradley A (1999) Mouse ENU mutagenesis. *Hum Mol Genet* 8: 1955–1963.

Keays DA, Clark TG, Flint J (2006) Estimating the number of coding mutations in genotypic- and phenotypic-driven N-ethyl-N-nitrosourea (ENU) screens. *Mamm Genome* 17: 230–238.

Keays DA, Clark TG, Campbell TG, Broxholme J, Valdar W (2007) Estimating the number of coding mutations in genotypic and phenotypic driven N-ethyl-N-nitrosourea (ENU) screens: revisited. *Mamm Genome* 18: 123–124.

Kemter E, Rathkolb B, Rozman J, Hans W, Schrewe A, Landbrecht C, Klaften M, Ivandic B, Fuchs H, Gailus-Durner V, Klingenspor M, Hrabé de Angelis M, Wolf E, Wanke R, Aigner B (2009) Novel missense mutation of uromodulin in mice causes renal dysfunction with alterations in urea handling, energy, and bone metabolism. *Am J Physiol Renal Physiol* 297: F1391–F1398.

Kemter E, Rathkolb B, Bankir L, Schrewe A, Hans W, Landbrecht C, Klaften M, Ivandic BT, Fuchs H, Gailus-Durner V, Hrabé de Angelis M, Wolf E, Wanke R, Aigner B (2010) Mutation of the Na+-K+-2Cl- cotransporter NKCC2 in mice is associated with severe polyuria and a urea-selective concentrating defect without

hpyerreninemia. *Am J Physiol Renal Physiol* 298: F1405–F1415.

Kitaura H, Tsujita M, Huber VJ, Kakita A, Shibuki K, Sakimura K, Kwee IL, Nakada (2009) Activity-dependent glial swelling is impaired in aquaporin-4 knockout mice. *Neurosci Res* 64: 208–212.

Lander ES (2011) Initial impact of the sequencing of the human genome. *Nature* 470: 187–197.

Lee TE, Philipson LH, Kuznetsov A, Nelson DJ (1994) Structural determinant for assembly of mammalian K+ channels. *Biophys J* 66: 667–673.

Li H, Leikauf G, Liu P, You M, Pitt B, Zhang L (2010) Genome-wide association study (GWAS) of ventilator-induced lung injury (VILI) using dense single nucleotide polymorphism (SNP) maps in mice. *Am J Respir Crit Care Med* 181: A1019.

Ma T, Yang B, Gillespie A, Carlson EJ, Epstein CJ, Verkman AS (1997) Generation and phenotype of a transgenic knockout mouse lacking the mercurial-insensitive water channel aquaporin-4. *J Clin Invest* 100: 957–962.

Manenti G, Galvan A, Pettinicchio A, Trincucci G, Spada E, Zolin A, Milani S, Gonzalez-Neira A, Dragani TA (2009) Mouse genome-wide association mapping needs linkage analysis to avoid false-positive loci. *PLoS Genet* 5: e1000331.

Majumdar A, Vainio S, Kispert A, McMahon J, McMahon AP (2003) Wnt11 and Ret/Gdnf pathways cooperate in regulating ureteric branching during metanephric kidney development. *Development* 130: 3175–3185.

Marfella CG, Ohkawa Y, Coles AH, Garlick DS, Jones SN, Imbalzano AN (2006) Mutation of the SNF2 family member Chd2 affects mouse development and survival. *J Cell Physiol* 209: 162–171.

McEvilly RJ, de Diaz MO, Schonemann MD, Hooshmand F, Rosenfeld MG (2002) Transcriptional regulation of cortical neuron migration by POU domain factors. *Science* 295: 1528–1532.

Mo L, Zhu XH, Huang HY, Shapiro E, Hasty DL, Wu XR (2004) Ablation of the Tamm-Horsfall protein gene increases susceptibility of mice to bladder colonization by type 1-fimbriated Escherichia coli. *Am J Physiol Renal Physiol* 286: F795–F802.

Moore KJ, Nagle DL (2000) Complex trait analysis in the mouse: The strengths, the limitations and the promise yet to come. *Annu Rev Genet* 34: 653–686.

Morishita Y, Matsuzaki T, Hara-chikuma M, Andoo A, Shimono M, Matsuki A, Kobayashi K, Ikeda M, Yamamoto T, Verkman A, Kusano E, Ookawara S, Takata K, Sasaki S, Ishibashi K (2005) Disruption of aquaporin-11 produces polycystic kidneys following vacuolization of the proximal tubule. *Mol Cell Biol* 25: 7770–7779.

Moser M, Pscherer A, Roth C, Becker J, Mücher G, Zerres K, Dixkens C, Weis J,Guay-Woodford L, Buettner R, Fässler R (1997) Enhanced apoptotic cell death of renal epithelial cells in mice lacking transcription factor AP-2 beta. *Genes Dev* 11: 1938–1948.

Moser M, Dahmen S, Kluge R, Gröne H, Dahmen J, Kunz D, Schorle H, Buettner R (2003) Terminal renal failure in mice lacking transcription factor AP-2 beta. *Lab Invest* 83: 571–578.

Müller-Röver S, Handjiski B, van der Veen C, Eichmüller S, Foitzik K, McKay IA, Stenn KS, Paus R (2001) A comprehensive guide for the accurate classification of murine hair follicles in distinct hair cycle stages. *J Invest Dermatol* 117: 3–15.

Munroe RJ, Bergstrom RA, Zheng QY, Libby B, Smith R, John SW, Schimenti KJ, Browning VL, Schimenti JC (2000) Mouse mutants from chemically mutagenized embryonic stem cells. *Nat Genet* 24: 318–321.

Nakai S, Sugitani Y, Sato H, Ito S, Miura Y, Ogawa M, Nishi M, Jishage K, Minowa O, Noda T (2003) Crucial roles of Brn1 in distal tubule formation and function in mouse kidney. *Development* 130: 4751–4759.

Newton CR, Graham A, Heptinstall LE, Powell SJ, Summers C, Kalsheker N, Smith JC, Markham AF (1989) Analysis of any point mutation in DNA. The amplification refractory mutation system (ARMS). *Nucleic Acids Res* 17: 2503–2516.

Ng SB, Turner EH, Robertson PD, Flygare SD, Bigham AW, Lee C, Shaffer T, Wong M, Bhattacharjee A, Eichler EE, Bamshad M, Nickerson DA, Shendure J (2009) Targeted capture and massively parallel sequencing of 12 human exomes. *Nature* 461: 272–276.

Ng SB, Buckingham KJ, Lee C, Bigham AW, Tabor HK, Dent KM, Huff CD, Shannon PT, Jabs EW, Nickerson DA, Shendure J, Bamshad MJ (2010) Exome sequencing identifies the cause of a mendelian disorder. *Nat Genet* 42: 30–35.

Nicklas W, Baneux P, Boot R, Decelle T, Deeny AA, Fumanelli M, Illgen-Wilcke B (2002) Recommendations for the health monitoring of rodent and rabbit colonies in breeding and experimental units. *Lab Anim* 36: 20–42.

Nolan PM, Peters J, Strivens M, Rogers D, Hagan J, Spurr N, Gray IC, Vizor L, Brooker D, Whitehill E, Washbourne R, Hough T, Greenaway S, Hewitt M, Liu X, McCormack S, Pickford K, Selley R, Wells C, Tymowska-Lalanne Z, Roby P, Glenister P, Thornton C, Thaung C, Stevenson JA, Arkell R, Mburu P, Hardisty R, Kiernan A, Erven A, Steel KP, Voegeling S, Guenet JL, Nickols C, Sadri R, Nasse M, Isaacs A, Davies K, Browne M, Fisher EM, Martin J, Rastan S, Brown SD, Hunter J (2000) A systematic, genome-wide, phenotype-driven mutagenesis programme for gene function studies in the mouse. *Nat Genet* 25: 440–443.

Norman LP, Jiang W, Han X, Saunders TL, Bond JS (2003) Targeted disruption of the meprin beta gene in mice leads to underrepresentation of knockout mice and changes in renal gene expression profiles. *Mol Cell Biol* 23: 1221–1230.

Noveroske JK, Weber JS, Justice MJ (2000) The mutagenic action of N-ethyl-N-nitrosourea in the mouse. *Mamm Genome* 11: 478–483.

Peltonen L, McKusick VA (2001) Genomics and medicine. Dissecting human disease in the postgenomic era. *Science* 291: 1224–1229.

Phillips K, Luisi B (2000) The virtuoso of versatility: POU proteins that flex to fit. *J Mol Biol* 302: 1023–1039.

Porter RM, Jahoda CA, Lunny DP, Henderson G, Ross J, McLean WH, Whittock NV, Wilson NJ, Reichelt J, Magin TM, Lane EB (2002) Defolliculated (dfl): a dominant mouse mutation leading to poor sebaceous gland differentiation and total elimination of pelage follicles. *J Invest Dermatol* 119: 32–37.

Prückl P (2011) Untersuchung zweier ENU-induzierter mutanter Mauslinien mit Fokus auf eine Linie mit einer Punktmutatin im Uromodulin-Gen. Dissertation, LMU München.

Rathkolb B, Decker T, Fuchs E, Soewarto D, Fella C, Heffner S, Pargent W,

Wanke R, Balling R, Hrabé de Angelis M, Kolb HJ, Wolf E (2000) The clinical-chemical screen in the Munich ENU Mouse Mutagenesis Project: screening for clinically relevant phenotypes. *Mamm Genome* 11: 543–546.

Runkel F, Marquardt A, Stoeger C, Kochmann E, Simon D, Kohnke B, Korthaus D, Wattler F, Fuchs H, Hrabé de Angelis M, Stumm G, Nehls M, Wattler S, Franz T, Augustin M (2004) The dominant alopecia phenotypes Bareskin, Rex-denuded, and Reduced Coat 2 are caused by mutations in gasdermin 3. *Genomics* 84: 824–835.

Russell WL, Kelly EM, Hunsicker PR, Bangham JW, Maddux SC, Phipps EL (1979) Specific-locus test shows ethylnitrosourea to be the most potent mutagen in the mouse. *Proc Natl Acad Sci USA* 76: 5818–5819.

Shen NV, Chen X, Boyer MM, Pfaffinger PJ (1993) Deletion analysis of K+ channel assembly. *Neuron* 11: 67–76.

Shibuya T, Morimoto K (1993) A review of the genotoxicity of 1-ethyl-1-nitrosourea. *Mutat Res* 297: 3–38.

Silver LM (1995) *Mouse Genetics: Concepts and Applications.* (New York: Oxford Univ. Press).

Singer B, Dosahjh MK (1990) Site-directed mutagenesis for quantitation of base-base interactions at defined sites. *Mutat Res* 233: 45–51.

Stogios P, Downs G, Jauhal J, Nandra S, Prive G (2005) Sequence and structural analysis of BTB domain proteins. *Genome Biol* 6: R82.

Su WL, Sieberts SK, Kleinhanz RR, Lux K, Millstein J, Molony C, Schadt EE (2010) Assessing the prospects of genome-wide association studies performed in inbred mice. *Mamm Genome* 21: 143–152.

Sumiyama K, Washio-Watanabe K, Saitou N, Hayakawa T, Ueda S (1996) Class III POU genes: generation of homopolymeric amino acid repeats under GC pressure in mammals. *J Mol Evol* 43: 170–178.

Sun L, Li XH, Du X, Benson K, Smart NG, Beutler B (2009) Record for "Fuzzy". MGI Direct Data Submission (http://www.informatics.jax.org).

Takahasi KR, Sakuraba Y, Gondo Y (2007) Mutational pattern and frequency of

induced nucleotide changes in mouse ENU mutagenesis. *BMC Mol Biol* 8: 52.

Tanaka S, Tamura M, Aoki A, Fujii T, Komiyama H, Sagai T, Shiroishi T (2007) A new Gsdma3 mutation affecting anagen phase of first hair cycle. *Biochem Biophys Res Commun* 359: 902–907.

Valdar W, Solberg LC, Gauguier D, Burnett S, Klenerman P, Cookson WO, Taylor MS, Rawlins JN, Mott R, Flint J (2006) Genome-wide genetic association of complex traits in heterogeneous stock mice. *Nat Genet* 38: 879–887.

Xu L, Li Y (2000) Positional Cloning. In Developmental biology protocols: overview II. *Methods in Molecular Biology*. 136: 285–296.

Yalcin B, Nicod J, Bhomra A, Davidson S, Cleak J, Farinelli L, Østerås M, Whitley A, Yuan W, Gan X, Goodson M, Klenerman P, Satpathy A, Mathis D, Benoist C, Adams DJ, Mott R, Flint J (2010) Commercially available outbred mice for genome-wide association studies. *PLoS Genet* 6: e1001085.

Zinovieva N, Vasicek D, Aigner B, Müller M, Brem G (1996) Short communication: single tube allele specific (STAS) PCR for direct determination of the mutation in the porcine ryanodine receptor gene associated with malignant hyperthermia. *Anim Biotechnol* 7: 173–177.

IX. ACKNOWLEDGEMENT

I would like to thank all, whose sincere efforts give a shape to this manuscript and first of all, I owe my deepest gratitude to my thesis supervisor, Prof. Dr. Bernhard Aigner, for providing me an opportunity to work on this project. His commitments, encouragement, guidance and support enabled me to develop an understanding of the subject. It is an honor for me to work under his supervision, who continuously sustains my consistency and moral.

I am indebted to Prof. Dr. Eckhard Wolf for his supportive attitude towards me. He is always the source of inspiration for me. Further, I want to acknowledge the Bayerische Forschungsstiftung for supporting my work financially. I also would like to show my gratitude to unseen heroes, brave mice which were bred and examined during the course of this work.

I express my sincere regards to Dr. Elisabeth, Dr. Nikolai and Dr. Tina for scientific guidance and suggestions. Further, I would like to thank Dr. Birgit and Elfi for clinical chemical analysis and Dr. Sibylle Wagner for linkage analysis. I am indebted to my colleagues Petra, Katrin, Pauline, Katinka, Marieke, Andrea, Stefanie, Kristin, Eva, Anne, Christina, Elisabeth, Dr. Myriam, Dr. Horst, Dr. Anne, Dr. Simone, and Dr. Barbara to support me during day-to-day work and sharing their valuable experiences during this study.

I also express my best regards to past and present members of Wilhelmshof 6, especially Mayuko, Jan, Katya, Jan Maxa, for sharing their daily life experiences and nice time. Further, I would like to thank all people from the mouse house facility, especially Helga for her helping hands to maintain the mouse lines.

Further, I express my sincere regards to Dr. Wolfgang Voss and Angelika for their superb administration support. I also express my best regards to Dr. Valeri and Tuna for sharing nice time during the study.

Additionally, I would like to thank my former supervisor Prof. M.L. Sangwan and the ABT staff and my friends RP, Harish, Arun, Manish, and my family friend Shailesh Varshney and his family. Thank you for being with me.

Lastly, I want to acknowledge my best regards to my extended family, my wife Rekha for her love, understanding and emotional support throughout the phase. I

am also indebted to my uncle, brothers, and their families for their affection and love. It is the blessings of my parents which enable me to achieve this milestone in my life.

Last but not least, I am indebted to almighty God who gives me power, energy, and patience every day.

Sudhir Kumar